1-1-2011

Role of the ARF Tumor Suppressor in Osteoclasts

Crystal Winkeler
Washington University in St. Louis

Washington University

Division of Biology and Biomedical Sciences

Molecular Cell Biology

Dissertation Examination Committee:

Jason Weber, Chair
Roberta Faccio
Loren Michel
Mark Sands
Katherine Weilbaecher
Zhongsheng You

Role of the Arf Tumor Suppressor in Osteoclasts

by

Crystal Lynn Winkeler

A dissertation presented to the
Graduate School of Arts and Sciences
of Washington University in
partial fulfillment of the
requirements for the degree
of Doctor of Philosophy

December 2011

Saint Louis, Missouri

ABSTRACT OF THE DISSERTATION

Role of the ARF Tumor Suppressor in Osteoclasts

by

Crystal Lynn Winkeler

Doctor of Philosophy in Biology and Biomedical Sciences

Molecular Cell Biology

Washington University in St. Louis, 2011

Dr. Jason D. Weber, Chairperson

The ARF tumor suppressor is upregulated upon oncogenic stress. ARF can suppress cell proliferation in both p53-dependent and -independent mechanisms. We have focused on ARF's ability to suppress protein synthesis in a p53-independent manner. Given that protein synthesis and the cell cycle are coordinately controlled, this arm of ARF tumor suppression also contributes to the restraint of cell proliferation. Our lab has recently shown that basal ARF suppresses protein synthesis in mitotic cells. The focus of my dissertation has been to determine whether basal ARF regulates cell growth in a post-mitotic setting.

We used the osteoclast (OC) as a model for post-mitotic growth. We attempted to generate osteoclast-specific *Arf* loss using a *Cre*-expressing mouse, in which *Cre* is controlled by the *Cathepsin K* promoter ($Ctsk^{Cre/+}$). Surprisingly, we generated $Arf^{-/-}$ mice as demonstrated by genotyping, loss of ARF expression in the testis, and a phenotype

comparable to traditional *Arf*$^{-/-}$ mice. Furthermore, both Cathepsin K and Cre are expressed in reproductive tissues, which results in Cre activity within gametes as confirmed by crossing *Ctsk*$^{Cre/+}$ mice with *ROSA* reporter mice. Finally, we found that *Cathepsin K* loss enhances serum estradiol levels. Together, this data suggests that *Cathepsin K*-driven *Cre* will not consistently result in OC-specific gene loss and may lead to misinterpretation of phenotypes generated to study the function of OC genes.

In parallel, we have analyzed the role of ARF during osteoclastogenesis *in vitro* and found that *Arf* loss enhances osteoclastogenesis as demonstrated by OC number and size, protein markers of osteoclastogenesis, and increased bone resorption. Enhanced osteoclastogenesis upon *Arf* loss is independent of both proliferation and p53. Furthermore, we demonstrated enhanced protein synthesis and ribosome activity during osteoclastogenesis in *Arf*$^{-/-}$ cells. As an alternative approach to studying *Arf* loss *in vivo*, we generated radiation chimeras and challenged them with RANKL. We found that *Arf* loss results in elevated bone resorption due, at least in part, to increased osteoclastogenesis *in vivo*. This data collectively suggests that ARF regulates proliferation-independent cell growth, a function that is physiologically relevant both *in vitro* and *in vivo*.

ACKNOWLEDGEMENTS

I would first like to thank my mentor, Jason Weber, for all of his support and advice along the way. I appreciate the times when he let me figure things out for myself while knowing exactly when to step in and lend me a hand. I am truly grateful for Jason's willingness to go beyond my expectations of a mentor and be someone who truly cares about my personal well-being and future. He is a role model for me as a successful scientist who manages to balance a career with a family. Also, I would like to extend my appreciation to the members of my thesis committee. It has been so beneficial to me to have such a wide spectrum of expertise to help guide my project. I would especially like to thank Kathy Weilbaecher for many one-on-one conversations about my project and future beyond graduate school.

Thank you to all the members of the Weber lab. My graduate school experience simply would not have been the same without them. I am so grateful that I was never far from someone to teach me a new protocol, talk over troublesome experiments, vent about life as a graduate student, or relieve stress with over lunch. They are a big part of the reason I will look back on my graduate career with fondness. Also, thank you to members of the bone group, especially Monica Croke and Michelle Hurchla. I certainly would not have been able to take on a project outside the realm of our lab's expertise without their willingness to help.

Finally, thank you to my friends and family. I can't emphasize enough how much it has meant to me to have been surrounded by so much love and support. I would

especially like to thank my parents, Jerry and Sharon Schulte, for their consistent encouragement and belief in me even when I doubted myself. I hope it goes without saying that I know I wouldn't have reached this point without them. Finally, I can never thank my husband, Corey, enough for his love and support. He has been the one person who has been there on a daily basis to encourage me and support me in any way needed. I look forward to sharing this accomplishment with him and our future together.

TABLE OF CONTENTS

LIST OF FIGURES

CHAPTER 1

CHAPTER 2

CHAPTER 3

CHAPTER 4

Chapter 1

Introduction

1.1 Unrestrained growth: a hallmark of cancer

There is no precise formula that drives a normal cell to become neoplastic. However, there are certain characteristics common among cancerous cells that have been described by Hanahan and Weinberg as the hallmarks of cancer. The founding hallmark capabilities include the ability to sustain proliferative signaling, evade growth suppressors, activate invasion and metastasis, enable replicative immortality, induce angiogenesis, and resist cell death (Hanahan and Weinberg, 2000). A decade later, additional hallmarks have been added to the original six, including reprogramming of energy metabolism and evading immune destruction. It is now also clear that genetic alterations largely underpin the ability of normal cells to acquire these characteristics. Furthermore, we must not only consider the individual cell but also the surrounding cells and tissues, known as the tumor microenvironment (Hanahan and Weinberg, 2011). My dissertation largely centers around two of the original cancer hallmarks: the ability to sustain proliferative signaling and the ability to evade growth suppression. Throughout this introduction, I will focus on cell growth (i.e. protein translation) as an essential and distinct component of proliferation. It will be important to remember that growth is just as necessary to proliferation as is the completion of mitosis; for without an increase in cell mass, daughter cells would become progressively smaller until they conceivably become nonfunctional and die.

Instructing a cell to grow via mTOR

In a normal cell, growth is only initiated when the proper nutrients and signals are present. The target of rapamycin (TOR) is a cellular sensor for signals that instruct a cell to grow. TOR (mTOR in mammals, also known as FRAP, RAFT, RAPT, or SEP) is an

evolutionarily conserved serine/threonine kinase and member of the phosphatidylinositol 3-kinase (PI3K)-related kinase (PIKK) superfamily (Brown et al., 1994; Chen et al., 1994; Chiu et al., 1994; Keith and Schreiber, 1995; Sabatini et al., 1995; Sabers et al., 1995). As its name suggests, TOR is bound by the bacterial compound rapamycin (Sehgal, 2003). In mammals, the binding of rapamycin to its target suppresses proliferation, emphasizing the importance of the mTOR pathway in regulating this process. To promote growth, mTOR shuttles from the cytoplasm to the nucleus, where it regulates two major proteins involved in translation: S6 kinase 1 (S6K1) and 4E-BP1 (eukaryotic initiation factor 4E (eIF4E)-binding protein, also known as PHAS-1) (Kim and Chen, 2000).

Phosphorylation of S6K1 by mTOR results in the subsequent phosphorylation of 40S ribosomal protein S6 (Jeno et al., 1988). It has been suggested that the phosphorylation of S6 is important for the enhanced translational efficiency of 5'-TOP (terminal oligopyrimidine)-containing mRNAs (Jefferies et al., 1997; Jefferies et al., 1994; Terada et al., 1994). Importantly, many components of the translational machinery contain a 5'-TOP sequence, thus the phosphorylation of S6K1 may result in an overall enhancement of protein synthesis. While this is an intriguing hypothesis, it has also been questioned by results demonstrating that S6K1 activity and S6 phosphorylation are dispensable in the upregulation of 5'-TOP mRNA translation. Furthermore, S6K1 is known to have other, albeit less-well studied, substrates that may contribute to enhanced protein synthesis (Fingar and Blenis, 2004; Ruvinsky and Meyuhas, 2006). So, while it is clear the S6K1 is important for cell growth, we do not yet fully understand the mechanism by which it exerts its functions.

In the absence of mTOR activation, 4E-BP1 binds tightly to eIF4E and inhibits its association with eIF4G to prevent the eIF4F complex from forming and thus protein synthesis from occurring. Upon phosphorylation by mTOR, 4E-BP1 releases eIF4E and allows for binding of eIF4E with eIF4G (Marcotrigiano et al., 1999), which is a scaffolding protein that recruits additional members of the initiation complex to promote cap-dependent translation. Clearly, 4E-BP1 and S6K1 are important modulators downstream of mTOR that instruct a cell to grow. As I mentioned above, cell growth is the production of macromolecules, and thus, in the next section I will give an overview of how the machinery for protein synthesis comes together.

The machinery for protein synthesis

Protein translation begins in nucleoli with the production of ribosomes. Nucleoli are composed of three structural regions: the fibrillar center, the dense fibrillar component, and the granular component. RNA polymerase I (Pol 1), HMG1 box architectural upstream binding factor (UBF), and the selectivity complex (SL1, also known as TIF-IB) are located in fibrillar centers, and this is where the transcription of ribosomal DNA (rDNA) occurs. With the exception of the 5S rRNA , all rRNAs all encoded in a polycistronic message (Fatica and Tollervey, 2002). The 5S subunit is separately transcribed by RNA polymerase III. The rRNA is then modified and processed by small nucleolar RNAs (snoRNAs), which guide both 2'-O-methylation and pseudouridylation (with the enzyme dyskerin) of individual nucleotides (Kiss, 2001). Subsequent cleavage by RNases eventually results in the mature ribosomal components. The 18S rRNA combines with ribosomal proteins to form the 40S ribosomal subunit

while the 60S subunit is formed by the joining of ribosomal proteins with 5S, 5.8S, and 28S subunits. The granular component is the site at which preribosomal subunits assemble with ribosomal proteins (Ruggero and Pandolfi, 2003). Finally, the small (40S) and large (60S) ribosomal subunits are ready to be transported to the cytoplasm for protein translation (Figure 1.1).

The ARF tumor suppressor: a sensor and modulator of cell growth

Given the importance of cell growth to tumor progression, it is important to understand the mechanisms by which a cell regulates ribosome production and protein synthesis. The ARF tumor suppressor is a key sensor of signals that instruct a cell to grow and is appropriately localized in nucleoli to limit unrestrained growth. In the following sections, I will introduce the ARF tumor suppressor, explain its known relevance in cancer, and highlight what is known about how it responds to cell growth signals.

1.2 ARF expression

The INK4a/Arf locus: organization and regulation

ARF is encoded on chromosome 9p21 as part of the *CDKN2a*, which includes both *INK4a* and *Arf* (Figure 1.2). The locus also contains *INK4b* (also known as *CDKN2b)*, which lies upstream of *Arf* and *INK4a*. *INK4b* is its own genetic entity, while *INK4a* and *Arf* share two of their three exons (Quelle et al., 1995; Sherr, 2000). It is also worth noting that a non-coding RNA, ANRIL (also known as *CDKN2b* antisense or *CDKN2BAS*), has recently been discovered at the *INK4b-Arf-INK4a* locus. It has been

proposed that ANRIL regulates the expression of the locus (Pasmant et al., 2007). Due to splicing events, unique promoters, and unique first exons, the transcription products of *INK4a* and *Arf* contain distinctive first exons (*INK4a* is encoded by exon 1α and *Arf* is encoded by exon 1β) but identical second and third exons. The two shared exons result in almost 70% sequence homology at the DNA level. However, *Arf* is translated in an alternative reading frame, for which it is named, from that of *INK4a* (Quelle et al., 1995). This results in two proteins that are distinctive following translation.

Both $p15^{INK4b}$ and $p16^{INK4a}$ bind and inhibit the cyclin-dependent kinases, CDK4 and CDK6 (Serrano et al., 1993; Sharpless, 2005). These kinases are important for the hyperphosphorylation of the retinoblastoma (Rb) tumor suppressor. When CDK4/6 are inhibited by $p15^{INK4b}$ and $p16^{INK4a}$, Rb is in a hypophosphorylated state, allowing it to bind and inhibit transcription factors of the E2F family (Sherr, 1996). Thus, $p15^{INK4b}$ and $p16^{INK4a}$ effectively halt the progression from G1 to S in the cell cycle. The first discovered role for ARF was also in regulating cell cycle progression as I will discuss further in the next section.

Regulating the Arf locus

Under normal conditions, it is important to keep *Arf* (and other members of the locus) repressed. This is primarily accomplished by polycomb repressive complexes (PRC). Generally speaking, the PRC2 complex first specifically methylates histone H3 at lysine 27, a process catalyzed by EZH2. The chromatin mark is then recognized by PRC1, which subsequently ubiquitinates histone H2A (Cao et al., 2002; Wang et al., 2004). The importance of this process in repressing *Arf* is evident by studies

demonstrating that overexpression of polycomb group (PcG) members retards senescence (Dietrich et al., 2007; Gil et al., 2004; Jacobs et al., 1999). In the case of Bmi-1 (a PcG member) overexpression, mouse embryonic fibroblasts (MEFs) become immortalized in culture. Furthermore, *bmi-1*$^{-/-}$ MEFs have heightened levels of ARF (and p16^{INK4a}) and are unable to enter S phase (Jacobs et al., 1999) . Upon oncogenic stress, it is important that a cell quickly be able to respond by upregulating the expression of ARF. This seems to be accomplished by a coordination of various factors and the exact mechanism may be different for different types of tissues or dependent upon the type of stress. For example, the expression of the methylating protein EZH2 can be downregulated (Bracken et al., 2007). Histone H3 can also be demethylated by demethylase enzymes such as JMJD3, which is upregulated in response to oncogenic Ras (Agger et al., 2009; Barradas et al., 2009). Finally, in selective tissues, oncogenic stress can cause the derepression of *Arf* by upregulating members of the chromatin remodeling SWI/SNF complex (Young and Jacks).

Arf loss in cancer

Mice containing individual loss of each of the three aforementioned genes have revealed that all are important in tumor suppression. p16^{INK4a} and ARF have synergistic tumor suppressive functions as mice containing loss of both are more tumor prone than those with the loss of only one or the other (Sharpless et al., 2004). Given the scope of my work, I will focus on alterations to *Arf* in cancer.

In order to specifically determine the role of *Arf* in tumor suppression, Sherr and colleagues selectively disrupted exon 1β in mice. These mice began developing tumors as

early as 8 weeks. After one year, 80% of the mice had died from spontaneous tumor development, with a mean survival latency of 38 weeks. Heterozygous mice also developed tumors, albeit after a longer latency compared to *Arf*$^{-/-}$ mice. Upon examination of *Arf*$^{+/-}$ mice, it was noted that tumor formation was accompanied by loss of the remaining allele. The tumor spectrum in *Arf*$^{-/-}$ mice included sarcomas (43%), lymphoid malignancies (29%), carcinomas (17%), and tumors of the nervous system (11%) (Kamijo et al., 1999). Consistent with this data is the work showing that mouse embryonic fibroblasts taken from *Arf*$^{-/-}$ mice are immortal and transformed upon the ectopic expression of oncogenic Ras (Kamijo et al., 1997). Furthermore, as wild-type cells are passaged, the expression of ARF increases, implying a role for ARF in limiting the proliferation of cultured cells.

In human cancers, one of the most frequent cytogenetic events is the homozygous loss of the *INK4b-Arf-INK4a* locus. In fact, the frequency of mutation at this locus is second only to the *p53* locus (Hainaut et al., 1997; Hall and Peters, 1996). In most cases of human cancer, all three proteins of the *INK4b-Arf-INK4a* locus are lost, making it difficult to determine their individual roles in human tumor suppression. However, there are specific examples in which only *Arf* appears to be affected in human cancer, and these cases appear to be most common in melanoma patients. Gene deletions in family with melanoma-neural system tumor syndrome have been shown to occur specifically in exon 1β (Randerson-Moor et al., 2001). Deletion of exon 1β has also been reported in members of a family predisposed to melanoma (Laud et al., 2006). In addition to melanoma cases, it has been reported that nine of fifty glioblastoma patients had specific deletion of *Arf* (Nakamura et al., 2001). Aside from deletions, mutations of exon 1β that

impair ARF function have been reported in a case of melanoma (Rizos et al., 2001). Furthermore, the *Arf* promoter contains a CpG island, and ARF expression can consequently be downregulated by promoter methylation (Robertson and Jones, 1998) (Furonaka et al., 2004; Kominami et al., 2009; Konishi et al., 2002; Melendez et al., 2000; Zemliakova et al., 2004; Zheng et al., 2000).

Arf transcription and translation

Arf transcription is upregulated in response to a host of oncogenic signals including c-Myc, Ras, E2F-1. E1A, and v-Abl (Sherr, 2001) . Perhaps the two most well-studied of these events, upregulation by c-Myc and Ras, were directly demonstrated *in vivo* using a construct in which GFP is controlled by the *Arf* promoter (Zindy et al., 2003). Given that oncogenic Ras plays an integral role in regulating cell growth, I will focus my attention on the upregulation of *Arf* transcription by Ras^{V12}. Research into the transcriptional regulation of *Arf* was initiated by searching the promoter for known binding sites of transcription factors. The *Arf* promoter contains a binding site for the DMP1 (cyclin D-binding Myb-like protein) transcription factor, namely a nonameric DNA consensus sequence containing G-G/T-A cores (Hirai and Sherr, 1996). The DMP1 transcription factor was a likely candidate for *Arf* regulation given that it is known to arrest mouse fibroblasts upon overexpression, and human *DMP1* is frequently deleted in myeloid leukemia (Bodner et al., 1999; Inoue and Sherr, 1998). In 1999, Inoue and colleagues demonstrated that DMP1 binds and activates the *Arf* promoter. Moreover, infection of wild-type MEFs with DMP1 induces ARF expression and a cell cycle arrest. Importantly, in the absence of *Arf*, DMP1 overexpression had no effect on the cell cycle,

indicating that DMP-1-induced arrest is dependent upon ARF (Inoue et al., 1999). Subsequent studies have now shown that DMP1 is a key mediator of Ras-induced ARF expression (Sreeramaneni et al., 2005). Until recently, ARF induction downstream oncogenic Ras has largely been considered a transcriptionally-activated process. However, Miceli and colleagues have demonstrated that Ras^{V12} can induce ARF levels in the absence of *Dmp1*. By signaling through the Ras/PI3K/TSC/mTOR pathway, this induction in *Dmp1*-null cells occurs in the absence of enhanced ARF mRNA levels (Miceli et al., 2011). Taken together, we now know that ARF is upregulated both transcriptionally and translationally in response to oncogenic Ras to induce cell cycle arrest.

ARF's structure, cellular location, and stabilization

The structure of ARF is important to consider when studying the protein's localization, stabilization, and binding partners. Mouse ARF ($p19^{ARF}$) contains 169 amino acids, while human ARF ($p14^{ARF}$) contains 132. Of this relatively small protein, nearly 20% of the residues are arginines, making ARF a highly basic protein. The basic nature of ARF renders it highly insoluble and is likely the reason for its lack of structure. Moreover, this property also renders ARF a very "sticky" protein, which makes it difficult to discern which of its proposed binding partners are physiologically relevant. It is likely that ARF requires consistent binding with another protein to bring its charge to a more neutral pH in order to function *in vivo* (Ozenne et al.; Quelle et al., 1995; Sherr, 2006). In fact, owing to a nucleolar localization signal, ARF is typically found within nucleoli bound in high molecular weight complexes with other proteins (Bertwistle et al.,

2004) . In consideration of ubiquitination on lysine residues, it is interesting that mouse ARF contains only one lysine (Lys26) while human ARF has none. ARF has a half-life of about 6h, at which point it is degraded by ubiquitin-mediated proteasomal degradation. However, studies have shown that the ubiquitin moiety is not added to the sole lysine in mouse ARF as removal of that lysine still results in ARF's degradation. Instead, both mouse and human ARF undergo N-terminal ubiquitination, which signals them for destruction (Kuo et al., 2004).

1.3 p53-dependent ARF tumor suppression

ARF's classical role as a tumor suppressor is to activate p53. Given that p53 is the most commonly mutated gene in human cancers, this is clearly a significant role of ARF. p53 can induce both cell cycle arrest and trigger apoptosis in response to oncogenic stimulation, DNA damage, and other cellular stressors. p53 exerts its functions by transactivating target genes such as p21 and PUMA. Interestingly, another target of p53 transactivation is its own negative regulator, murine double minute 2 (MDM2, HDM2 in humans) (Sherr and Weber, 2000). In the absence of cellular stress, p53 is bound by MDM2. When MDM2 is bound to p53, p53 is physically unable to bind to target genes and exert its function as a transcription factor (Momand et al., 1992; Oliner et al., 1993). MDM2 also results in the nuclear export and eventual proteasomal degradation of p53 (Roth et al., 1998). Furthermore, MDM2 contains a RING domain, allowing it to act as an E3 ubiquitin ligase and contribute to the ubiquitination of p53 (Haupt et al., 1997; Honda et al., 1997; Kubbutat et al., 1997). The importance of the MDM2-p53 interaction

is underscored by work demonstrating that *mdm2-/-* mice are embryonic lethal but can be rescued by concomitant deletion of *p53* (Jones et al., 1995).

When prompted by oncogenic signals such as Ras^{V12} (Palmero et al., 1998) or Myc overexpression (Zindy et al., 1998), ARF is upregulated. ARF then binds MDM2 via amino acids 1-14 and sequesters it in the nucleolus (Weber et al., 1999). The residues important for the nucleolar localization of ARF are also within the first 37 residues of exon 1β, and only these residues are necessary for fully functional ARF (I will later discuss other roles of these residues). MDM2 likely also contributes to the nucleolar localization of the complex as binding to ARF reveals MDM2's nucleolar localization signal (Lohrum et al., 2000). Nucleolar localization prevents the binding of MDM2 to p53 and the ability of MDM2 to shuttle between the nucleus and cytoplasm, thereby impeding its ability to transport p53 to the cytoplasm for degradation (Tao and Levine, 1999). As is the case for *Mdm2*, *Arf* is a transcriptional target of p53, adding to the negative feedback loop of p53 activation (Stott et al., 1998).

The importance of the ARF-MDM2 interaction is highlighted by studies demonstrating that oncogenic insult is incapable of inducing p53 responses when ARF is lost (Kamijo et al., 1997; Palmero et al., 1998). This suggests that ARF activity could be mimicked by generating therapeutics to inhibit MDM2 in p53-positive cancers. A synthetic class of molecules, called nutlins, was perhaps the most promising of MDM2 inhibitors, especially in the absence of ARF. They free p53 from MDM2's negative regulation via binding a hydrophobic pocket of MDM2 that is critical for its interaction with p53 (Vassilev et al., 2004). Initially, nutlins seemed as though they would be a successful cancer therapy; upon nutlin treatment, p53-positive cancer cells either became

senescent or underwent apoptosis. Nutlins also seemed promising *in vivo* when they were successfully used to reduce tumor xenograft growth in mice (Vassilev et al., 2004). Unfortunately, it became evident that nutlins would be too toxic due to prolonged p53 activity. The embryonic lethality of *Mdm*-2 mice supported this theory. When considering that p53/*Mdm2*-null mice are viable, the *Mdm2*-null phenotype indicates that unchecked p53 is deleterious during development (Jones et al., 1995; Montes de Oca Luna et al., 1995). Furthermore, when p53 activity was conditionally upregulated in *Mdm2*-null mice, the mice died within 1 week (Ringshausen et al., 2006). While this data was unfortunate, it may have heightened the interest in identifying other, p53-independent targets of the ARF tumor suppressor that could lead to additional therapeutic targets in the absence of functional ARF.

1.4 p53-independent functions of ARF

It was not initially clear that ARF tumor suppression went beyond the scope of p53. The first clue presented when mice were engineered to overexpress *c-Myc*. These mice developed B-cell lymphomas with a mean survival of 6 months (Eischen et al., 1999). It was previously known that oncogenic c-Myc activates the p53-MDM2-ARF pathway in culture (Zindy et al., 1998). Therefore, the authors examined this pathway in the mouse tumors. As may have been expected, a number of tumors either displayed *p53* mutation, biallelic *Arf* loss, or MDM2 overexpression. Interestingly, some tumors also presented either *p53* mutations or biallelic *Arf* loss in conjunction with MDM2 overexpression (Eischen et al., 1999), which could be interpreted as MDM2 having p53-independent tumor suppressive properties. However, it was also suggested that ARF may

have p53-independent tumor suppressive functions based on this data. In 2000, Weber *et al.* published their results of genetically engineered mice that were nullizygous for *p53*, *Mdm2*, and *Arf* (known as triple knock-out, or TKO, mice). When compared to mice lacking either *p53* or *Arf* alone, mice lacking both *p53* and *Arf* (with or without loss of *Mdm2*) displayed a wider tumor spectrum and an increase in the number of primary tumors (Weber et al., 2000). If ARF only exerted its tumor suppressive functions through p53, we would have expected the TKO mice to display the same types of tumors as *p53*-null mice. Furthermore, the results demonstrated that MDM2 antagonizes the p53-independent tumor suppressive functions. Ectopically expressed ARF was unable to arrest *p53/Arf*-null MEFs. However, ARF was able to rescue to these cells with concomitant deletion of *Mdm2*. This phenomenon was explained by results showing that an *Arf* mutant lacking amino acids 1-14, which are necessary for ARF's ability to bind MDM2, are required for ARF to arrest TKO cells. In other words, ARF is unable to arrest *p53/Arf*-null cells in the presence of antagonistic MDM2. Moreover, the amino terminal 14 amino acids of ARF are necessary for both its p53-dependent and -independent tumor suppressive functions. In future sections, I will touch upon some of the reported ARF-interacting proteins that have emerged since the genetic evidence of p53-independent ARF tumor suppression was presented.

Arf-interacting proteins beyond the realm of p53-dependent tumor suppression

In 2006, at least 30 proteins had been reported to interact with ARF (Sherr, 2006). For a majority of the reported ARF-interacting partners, it is still too early to determine whether their interaction is physiologically relevant, partially due to the promiscuity of

ARF's binding. Interestingly, ARF is known to interact with another E3 ubiquitin ligase aside from MDM2: ARF-BP1. ARF-BP1 contains a HECT domain and has been shown to ubiquitinate p53. When bound to ARF, the ubiquitin ligase activity of ARF-BP1 is inhibited (Chen et al., 2005). ARF is also known to interact with DP1, a binding partner of the E2F family of transcription factors. The ARF-DP1 interaction inhibits the ability of DP1 to activate the *dhfr* gene, which promotes cell cycle arrest (Datta et al., 2005). ARF has also been shown to interact with MYC. Two studies were simultaneously published that demonstrated the ability of ARF to block transcriptional activation by MYC in a p53-independnet manner (Datta et al., 2004; Qi et al., 2004). One group further reported that ARF exerts this function by sequestering MYC in the nucleolus (Datta et al., 2004). UBC9 is another ARF-interacting protein (Rizos et al., 2005). UBC9 is a SUMO conjugating enzyme that is of particular interest given recent reports demonstrating the ability of ARF to promote protein sumoylation. Finally, I will highlight the ARF-NPM interaction in forthcoming sections of this chapter as NPM is an important component of my dissertation.

The relationship between ARF and NPM

One of the most well-studied and relevant ARF-interacting proteins is nucleophosmin (NPM; also known as B23, numatrin, and NO38). NPM was first identified as an ARF-interacting protein by four independent laboratories, all of which reported slightly different stories on the physiological function of the interaction. Itahana and colleagues reported that ARF-binding induces the ubiquitination and proteasomal degradation of NPM (Itahana et al., 2003). This theory is somewhat tantalizing given

that, at the time, ARF had published roles in inhibiting ribosomal RNA processing (Sugimoto et al., 2003) while others had already published that NPM promotes this process (Savkur and Olson, 1998). So, the authors suggested that their data provided the mechanism by which ARF negatively regulates NPM's pro-growth properties (Itahana et al., 2003). However, none of the other laboratories were able to reproduce the ubiquitination and subsequent degradation of NPM by ARF. A few months later, Bertwistle and colleagues reported that ARF interacts with NPM using the same amino-terminal 14 amino acids that are required for its interaction with MDM2. Furthermore, they suggested that NPM's interaction with ARF compromises ARF's ability to prevent ribosomal processing (Bertwistle et al., 2004). Brady and colleagues proposed a model in which ARF binds NPM, and inhibits its shuttling from the nucleus to the cytoplasm, resulting in cell cycle arrest. Their data went on to verify that amino acids 1-14 of ARF were necessary for binding NPM as an ARF mutant lacking this domain (ARF Δ1-14) did not coimmunoprecipitate NPM (Brady et al., 2004). Furthermore, the ARF-NPM is MDM-2-sensitive as reintroduction of MDM2 releases NPM from ARF (Brady et al., 2004). The final group again verified that ARF's interaction with NPM was dependent upon its first 14 amino acids. However, they suggest that the interaction is important to prevent ARF from exerting its p53-*dependent* tumor suppressive functions (Korgaonkar et al., 2005). This data is in direct contrast to the aforementioned results that demonstrated a preferential binding of ARF to MDM2. If we can gather one thing from the four individual reports, it is that NPM is a bona fide interaction partner of ARF. Given this interaction and that my work has centered on the p53-independent growth

regulatory properties of ARF, I will now focus on what we have since learned about NPM in promoting cell growth.

NPM and cell growth

NPM is a highly conserved 37kDa phosphoprotein. Although originally described as a nucleolar resident, NPM is capable of shuttling between the nucleoplasm and cytoplasm (Kang et al., 1974; Kang et al., 1975), a function that is important for ribosome export as will be discussed later. NPM is highly expressed under basal conditions, and its expression is exacerbated upon mitogenic stimulation. Work from our lab has shown that oncogenic Ras signals through mTOR to upregulate the translation of NPM (Pelletier et al., 2007). Furthermore, the upregulation of NPM protein was independent of changes at the mRNA level (Pelletier et al., 2007). Olanich and colleagues have since shown that the 3'-UTR of NPM is sufficient to mediation upregulated translation through mTOR (Olanich et al.). Both studies have additionally demonstrated that the translational upregulation of NPM via mTOR results in higher rates of protein synthesis and enhanced proliferation in the absence of *p53* (Olanich et al.; Pelletier et al., 2007). Furthermore, NPM is progrowth as its overexpression has been shown to increase cell size in $Arf^{-/-}$ MEFs and transform $p53^{-/-}$ MEFs in soft agar (Brady et al., 2009). *Npm1*-null mouse models have demonstrated the importance of NPM in the maintenance of cell growth and proliferation as they are embryonic lethal (Grisendi et al., 2005). Furthermore, in highly proliferative and tumorigenic cells, NPM expression is elevated compared to normal cells. These data were some of the first to suggest a role for NPM in regulating cell growth and proliferation (Borer et al., 1989; Yun et al., 2003). Since then, multiple

groups have reported that NPM is overexpressed in a variety of human tumors (Bernard et al., 2003; Brady et al., 2009; Nozawa et al., 1996; Shields et al., 1997; Skaar et al., 1998; Subong et al., 1999; Tanaka et al., 1992; Tsui et al., 2004). On the other hand, NPM expression is known to be reduced in a number of human cancers as a result of either gene deletion or genetic alterations. Considering this data alone, it is not surprising that NPM has been ascribed both oncogenic and tumor suppressive roles (Grisendi et al., 2006). In future sections, I will largely focus on oncogenic NPM as it is directly related to NPM's role in ribosome biogenesis and cell growth.

NPM's nucleocytoplasmic shuttling is CRM-1 dependent and required for the export of ribosomal components (Borer et al., 1989; Maggi et al., 2008; Yu et al., 2006). Ribosomal protein L5 (rpL5) is a chaperone for the 5S rRNA and the first reported component of the ribosomal machinery to be exported by NPM (Yu et al., 2006). In this study, the authors created a shuttling-deficient mutant of NPM, in which two leucines within the nuclear export sequence of NPM were mutated to alanines. The mutation completely abrogated the nucleocytoplasmic shuttling ability of NPM, blocked the export of both rpL5 and 5S rRNA, and ultimately resulted in cell cycle arrest (Yu et al., 2006). In an effort to determine if NPM interacted with other components of the ribosome machinery, Maggi *et al.* generated a polyclonal NPM affinity column. Their efforts resulted in a list of 10 components of the 40S and 60S subunits and an additional 9 proteins known to be important in translation (Maggi et al., 2008). NPM was also demonstrated to be required for protein synthesis by use of the shuttling-deficient mutant as well as siRNA-mediated kncokdown of NPM (Maggi et al., 2008). Furthermore, the importance of NPM's role in shuttling ribosomal components out into the cytoplasm is

highlighted by electron micrographs of the nuclear/cytosol boundary from *Npm* $^{hy/hy}$ (hypomorphic NPM alleles that express nearly undectectable levels of NPM) (Grisendi et al., 2005) MEFs, where one can clearly see the accumulation of ribosomes along the inside perimeter of the nucleus (Maggi et al., 2008). NPM mutations in acute myeloid leukaemia underscore the importance of NPM's shuttling function (Falini et al., 2005). The NPM mutation causes a frameshift that results in an additional NES and concomitant loss of NPM's nucleolar localization motif (Bolli et al., 2007; Falini et al., 2006). These changes result in the cytoplasmic localization of NPM and thus, this mutant has been designated NPM cytoplasmic positive or NPMc+. Cheng and colleagues subsequently demonstrated that NPMc+ is an oncogene in that it can transform mouse embryonic fibroblasts in cooperation with E1A in soft agar assays (Cheng et al., 2007). Cheng *et al*. went on to show that oncogneic potential of NPMc+ was relevant *in vivo* by creating transgenic mice that express the NPMc+ mutant. The mutant mice developed myeloproliferation in bone marrow and spleen whereas expression of wild-type NPM did not result in disease (Cheng et al.). This NPM mutation also brings forth an important aspect of the ARF-NPM interaction. NPM has been demonstrated to maintain the stability of ARF within the nucleolus (Colombo et al., 2005; Colombo et al., 2006; Korgaonkar et al., 2005). In fact, the NPMc+ mutant takes ARF along as it aberrantly shuttles to the cytoplasm, which reduces the stability of ARF and interferes with both p53-dependent and p53-independnet tumor suppressive functions of ARF (Colombo et al., 2006; den Besten et al., 2005). Given the importance of the ARF-NPM interaction in cell growth, I will outline future experiments in Chapter 4 to determine the role of NPM in post-mitotic cells.

1.5 What is basal ARF doing?

While ARF is primarily recognized as a protein upregulated in the face of oncogenic distress, there has been recent data suggesting important roles for basal ARF. It is becoming increasingly clearer that even thought ARF is nearly undetectable in many cells lines, it plays an integral role based on studies analyzing the effects of its loss. This emerging field is of particular importance to my project as we have studied the effects of basal *Arf* loss during osteoclastogenesis. In this section, I will cover the known roles of basal ARF in regulating mouse eye development, male germ cell production, and protein synthesis. In the following section, I will discuss what we know about the role of basal ARF in osteoblasts.

The role of ARF in mouse eye development

Initially, $Arf^{-/-}$ mice seemed developmentally normal despite the fact that their eyes were slightly smaller compared to the eyes of wild-type mice (Kamijo et al., 1999; Kamijo et al., 1997; McKeller et al., 2002). Upon closer examination, McKeller and colleagues noticed that $Arf^{-/-}$ mice had a funnel-shapped mass of cells in the vitreous of their eyes just behind the lens. During postnatal day 1 through 10, this mass of cells is present and at least some of the cells are dividing. Although the authors did not notice an increase in the overall size of the cell mass as the mice aged, they did record its presence through 8 months of age. Notably, this retrolental mass of cells was not present in wild-type or $Arf^{+/-}$ mice (McKeller et al., 2002). Wild-type mice are born with elements of the hyaloid vascular system (HVS), including endothelial cells, perivascular cells forming the

hyaloid artery, and several other types of perivascular cells that form the structures of the vasa hyaloidea propria (VHP), the tunica vasculosa lentis, which surrounds the lens, and the pupillary membrane. Normally, the HVS will regress by postnatal day 14 (Ito and Yoshioka, 1999). Although the HVS was still present in *Arf*$^{-/-}$ P10 mice, the authors did not detect any cellular components of the HVS by postnatal day 10 in wild-type mice (McKeller et al., 2002). Expression of ARF mRNA was examined in gross sections of the eye and found primarily in the vitreous. Given the localization of ARF and that most of the retrolental mass was centered within the region of the VHP, the authors suggested that ARF might regulate VHP regression (Ito and Yoshioka, 1999). Regression of the HVS, which includes the VHP, is important for normal eye development; failed regression results in a human eye disease known as persistent hyperplastic primary vitreous or PHPV and results in microphthalmia (abnormally small eyes) (Goldberg, 1997; Haddad et al., 1978). *Arf*$^{-/-}$mice were examined for two primary characteristics of PHPV: retrolental fibrovascular tissue lining the inner neuroretina resulting in retinal abnormalities and retrolental fibrovascular tissue that adheres to the posterior of the lens (Haddad et al., 1978). For the most part, the neuroretina and lens of *Arf*$^{-/-}$mice appeared normal through P10. However, beginning at P14, *Arf*$^{-/-}$mice displayed both defects in the neurorentina and the lens, which ultimately results in blindness (McKeller et al., 2002). Importantly, the characteristics of PHPV were not observed in *p53*$^{-/-}$ mice, indicating that the role of ARF in hyaloid vascular regression is independent of p53 (McKeller et al., 2002). To better understand the molecular mechanisms by which ARF regulates HVS regression, Silva and colleagues examined *Arf*$^{Gfp/+}$ mice. In these mice, one allele of *Arf* is replaced by *Gfp*, allowing for a more sensitive means of detecting tissues and cells in

which *Arf* expression occurs *in vivo* (Zindy et al., 2003). Results showed that ARF was expressed in the vitreal perivascular structures between embryonic day 11.5 (E11.5) and E18.5. Postnatally, GFP-positive cells were detected in mural cells expressing Pdgfrβ (Silva et al., 2005). In normal development, endolthelial cells within the vitreal HVS secrete PDGF-β, which then binds to cognate receptors on pericyte-like mural cells to support the developing lens (Gerhardt and Betsholtz, 2003; Ito and Yoshioka, 1999; Lindahl et al., 1997; Zhu et al., 1999). We now know that ARF regulates the proliferation of pericyte-like mural cells that express the PDGF-β receptor; and without ARF, these cells abnormally proliferation, resulting in lack of complete HVS regression, and ultimately, blindness (Gromley et al., 2009; Silva et al., 2005).

The role of ARF in male germ cell development

In addition to ARF expression within the eye, the $Arf^{Gfp/+}$ mice also revealed expression of ARF in one other normal cell: male spermatogonia (Zindy et al., 2003). Using a more sensitive system that is capable of detecting transient expression of ARF, Gromey and colleagues confirmed ARF's presence during male germ cell development (Gromley et al., 2009). In mice, spermatogenesis occurs within the first month of life. Spermatogonia are cells that line the basement membrane of each seminiferous tubule; these are the cells that express ARF (Gromley et al., 2009). Spermatogonia will enter meiosis I, moving toward the lumen of the tubule as they progress, during P7-P10. During this stage the cells are known as spermatocytes and undergo homologous recombination between homologous chromosomes. By P18, meiosis I is complete and the spermatocytes move directly into meiosis II to form haploid cells. Spermatogenesis is

complete once the spermatocytes differentiate into mature spermatozoa around P35 (Cole et al.) *Arf*$^{-/-}$ mice have reduced sperm number compared to that in wild-type mice due to an increase in apoptosis during germ cell development (Churchman et al.; Cole et al.). Notably, there was no increase in the proliferation of spermatogonia during germ cell development upon *Arf* loss (Churchman et al.). While the apoptosis of these cells is dependent upon p53, the functions of ARF that regulate apoptosis are independent of p53. Cells void of *Arf* display increased levels of phosphorylated histone H2AX (Churchman et al.). H2AX is normally phosphorylated at the leptene stage of meiosis, but disappears by early pachytene upon synapsis of homologous chromosomes (Inagaki et al.; Mahadevaiah et al., 2001). Thus far, the data suggest that persistent phosphorylated H2AX signals cells for apoptosis, although this has not been convincingly demonstrated. Importantly, deletion of *p53* was unable to rescue the defect in H2AX phosphorylation (Churchman et al.). Taken together, this role of ARF in male germ cell development is counterintuitive given what we already know about the ARF-p53 interaction; ARF actually *prevents* p53 from inducing apoptosis in primary spermatocytes (Churchman et al.).

Basal ARF regulates nucleolar structure and function

Given the nucleolar localization of ARF and its interaction with NPM, Apicelli and colleagues examined the role of basal ARF in maintaining nucleolar structure and limiting protein synthesis (Apicelli et al., 2008). *Arf* loss resulted in an increase in both the number and size of AgNORs in mouse embryonic fibroblasts (MEFs) (Apicelli et al., 2008). AgNORs highlight argyrophilic proteins that surround nucleoli. An increased

AgNOR index has classically been associated with poor prognoses in cancer (Pich et al., 2000) and, thus, this data suggested that ARF maintains the structure and likely function of proteins within nucleoli. This data was corroborated by *in situ* AgNOR staining on tissues from *Arf*$^{-/-}$ mice. Both intestine and liver tissue exhibited an increase in total AgNOR area in the absence of *Arf* (Apicelli et al., 2008). In low-passage MEFs, *Arf* loss also enhances protein synthesis as assessed by ^{35}S-methionine incorporation, resulting in a increase in both protein content and cell volume (Apicelli et al., 2008). Importantly, enhanced protein synthesis in these cells was shown to be independent of proliferation as the total cell number did not increase over 7 days. Again, the increases in protein synthesis upon *Arf* loss was supported by *in vivo* results demonstrating that *Arf* loss in liver tissue also causes an increase in protein synthesis by ^{35}S-methionine incorporation (Apicelli et al., 2008). To determine if enhanced protein synthesis could, at least partially, be attributed to an increase in protein output, Apicelli and colleagues isolated cytosolic fractions from WT and *Arf*$^{-/-}$ MEFs, ran the fractions over a sucrose gradient, and monitored the RNA absorption. An increase in ribosome output upon *Arf* loss was observed *in vitro* and supported by identical experiments done using liver tissue from *Arf*$^{-/-}$mice (Apicelli et al., 2008). Together, this data demonstrates that basal *Arf* loss profoundly enhances cell growth in mitotic cells over time. To determine if acute *Arf* loss would have the same effects on mitotic cell growth, Apicelli and colleagues knocked down ARF by lentiviral transduction with an shRNA against exon1β. Again, the authors observed an increase in the number of AgNORs upon *Arf* loss as well as an increase in total AgNOR area (Apicelli et al., 2008). In fact, these changes were even more pronounced than those observed with chronic loss of *Arf*, which suggests that cells with

chronic *Arf* loss may have a means in which to compensate and control nucleolar morphology. Acute *Arf* loss also resulted in enhanced protein synthesis and ribosome output (Apicelli et al., 2008). Taking a step back in the production of ribosomes, the authors examined the transcription of rDNA and the processing of rRNA given that previous studies had demonstrated a role for ARF in both of these processes (Ayrault et al., 2006; Ayrault et al., 2004; Qi et al., 2004; Sugimoto et al., 2003). Furthermore, it is conceivable that ARF could simultaneously dampen multiple aspects of ribosome biogenesis as serial immunoprecipitation experiments have shown that only some of the ARF protein in the cell is bound to NPM (Apicelli et al., 2008). Loss of *Arf* resulted in a significant increase in newly transcribed 47S transcripts as demonstrated by quantitative RT-PCR, a result that was independent of shRNA-mediated knockdown of Myc. The data further suggests that *Arf* loss results in enhanced processing of the newly transcribed 47S rRNA, which supports previous findings (Apicelli et al., 2008; Sugimoto et al., 2003). Specifically, in accordance with previously published data from Sugimoto and colleagues, the data suggested that ARF impedes processing of the 47S rRNA into the 32S rRNA intermediate (Apicelli et al., 2008; Sugimoto et al., 2003). The final step of ribosome biogenesis is the export of the ribosomal subunits. By radioactively labeling the rRNA subunits with ^{3}H-methyl methionine, it was demonstrated that *Arf*$^{-/-}$ MEFs export ribosomal subunits into the cytoplasm at a faster rate than that observed in wild-type cells (Apicelli et al., 2008). This result is in accordance with previously published data showing that ARF interacts with NPM, which is known to be important for shuttling ribosomes from the nucleus to the cytoplasm (Maggi et al., 2008; Pelletier et al., 2007; Yu et al., 2006). Importantly, Apicelli and colleagues made the point that the enhanced

export of ribosomes is not solely reflective of the fact that *Arf* loss enhances the transcription and processing of rRNA; instead, *Arf* loss amplifies each of the three steps in ribosomal biogenesis: transcription, processing, and export (Apicelli et al., 2008). Finally, the authors used shRNA-mediated knockdown of NPM to determine if the enhanced protein synthesis observed in $Arf^{-/-}$ MEFs was due to unrestrained NPM activity. Upon testing the three steps in ribosomal biogenesis, it was determined that unrestrained NPM activity could explain the enhanced export of ribosomal subunits upon *Arf* loss. Furthermore, knockdown of NPM in $Arf^{-/-}$ MEFs brought overall rates of protein synthesis back to levels observed in wild-type cells (Apicelli et al., 2008). Taken together, the work from Apicelli and colleagues, in association with other groups, suggests that basal ARF limits the amount of protein synthesis in mitotic cells by impeding multiple steps of ribosome biogenesis (Figure 1.3).

1.6 Modeling proliferation-independent growth

Given the aforementioned role of basal ARF in regulating ribosome biogenesis and protein synthesis, Apicelli and colleagues initiated the study of ARF in osteoclasts. The goal of this work was to demonstrate the physiological relevance of ARF's growth control. The osteoclast is a unique model in which to focus on cell growth regulation because they require protein synthesis to differentiate and be fully functional, and they are post-mitotic in their mature state. Before discussing the results of this initial study, I would first like to review osteoclast differentiation and the features of mature osteoclasts.

Osteoclast differentiation

Osteoclasts are the bone resorbing cells of the body. They are essential for normal bone turnover or remodeling as evidenced by skeletal diseases such as osteoporosis that occur when they dysfunction. Skeletal diseases may also result due to enhanced or delayed differentiation of osteoclasts. Osteoclasts are derived from the monocyte/macrophage family in the hematopoietic lineage (Coccia et al., 1980). The use of animal models has revealed important factors during osteoclastogenesis (Figure 1.4). The earliest known transcription factor important for osteoclastogenesis is PU.1. In the absence of *PU.1*, mice do not generate bone marrow macrophages resulting in osteopetrosis (Henkel et al., 1996; Scott et al., 1994; Tondravi et al., 1997). PU.1 is important for the transcription of lineage-specific cytokine receptors including the macrophage colony-stimulating factor (M-CSF) receptor, c-fms (Singh et al., 1999) and the receptor activator of NF-κB (RANK) (Kwon et al., 2005). In conjunction with other transcription factors, PU.1 also induces the transcription of two of the most well-characterized OC-specific target genes: *Cathepsin K* and *tartrate-resistant acid phosphatase (TRAP)* (Matsumoto et al., 2004; Partington et al., 2004). Clearly, PU.1 is important throughout osteoclast development, which explains why its levels nearly triple during osteoclastogenesis (Tondravi et al., 1997). Another early transcription factor that collaborates with PU.1 is MITF, which is encoded by the *microphthalmia (mi)* locus. Loss of *Mitf* results in osteopetrosis as a result of inadequate osteoclasts (Hershey and Fisher, 2004). This is due to the fact that MITF is necessary for the transcription of essential osteoclast genes including *TRAP* and *carbonic anhydrase II (CAII)* (Luchin et

al., 2000; Luchin et al., 2001). However, *Mitf*-null mice do form macrophages, placing MITF downstream of PU.1 in osteoclastogenesis (Thesingh and Scherft, 1985).

M-CSF, which is expressed by osteoblasts, plays a pivitol role in osteoclastogenesis. M-CSF-deficient (*op/op*) mice are osteopetrotic due to insufficient osteoclasts (Yoshida et al., 1990). M-CSF promotes differentiation, the proliferation and survival of precursors, and cytoskeletal reorganization (Insogna et al., 1997; Sherr et al., 1988; Tanaka et al., 1993; Woo et al., 2002). In order to carry out its functions, M-CSF must bind to its reception, c-Fms. Thus, loss of *c-fms* also results in osteopetrosis in mice as a result of an osteoclast deficiency (Dai et al., 2002). Upon binding to c-Fms, M-CSF exerts a number of downstream intracellular events including the induction of genes necessary for the cell to respond to interleukins and RANKL (Cappellen et al., 2002). In particular, M-CSF upregulates the expression of RANK (Cappellen et al., 2002), which is the receptor for RANKL and the only other cytokine that , together with M-CSF, is required for osteoclast differentiation *in vitro* (Lacey et al., 1998; Yao et al., 2002; Yasuda et al., 1998). Notably, upon binding its ligand, c-Fms autophosphorylates, which leads to the recruitment of adaptor molecules. One of the most well-studied and important of these adaptor proteins is c-Src, which is discussed further in this section (Feng et al., 2002).

Perhaps the most essential component of osteoclastogenesis is RANKL, also known as TNF-related activation-induced cytokine (TRANCE), osteoprotegrin ligand (OPGL), or OC differentiation factor (ODF). As one of the alternative names suggest, RANKL is a member of the tumor necrosis factor (TNF) family. A major discovery in delineating the molecular events promoting osteoclastogenesis came when Suda and

colleagues demonstrated that osteoclast precursors must come in contact with osteoblasts (or their precursors) for osteoclastogenesis to ensue (Udagawa et al., 1990). This finding paved the way for the understanding that RANKL is produced by osteoblasts and then binds to RANK on the surface of macrophages to induce osteoclastogenesis. The importance of this interaction is underscored by the fact that knockout mice of either the ligand or the receptor do not make osteoclasts and are severely osteopetrotic (Dougall et al., 1999; Lacey et al., 1998; Li et al., 2000). RANK activation recruits adaptor molecules of the TNF receptor-associated family (TRAFs) (Darnay et al., 1999; Galibert et al., 1998). TRAFs relay the RANKL signal to activate all three MAP kinase pathways, including ERK, p38, and JNK, as well as PI-3K and NF-κB (Del Fattore et al., 2008). Finally, it is important to note that in addition to advancing osteoclastogenesis, RANKL both induces osteoclast resorption and promotes osteoclast survival (Burgess et al., 1999). One of the most well-characterized and important downstream effectors of RANKL is the transcription factor, nuclear factor of activated T-cells cytoplasmic 1 (NFATc1). NFATc1 belongs to a family of NFAT transcription factors and is the major NFAT found in osteoclasts (Day et al., 2005). Osteoclastogenesis is halted in the absence of NFATc1 (Takayanagi et al., 2002). More importantly, overexpression of NFATc1 can rescue RANKL deficiency, indicating that it is the primary transcription factor downstream of RANKL that is responsible for osteoclast differentiation (Takayanagi et al., 2002). In cooperation with other transcription factors, namely Fos and Jun proteins, NFATc1 induces genes critical for osteoclast function, such as the calcitonin receptor, cathepsin K, and β3 integrin (Crotti et al., 2005; Ikeda et al., 2004; Kim et al., 2005a; Kim et al., 2005b; Matsumoto et al., 2004).

As previously mentioned, NF-κB is one of the primary pathways activated by RANKL. NF-κB is family of five transcription factors that includes p50 (NF-κB1), p52 (NF-κB2), p65 (RelA), c-Rel, and RelB. The Rel domains in each of these proteins allows for dimerization and DNA binding (Thanos and Maniatis, 1995). In the absence of RANKL, NF-κB is bound by IκB proteins, keeping it inactive in the cytosol. Upon RANKL activation, IκB is phosphorylated by IKK (IκB kinase), leading to its degradation. NF-κB is then free to translocate to the nucleus and promote the transcription of OC-specific genes (Thanos and Maniatis, 1995). Without the NF-κB pathway, mice are osteopetrotic as a result of insufficient osteoclastogenesis (Abu-Amer et al., 2001).

In corroboration with NF-κB, AP-1 induces the transcription of genes important for osteoclastogenesis. There are two primary components of AP-1: Fos and Jun proteins (Wagner and Eferl, 2005). RANKL promotes the induction of c-Fos (David et al., 2002). Mice lacking c-Fos do not produce osteoclasts and are therefore osteopetrotic (Grigoriadis et al., 1994; Johnson et al., 1992; Wang et al., 1992). One of the most notable targets of Fos transcription is NFATc1. In fact, overexpression of NFATc1 can rescue loss of Fos (Matsuo et al., 2004). Loss of c-Jun activity also results in deficient osteoclastogenesis and resultant osteopetrosis (Ikeda et al., 2004). As with c-Fos, RANKL stimulation results in the activation of c-Jun (Kim et al., 1999). In summary, RANKL induces the activation of various downstream transcription factors including NFATc1, NF-κB, and AP-1, and results in a cell committed to the osteoclast lineage. In the next section, I will discuss the final steps in becoming a fully functional osteoclast.

The making of a fully functional osteoclast

Once committed to the osteoclast lineage, the initial step in bone resorption is binding the bone. The formation of a tight seal to bone requires integrins. Integrins such as $\alpha_v\beta_3$ bind actin complexes within the osteoclast and proteins in the bone matrix containing RDG (ArgGlyAsp) motifs (Aubin, 1992). *Itgb3*$^{-/-}$ (β_3 integrin-null) mice have an enhanced number of osteoclasts. However, the osteoclasts are unable to resorb bone, resulting in increased bone mass by 4 months of age. Upon closer examination, researchers found that the osteoclasts in these mice do not adhere to bone, have an abnormal cytoskeletal arrangement, and do not form a ruffled border, all of which are important for osteoclast function (McHugh et al., 2000). Src is also an important mediator of these functions, namely cytoskeletal rearrangements and ruffled border formation. Similar to *Itgb3*$^{-/-}$ mice, *Src*$^{-/-}$ mice have adequate numbers of osteoclasts (Soriano et al., 1991). However, they have faulty bone resorption due to defective osteoclast spreading and a reduction in the number of H^+-ATPases at the resorptive front (Boyce et al., 1992). In terms of osteoclast spreading, Src is believed to be important for transmitting signals emanating from the bone matrix and mediated through $\alpha_v\beta_3$ to the cytoskeleton (Teitelbaum and Ross, 2003). Cytoskeletal rearrangements are important for the vesicular trafficking of bone resorptive components to the cell-bone membrane interface, known as the ruffled border. The ruffling of the membrane is formed at the site of active resorption as a result of the insertion of many H^+-ATPases. Hence, without Src to mediate the cytoskeleton and allow for trafficking of the proton pumps, there are fewer H^+-ATPases at the resorptive front and a ruffled border is not formed (Boyce et al., 1992).

The bone matrix is composed of both a mineralized component and an organic component, both of which are resorbed by the osteoclast (Blair, 1998). Importantly, the resorptive lacunae is the area of active resorption and can be locally acidified without affecting the pH of the surrounding area due to the tight seal formed by the aforementioned integrin and actin contacts with the bone. The importance of acidification in bone resorption explains the need for trafficking of many H^+-ATPases to the ruffled border (i.e. the part of the osteoclast membrane contact the resorptive lacunae). A lowered pH (around 4.5) is sufficient to dissolve the mineralized component of the bone. Furthermore, as verified by mouse models, acidification of the resorption lacunae is also necessary for the activation of bone-degrading enzymes. In mice lacking a necessary component of the proton pump, enzyme activity was diminished and resorption was reduced (Scimeca et al., 2000). While the presence of a fully functioning proton pump is critical to osteoclast function, it is meaningless without an adequate supply of protons from within the cell. To generate protons, enzymatic carbonic anhydrase II (CA-II) converts H_2O and CO_2 into H_2CO_3. The H_2CO_3 then dissociates to form HCO_3^- and the necessary protons (Sly and Hu, 1995). Thus, CA-II is critical for osteoclast function and without it, mice have a trabecular bone volume that is 50% greater than that in wild-types (Margolis et al., 2008). Importantly, the HCO_3^- ions are exchanged on the cell membrane for Cl^- ions; this occurs on a portion of the membrane outside of the sealing zone. The Cl^- ions are important because they are subsequently exported into the resorption lacunae as protons are being pumped out, which allows the intracellular pH to remain neutral (Kornak et al., 2001; Schlesinger et al., 1997).

Cathepsin K is arguably the most important enzyme in the degradation of the organic components of the bone. It is localized within lysosome of osteoclasts and secreted in the resorption lacuae. Humans lacking Cathepsin K have pycnodysostosis, which is characterized by short stature, dense bones, and other bone malformations (Gelb et al., 1996). These defects are recapitulated in *CtsK*$^{-/-}$ mice, which are also osteopetrotic (Saftig et al., 1998). While the mice have normal numbers of osteoclasts, they are unable to properly resorb bone (Nishi et al., 1999; Saftig et al., 1998). Cathepsin K is further discussed in Chapter 2. Matrix metalloproteinases (MMPs) are also important to the functioning osteoclast. They are known to cleave cytokines and growth factors in addition to the organic matrix of bone (Krane and Inada, 2008). *MMP13*-null mice exhibit increase bone density as a result of decreased osteoclast function (Kosaki et al., 2007; Stickens et al., 2004). Additionly, both MMP13 and MMP9 have been shown to regulate osteoclast recruitment and invasion, which may highlight the more important roles of MMPs in osteoclast function (Inada et al., 2004; Vu et al., 1998). One final enzyme that is a canonical marker of osteoclast function is tartrate-resistant acid phosphatase (TRAP). TRAP is expressed in both macrophages and osteoclasts and has long been used as a histochemical marker for osteoclasts (Burstone, 1959; Minkin, 1982). TRAP is a secreted protein, although its exact function is somewhat unclear (Kirstein et al., 2006). The most well-characterized function of TRAP is the hydrolysis of the phosphoprotein, osteopontin (OPN) (Suter et al., 2001). OPN is a protein important for osteoclast attachment to the bone. It has been proposed that TRAP dephosphorylates OPN, which would then allow the osteoclast to migrate to another area for resorption (Ek-Rylander et al., 1994). The importance of TRAP to osteoclast function is emphasized

by the phenotype of mice lacking TRAP. *TRAP*$^{-/-}$ mice display a myriad of skeletal malformations including mild osteopetrosis and increased bone density (Hayman et al., 1996).

The role of Arf in bone

Finally, I would like to discuss the known roles of ARF in bone turnover. First, given the physiological communication between osteoclasts and osteoblasts, it is important to consider the role of ARF in osteoblasts.

The role of Arf in osteoblasts

Under osteogenic conditions, bone marrow stromal cells can be differentiated into osteoblasts (OBs). *Arf*$^{-/-}$ stromal cells exhibit enhanced osteoblastogenesis compared to wild-type counterparts when assessed by alkaline phosphatase (ALP) expression and mineralization *in vitro* (Rauch et al.). Data also suggests that ARF regulation of osteoblastogenesis is relevant *in vivo*. Long bones taken from 8-week-old *Arf*$^{-/-}$ displayed elevated levels of OB differentiation markers compared to bones from wild-type mice. This is correlated to increased bone formation as quantified by double calcein labeling as well as elevated serum osteocalcin levels, which is a biomarker of mature OBs. Finally, when comparing *Arf*$^{-/-}$ mice to wild-types, the authors observed an overall increase in trabecular bone volume in conjunction with higher levels of bone mineral density, trabecular number, and trabecular thickness as assessed by microCT (Rauch et al.). Importantly, Hurchla and colleagues subsequently determined that enhanced

osteoblastogenesis was at least partially due to enhanced proliferation of osteoblast precursors upon *Arf* loss (unpublished communicated data).

Initial study of ARF in osteoclasts

As previously mentioned, the study of ARF in osteoclasts was initiated to determine if the changes in protein synthesis upon loss of basal *Arf* were physiologically relevant; in other words, would loss of *Arf* have an impact on the function of a cell with obvious protein synthesis demands? Apicelli and colleagues first differentiated bone marrow-derived macrophages from wild-type or $Arf^{-/-}$ mice in the presence of M-CSF and RANKL. After three days in the osteoclastogenic media, they observed an increase in the number of TRAP-positive (via staining with a TRAP substrate) multinucleated osteoclasts in the absence of *Arf* (Apicelli et al., 2008). *Arf* loss also appears to enhance the activity of mature osteoclasts. Upon plating equal numbers of TRAP-positive cells, day 4 WT osteoclasts were compared to day 3 $Arf^{-/-}$ osteoclasts. $Arf^{-/-}$ osteoclasts had nearly twice as much TRAP activity as WT osteoclasts as assessed by the addition of a TRAP substrate (Apicelli et al., 2008). Furthermore, the authors assessed *in vivo* activity of osteoclasts by serum TRAP activity. $Arf^{-/-}$ mice exhibited a significant increase in serum TRAP activity relative to that observed in WT mice (Apicelli et al., 2008). Importantly, BrdU incorporation experiments done using bone marrow macrophages *in vitro* did not show a difference in proliferation upon *Arf* loss (Apicelli et al., 2008). Together, this suggests that *Arf* loss enhanced osteoclast activity both *in vitro* and *in vivo* and is independent of precursor proliferation (Figure 1.5). Finally, Apicelli and colleagues demonstrated that loss of NPM by shRNA-mediated knockdown abrogates the

enhanced osteoclastogenesis observed in *Arf*$^{-/-}$ cells (Apicelli et al., 2008). This data suggests that ARF may be regulating osteoclastogenesis by impeding protein synthesis (Figure 1.6).

1.6 Dissertation objectives

At the onset of this project, the ARF field was well aware that ARF levels are induced in the presence of oncogenic stress to impede cell proliferation. The mechanism of ARF tumor suppression has long been appreciated to include the sequestration of MDM2 and thus, the activation of p53 activity. As demonstrated by the myriad of ARF-interacting targets aside from MDM2, it is clear that the ARF field has embraced the idea of p53-independent ARF tumor suppression. Our lab has largely focused on the ability of ARF to bind NPM and prohibit its nucleocytoplasmic shuttling, which certainly contributes to decreased protein synthesis and cell growth. Given that cell growth is intimately tied to the progression of the cell cycle, one of the primary questions of my project was to determine if ARF regulates protein synthesis in a proliferation-independent context. Furthermore, the ARF field has more recently focused on the function of basal ARF. While the importance of enhanced ARF levels upon oncogenic stress is becoming overwhelmingly clear, the significance of basal ARF is still in its infancy. There have been minimal reports demonstrating a physiologically-relevant function of basal ARF including the role of ARF in eye development, male germ cell development, osteoblast activity. Our lab has most recently demonstrated a role for basal ARF in the maintenance of nucleolar structure and function, which ultimately results in the regulation of protein synthesis. These studies were done using mitotic cells. Therefore, we were inclined to

study this function of ARF in a post-mitotic setting such that we could satisfy the first goal of the project: does ARF regulate protein synthesis in a proliferation-independent context? Importantly, we also wanted to choose a physiologically-relevant setting. We choose the osteoclasts as a model given our preliminary published results and realizing that osteoclasts have a demand for protein synthesis to properly function. Using this system, we additionally satisfied a second goal of the project: to determine if basal ARF regulation of protein synthesis is physiologically-relevant. Finally, we anticipated that the completion of this project would allow the field to better understand the teleological function of ARF, namely that ARF is first and foremost a regulator of protein production.

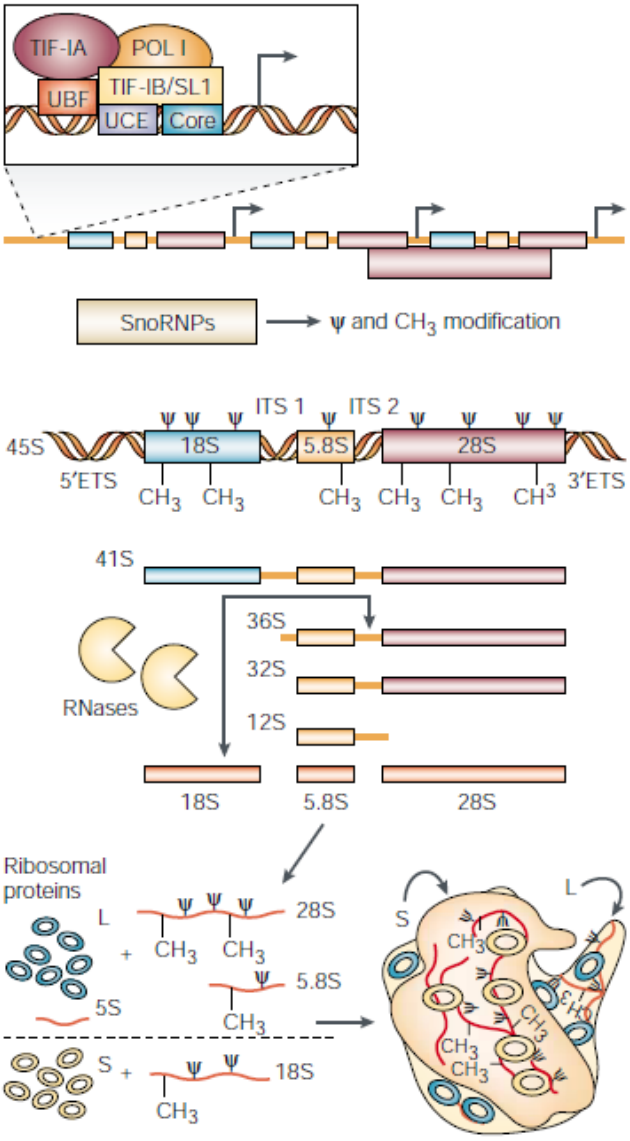

Figure 1.1

Ribosome production. Ribosome production begins with the transcription of the ribosomal DNA. The transcript is then modified, a process that is guided by small nucleolar RNAs (snoRNAs). RNases cleave the transcript to produce the mature 18S,

5.8S, and 28S rRNAs. These rRNAs further associate with ribosomal proteins to ultimately form the small (40S) and large (60S) ribosomal subunits. The subunits are then exported to the cytoplasm for protein synthesis. Adapted from Ruggero and Pandolfi, 2003.

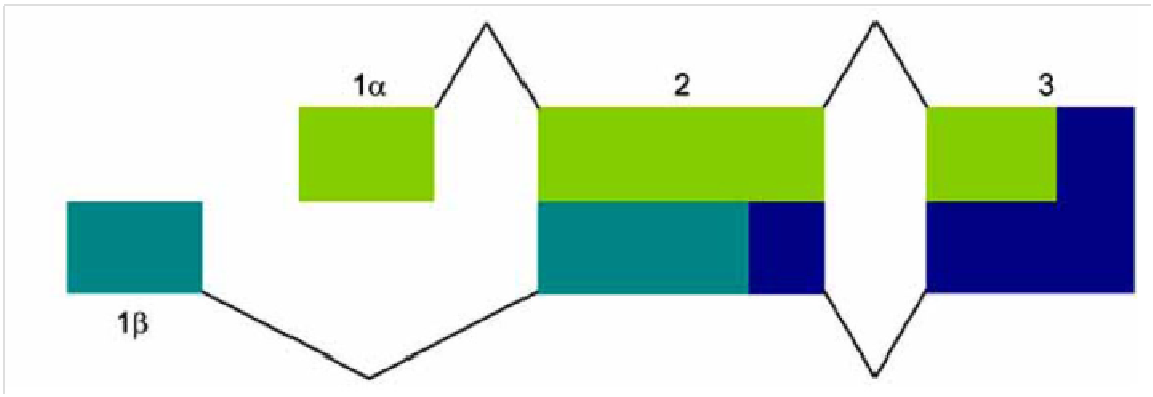

Figure 1.2

Organization of the *INK4a/Arf* locus. INK4a and ARF share exons 2 and 3. Exon1α is unique to INK4a, while exon1β is unique to ARF. The first exons of INK4a and ARF splice into exon 2 in alternative reading frames such that the light green portion encodes for INK4a and the dark green portion encodes for ARF. Adapted from Saporita *et al.* 2007.

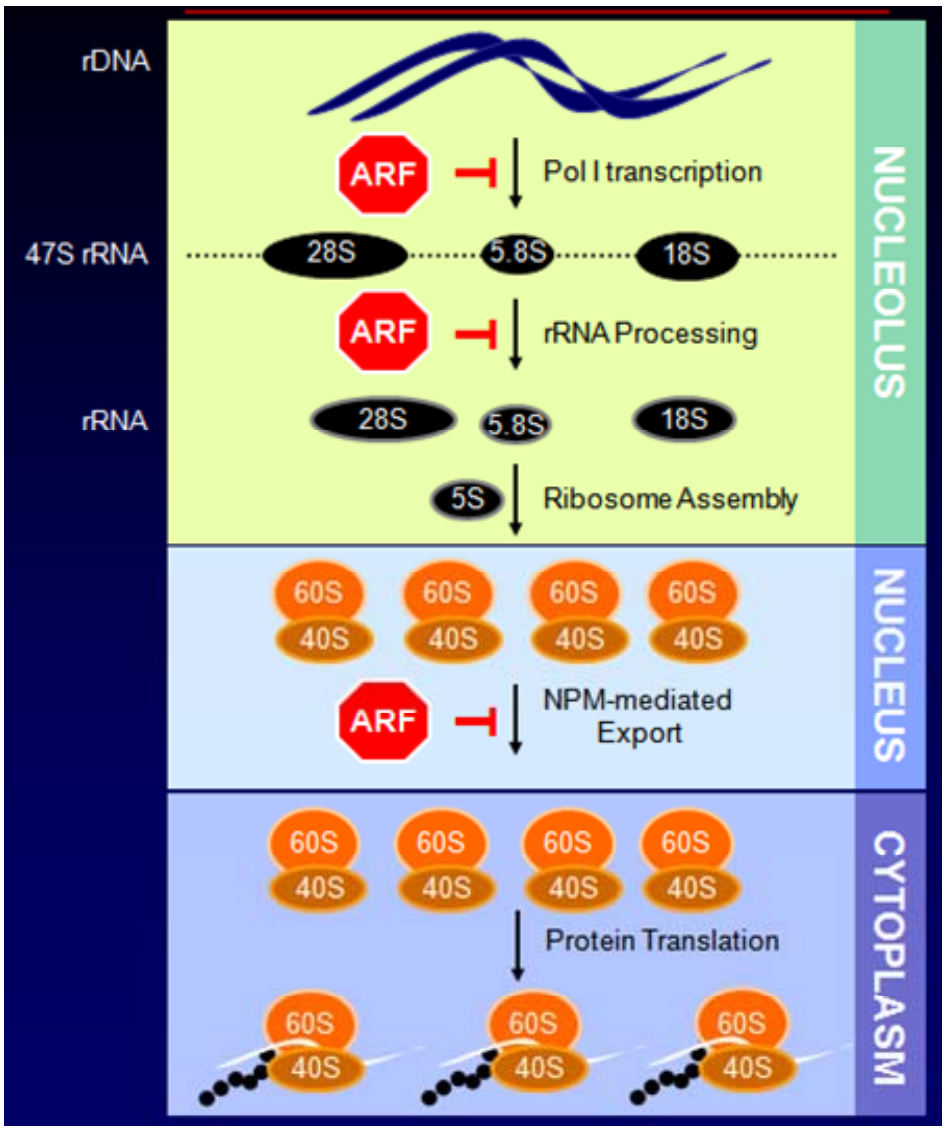

Figure 1.3

Basal ARF is known to regulate multiple steps in the control of protein synthesis. *Arf* loss results in increased transcription of ribosomal DNA (rDNA), suggesting that ARF impedes rDNA transcription in the nucleolus. Within the nucleolus, ARF also inhibits the processing of the newly transcribed 47S rRNA into the mature 28S, 5.8S, and 18S ribosomal subunits. In the nucleus, ARF impedes NPM-mediated export of mature

ribosomal subunits to the cytoplasm. The role of ARF in limiting these steps of ribosomal biogenesis results in the overall maintenance of protein synthesis in the cytoplasm. Adapted from Saporita *et al.* 2007.

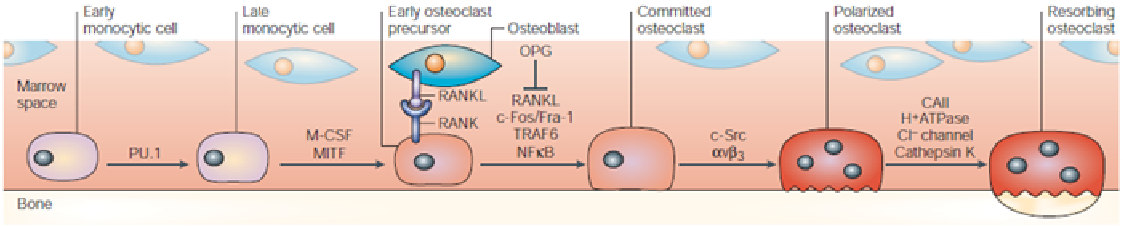

Figure 1.4

Osteoclastogenesis. Osteoclasts are members of the monocyte/macrophage family. Specific genes are sequentially activated as macrophages differentiate into mature, resorbing osteoclast. Notably, RANKL, which is largely found on the membrane of osteoblasts induces the commitment of cells to the osteoclast lineage. Adapted from Teitelbaum and Ross, 2003.

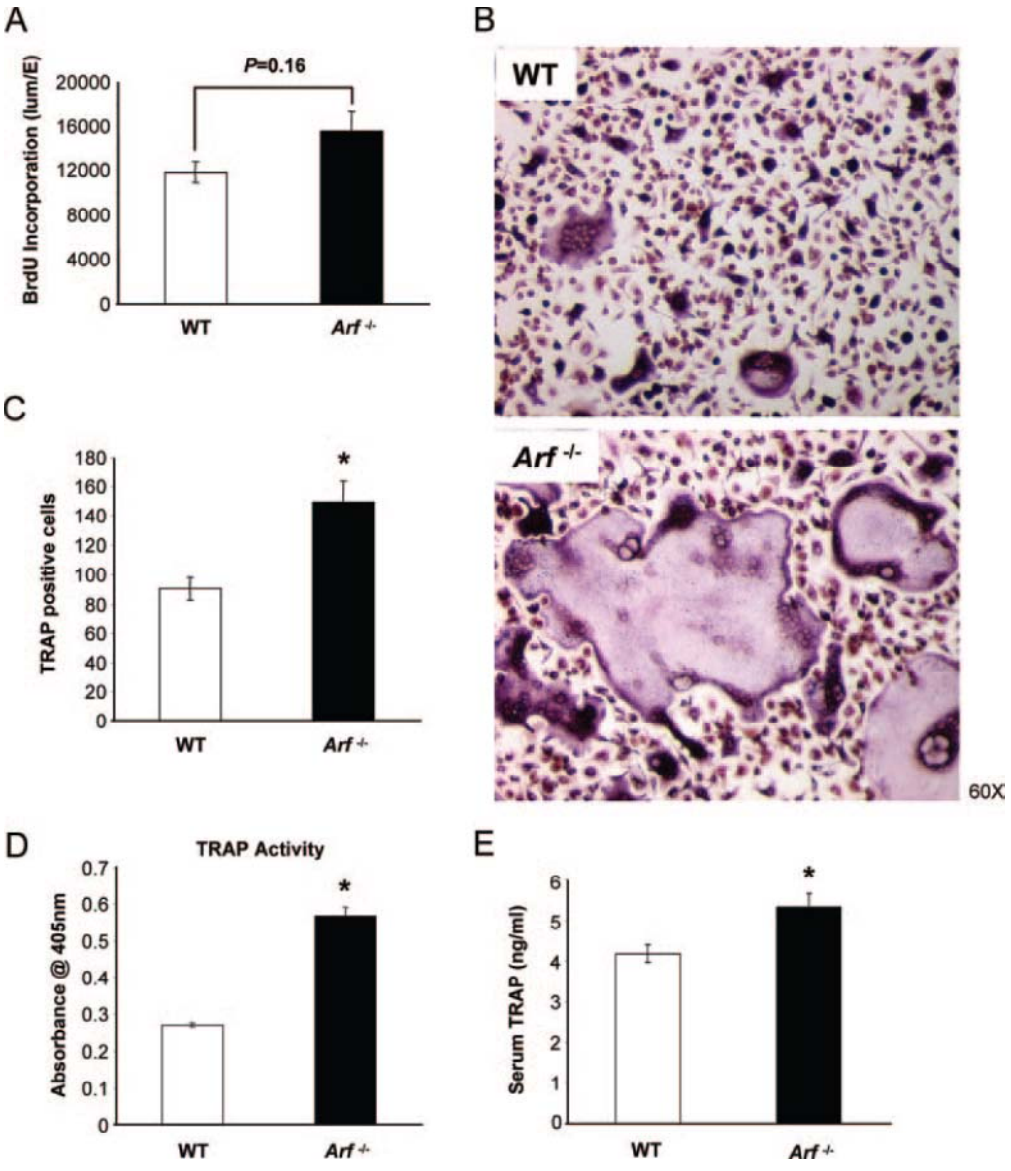

Figure 1.5

***Arf* loss affects osteoclastogenesis *in vitro*.** (A) BrdU incorporation suggests there is no difference between wild-type and *Arf*$^{-/-}$ macrophages. (B). BMMs differentiated for 3 days in the presence of M-CSF (1/20 vol) and 100ng/mL RANKL and then TRAP stained. (C) Quantification of TRAP-positive cells with greater than five nuclei from day 3 osteoclast images (p = 0.01). (D) TRAP solution assay from equal numbers of day 4

wild-type osteoclasts and day 4 *Arf*$^{-/-}$ osteoclasts. Cells were lysed and incubated in a colorimetric assay with a substrate for TRAP ($p = 0.01$) (E) Levels of serum TRAP from age-matched wild-type and *Arf*$^{-/-}$ mice ($p = 0.03$, $n=5$). Adapted from Apicelli *et al.* 2008.

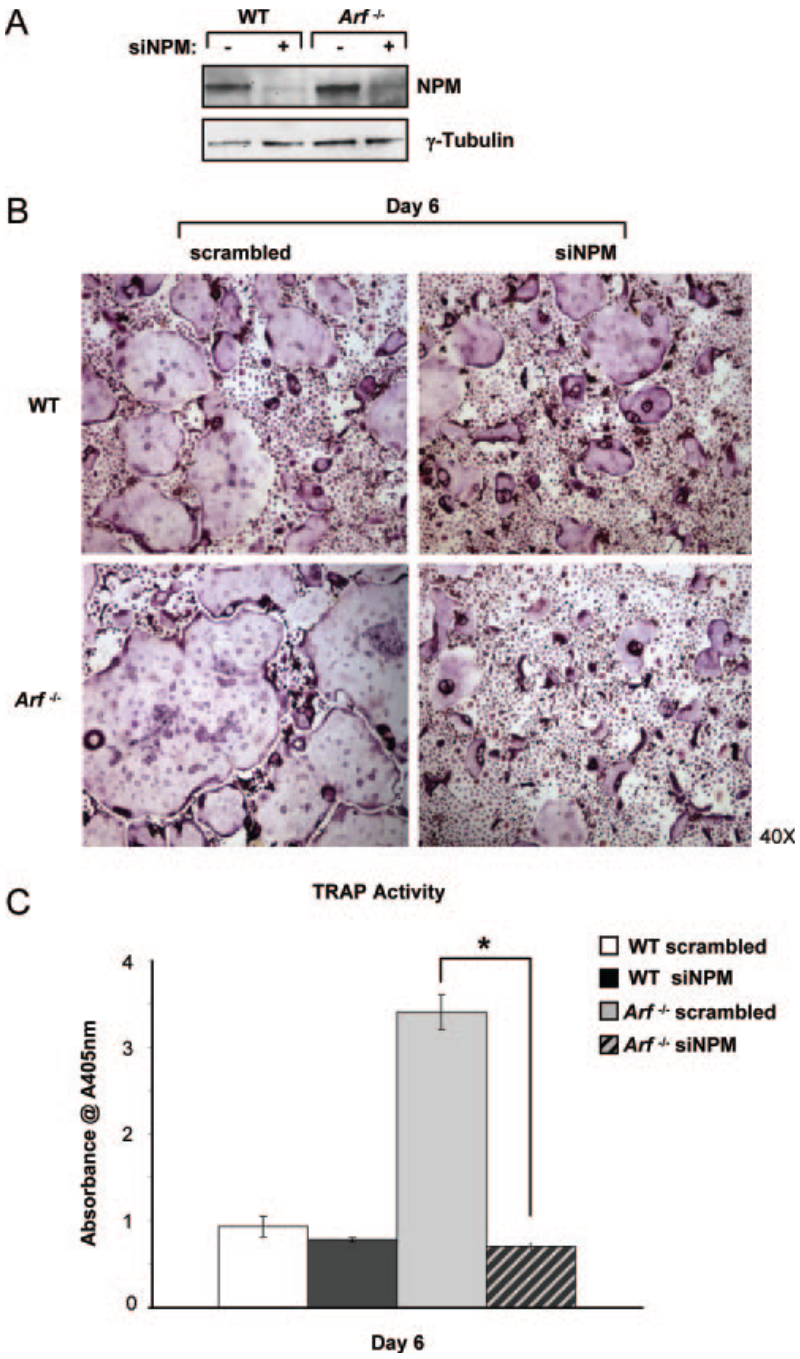

Figure 1.6

Loss of NPM reverses the *Arf*$^{-/-}$ osteoclast phenotype. (A) NPM is knocked down by lentivirus-targeted shRNA in wild-type and *Arf*$^{-/-}$ macrophages and confirmed by immunoblotting. (B) Macrophages with or without NPM knockdown are differentiated is

osteoclastogenic media for 6 days and then stained for TRAP. (C) TRAP activity is quantified in day 6 osteoclasts. Loss of NPM reverses the *Arf*$^{-/-}$ osteoclast phenotype such that they are equivalent to wild-type osteoclasts ($p < 0.01$). Adapted from Apicelli *et al.* 2008.

1.7 References

Abu-Amer, Y., Dowdy, S.F., Ross, F.P., Clohisy, J.C., and Teitelbaum, S.L. (2001). TAT fusion proteins containing tyrosine 42-deleted IkappaBalpha arrest osteoclastogenesis. J Biol Chem *276*, 30499-30503.

Agger, K., Cloos, P.A., Rudkjaer, L., Williams, K., Andersen, G., Christensen, J., and Helin, K. (2009). The H3K27me3 demethylase JMJD3 contributes to the activation of the INK4A-ARF locus in response to oncogene- and stress-induced senescence. Genes Dev *23*, 1171-1176.

Apicelli, A.J., Maggi, L.B., Jr., Hirbe, A.C., Miceli, A.P., Olanich, M.E., Schulte-Winkeler, C.L., Saporita, A.J., Kuchenreuther, M., Sanchez, J., Weilbaecher, K.*, et al.* (2008). A non-tumor suppressor role for basal p19ARF in maintaining nucleolar structure and function. Mol Cell Biol *28*, 1068-1080.

Aubin, J.E. (1992). Osteoclast adhesion and resorption: the role of podosomes. J Bone Miner Res *7*, 365-368.

Ayrault, O., Andrique, L., Fauvin, D., Eymin, B., Gazzeri, S., and Seite, P. (2006). Human tumor suppressor p14ARF negatively regulates rRNA transcription and inhibits UBF1 transcription factor phosphorylation. Oncogene *25*, 7577-7586.

Ayrault, O., Andrique, L., Larsen, C.J., and Seite, P. (2004). Human Arf tumor suppressor specifically interacts with chromatin containing the promoter of rRNA genes. Oncogene *23*, 8097-8104.

Barradas, M., Anderton, E., Acosta, J.C., Li, S., Banito, A., Rodriguez-Niedenfuhr, M., Maertens, G., Banck, M., Zhou, M.M., Walsh, M.J.*, et al.* (2009). Histone demethylase JMJD3 contributes to epigenetic control of INK4a/ARF by oncogenic RAS. Genes Dev *23*, 1177-1182.

Bernard, K., Litman, E., Fitzpatrick, J.L., Shellman, Y.G., Argast, G., Polvinen, K., Everett, A.D., Fukasawa, K., Norris, D.A., Ahn, N.G.*, et al.* (2003). Functional proteomic analysis of melanoma progression. Cancer Res *63*, 6716-6725.

Bertwistle, D., Sugimoto, M., and Sherr, C.J. (2004). Physical and functional interactions of the Arf tumor suppressor protein with nucleophosmin/B23. Mol Cell Biol *24*, 985-996.

Blair, H.C. (1998). How the osteoclast degrades bone. Bioessays *20*, 837-846.

Bodner, S.M., Naeve, C.W., Rakestraw, K.M., Jones, B.G., Valentine, V.A., Valentine, M.B., Luthardt, F.W., Willman, C.L., Raimondi, S.C., Downing, J.R.*, et al.* (1999). Cloning and chromosomal localization of the gene encoding human cyclin D-binding Myb-like protein (hDMP1). Gene *229*, 223-228.

Bolli, N., Nicoletti, I., De Marco, M.F., Bigerna, B., Pucciarini, A., Mannucci, R., Martelli, M.P., Liso, A., Mecucci, C., Fabbiano, F.*, et al.* (2007). Born to be exported: COOH-terminal nuclear export signals of different strength ensure cytoplasmic accumulation of nucleophosmin leukemic mutants. Cancer Res *67*, 6230-6237.

Borer, R.A., Lehner, C.F., Eppenberger, H.M., and Nigg, E.A. (1989). Major nucleolar proteins shuttle between nucleus and cytoplasm. Cell *56*, 379-390.

Boyce, B.F., Yoneda, T., Lowe, C., Soriano, P., and Mundy, G.R. (1992). Requirement of pp60c-src expression for osteoclasts to form ruffled borders and resorb bone in mice. J Clin Invest *90*, 1622-1627.

Bracken, A.P., Kleine-Kohlbrecher, D., Dietrich, N., Pasini, D., Gargiulo, G., Beekman, C., Theilgaard-Monch, K., Minucci, S., Porse, B.T., Marine, J.C*., et al.* (2007). The Polycomb group proteins bind throughout the INK4A-ARF locus and are disassociated in senescent cells. Genes Dev *21*, 525-530.

Brady, S.N., Maggi, L.B., Jr., Winkeler, C.L., Toso, E.A., Gwinn, A.S., Pelletier, C.L., and Weber, J.D. (2009). Nucleophosmin protein expression level, but not threonine 198 phosphorylation, is essential in growth and proliferation. Oncogene *28*, 3209-3220.

Brady, S.N., Yu, Y., Maggi, L.B., Jr., and Weber, J.D. (2004). ARF impedes NPM/B23 shuttling in an Mdm2-sensitive tumor suppressor pathway. Mol Cell Biol *24*, 9327-9338.

Brown, E.J., Albers, M.W., Shin, T.B., Ichikawa, K., Keith, C.T., Lane, W.S., and Schreiber, S.L. (1994). A mammalian protein targeted by G1-arresting rapamycin-receptor complex. Nature *369*, 756-758.

Burgess, T.L., Qian, Y., Kaufman, S., Ring, B.D., Van, G., Capparelli, C., Kelley, M., Hsu, H., Boyle, W.J., Dunstan, C.R*., et al.* (1999). The ligand for osteoprotegerin (OPGL) directly activates mature osteoclasts. J Cell Biol *145*, 527-538.

Burstone, M.S. (1959). Histochemical demonstration of acid phosphatase activity in osteoclasts. J Histochem Cytochem *7*, 39-41.

Cao, R., Wang, L., Wang, H., Xia, L., Erdjument-Bromage, H., Tempst, P., Jones, R.S., and Zhang, Y. (2002). Role of histone H3 lysine 27 methylation in Polycomb-group silencing. Science *298*, 1039-1043.

Cappellen, D., Luong-Nguyen, N.H., Bongiovanni, S., Grenet, O., Wanke, C., and Susa, M. (2002). Transcriptional program of mouse osteoclast differentiation governed by the macrophage colony-stimulating factor and the ligand for the receptor activator of NFkappa B. J Biol Chem *277*, 21971-21982.

Chen, D., Kon, N., Li, M., Zhang, W., Qin, J., and Gu, W. (2005). ARF-BP1/Mule is a critical mediator of the ARF tumor suppressor. Cell *121*, 1071-1083.

Chen, Y., Chen, H., Rhoad, A.E., Warner, L., Caggiano, T.J., Failli, A., Zhang, H., Hsiao, C.L., Nakanishi, K., and Molnar-Kimber, K.L. (1994). A putative sirolimus (rapamycin) effector protein. Biochem Biophys Res Commun *203*, 1-7.

Cheng, K., Grisendi, S., Clohessy, J.G., Majid, S., Bernardi, R., Sportoletti, P., and Pandolfi, P.P. (2007). The leukemia-associated cytoplasmic nucleophosmin mutant is an oncogene with paradoxical functions: Arf inactivation and induction of cellular senescence. Oncogene *26*, 7391-7400.

Cheng, K., Sportoletti, P., Ito, K., Clohessy, J.G., Teruya-Feldstein, J., Kutok, J.L., and Pandolfi, P.P. The cytoplasmic NPM mutant induces myeloproliferation in a transgenic mouse model. Blood *115*, 3341-3345.

Chiu, M.I., Katz, H., and Berlin, V. (1994). RAPT1, a mammalian homolog of yeast Tor, interacts with the FKBP12/rapamycin complex. Proc Natl Acad Sci U S A *91*, 12574-12578.

Churchman, M.L., Roig, I., Jasin, M., Keeney, S., and Sherr, C.J. Expression of arf tumor suppressor in spermatogonia facilitates meiotic progression in male germ cells. PLoS Genet *7*, e1002157.

Coccia, P.F., Krivit, W., Cervenka, J., Clawson, C., Kersey, J.H., Kim, T.H., Nesbit, M.E., Ramsay, N.K., Warkentin, P.I., Teitelbaum, S.L*., et al.* (1980). Successful bone-marrow transplantation for infantile malignant osteopetrosis. N Engl J Med *302*, 701-708.

Cole, F., Keeney, S., and Jasin, M. Evolutionary conservation of meiotic DSB proteins: more than just Spo11. Genes Dev *24*, 1201-1207.

Colombo, E., Bonetti, P., Lazzerini Denchi, E., Martinelli, P., Zamponi, R., Marine, J.C., Helin, K., Falini, B., and Pelicci, P.G. (2005). Nucleophosmin is required for DNA integrity and p19Arf protein stability. Mol Cell Biol *25*, 8874-8886.

Colombo, E., Martinelli, P., Zamponi, R., Shing, D.C., Bonetti, P., Luzi, L., Volorio, S., Bernard, L., Pruneri, G., Alcalay, M*., et al.* (2006). Delocalization and destabilization of the Arf tumor suppressor by the leukemia-associated NPM mutant. Cancer Res *66*, 3044-3050.

Crotti, T.N., Flannery, M., Walsh, N.C., Fleming, J.D., Goldring, S.R., and McHugh, K.P. (2005). NFATc1 directly induces the human beta3 integrin gene in osteoclast differentiation. J Musculoskelet Neuronal Interact *5*, 335-337.

Dai, X.M., Ryan, G.R., Hapel, A.J., Dominguez, M.G., Russell, R.G., Kapp, S., Sylvestre, V., and Stanley, E.R. (2002). Targeted disruption of the mouse colony-stimulating factor 1 receptor gene results in osteopetrosis, mononuclear phagocyte deficiency, increased primitive progenitor cell frequencies, and reproductive defects. Blood *99*, 111-120.

Darnay, B.G., Ni, J., Moore, P.A., and Aggarwal, B.B. (1999). Activation of NF-kappaB by RANK requires tumor necrosis factor receptor-associated factor (TRAF) 6 and NF-kappaB-inducing kinase. Identification of a novel TRAF6 interaction motif. J Biol Chem *274*, 7724-7731.

Datta, A., Nag, A., Pan, W., Hay, N., Gartel, A.L., Colamonici, O., Mori, Y., and Raychaudhuri, P. (2004). Myc-ARF (alternate reading frame) interaction inhibits the functions of Myc. J Biol Chem *279*, 36698-36707.

Datta, A., Sen, J., Hagen, J., Korgaonkar, C.K., Caffrey, M., Quelle, D.E., Hughes, D.E., Ackerson, T.J., Costa, R.H., and Raychaudhuri, P. (2005). ARF directly binds DP1: interaction with DP1 coincides with the G1 arrest function of ARF. Mol Cell Biol *25*, 8024-8036.

David, J.P., Sabapathy, K., Hoffmann, O., Idarraga, M.H., and Wagner, E.F. (2002). JNK1 modulates osteoclastogenesis through both c-Jun phosphorylation-dependent and -independent mechanisms. J Cell Sci *115*, 4317-4325.

Day, C.J., Kim, M.S., Lopez, C.M., Nicholson, G.C., and Morrison, N.A. (2005). NFAT expression in human osteoclasts. J Cell Biochem *95*, 17-23.

Del Fattore, A., Teti, A., and Rucci, N. (2008). Osteoclast receptors and signaling. Arch Biochem Biophys *473*, 147-160.

den Besten, W., Kuo, M.L., Williams, R.T., and Sherr, C.J. (2005). Myeloid leukemia-associated nucleophosmin mutants perturb p53-dependent and independent activities of the Arf tumor suppressor protein. Cell Cycle *4*, 1593-1598.

Dietrich, N., Bracken, A.P., Trinh, E., Schjerling, C.K., Koseki, H., Rappsilber, J., Helin, K., and Hansen, K.H. (2007). Bypass of senescence by the polycomb group protein CBX8 through direct binding to the INK4A-ARF locus. EMBO J *26*, 1637-1648.

Dougall, W.C., Glaccum, M., Charrier, K., Rohrbach, K., Brasel, K., De Smedt, T., Daro, E., Smith, J., Tometsko, M.E., Maliszewski, C.R*., et al.* (1999). RANK is essential for osteoclast and lymph node development. Genes Dev *13*, 2412-2424.

Eischen, C.M., Weber, J.D., Roussel, M.F., Sherr, C.J., and Cleveland, J.L. (1999). Disruption of the ARF-Mdm2-p53 tumor suppressor pathway in Myc-induced lymphomagenesis. Genes Dev *13*, 2658-2669.

Ek-Rylander, B., Flores, M., Wendel, M., Heinegard, D., and Andersson, G. (1994). Dephosphorylation of osteopontin and bone sialoprotein by osteoclastic tartrate-resistant acid phosphatase. Modulation of osteoclast adhesion in vitro. J Biol Chem *269*, 14853-14856.

Falini, B., Bolli, N., Shan, J., Martelli, M.P., Liso, A., Pucciarini, A., Bigerna, B., Pasqualucci, L., Mannucci, R., Rosati, R*., et al.* (2006). Both carboxy-terminus NES motif and mutated tryptophan(s) are crucial for aberrant nuclear export of nucleophosmin leukemic mutants in NPMc+ AML. Blood *107*, 4514-4523.

Falini, B., Mecucci, C., Tiacci, E., Alcalay, M., Rosati, R., Pasqualucci, L., La Starza, R., Diverio, D., Colombo, E., Santucci, A*., et al.* (2005). Cytoplasmic nucleophosmin in acute myelogenous leukemia with a normal karyotype. N Engl J Med *352*, 254-266.

Fatica, A., and Tollervey, D. (2002). Making ribosomes. Curr Opin Cell Biol *14*, 313-318.

Feng, X., Takeshita, S., Namba, N., Wei, S., Teitelbaum, S.L., and Ross, F.P. (2002). Tyrosines 559 and 807 in the cytoplasmic tail of the macrophage colony-stimulating factor receptor play distinct roles in osteoclast differentiation and function. Endocrinology *143*, 4868-4874.

Fingar, D.C., and Blenis, J. (2004). Target of rapamycin (TOR): an integrator of nutrient and growth factor signals and coordinator of cell growth and cell cycle progression. Oncogene *23*, 3151-3171.

Furonaka, O., Takeshima, Y., Awaya, H., Ishida, H., Kohno, N., and Inai, K. (2004). Aberrant methylation of p14(ARF), p15(INK4b) and p16(INK4a) genes and location of the primary site in pulmonary squamous cell carcinoma. Pathol Int *54*, 549-555.

Galibert, L., Tometsko, M.E., Anderson, D.M., Cosman, D., and Dougall, W.C. (1998). The involvement of multiple tumor necrosis factor receptor (TNFR)-associated factors in the signaling mechanisms of receptor activator of NF-kappaB, a member of the TNFR superfamily. J Biol Chem *273*, 34120-34127.

Gelb, B.D., Shi, G.P., Chapman, H.A., and Desnick, R.J. (1996). Pycnodysostosis, a lysosomal disease caused by cathepsin K deficiency. Science *273*, 1236-1238.

Gerhardt, H., and Betsholtz, C. (2003). Endothelial-pericyte interactions in angiogenesis. Cell Tissue Res *314*, 15-23.

Gil, J., Bernard, D., Martinez, D., and Beach, D. (2004). Polycomb CBX7 has a unifying role in cellular lifespan. Nat Cell Biol *6*, 67-72.

Goldberg, M.F. (1997). Persistent fetal vasculature (PFV): an integrated interpretation of signs and symptoms associated with persistent hyperplastic primary vitreous (PHPV). LIV Edward Jackson Memorial Lecture. Am J Ophthalmol *124*, 587-626.

Grigoriadis, A.E., Wang, Z.Q., Cecchini, M.G., Hofstetter, W., Felix, R., Fleisch, H.A., and Wagner, E.F. (1994). c-Fos: a key regulator of osteoclast-macrophage lineage determination and bone remodeling. Science *266*, 443-448.

Grisendi, S., Bernardi, R., Rossi, M., Cheng, K., Khandker, L., Manova, K., and Pandolfi, P.P. (2005). Role of nucleophosmin in embryonic development and tumorigenesis. Nature *437*, 147-153.

Grisendi, S., Mecucci, C., Falini, B., and Pandolfi, P.P. (2006). Nucleophosmin and cancer. Nat Rev Cancer *6*, 493-505.

Gromley, A., Churchman, M.L., Zindy, F., and Sherr, C.J. (2009). Transient expression of the Arf tumor suppressor during male germ cell and eye development in Arf-Cre reporter mice. Proc Natl Acad Sci U S A *106*, 6285-6290.

Haddad, R., Font, R.L., and Reeser, F. (1978). Persistent hyperplastic primary vitreous. A clinicopathologic study of 62 cases and review of the literature. Surv Ophthalmol *23*, 123-134.

Hainaut, P., Soussi, T., Shomer, B., Hollstein, M., Greenblatt, M., Hovig, E., Harris, C.C., and Montesano, R. (1997). Database of p53 gene somatic mutations in human tumors and cell lines: updated compilation and future prospects. Nucleic Acids Res *25*, 151-157.
Hall, M., and Peters, G. (1996). Genetic alterations of cyclins, cyclin-dependent kinases, and Cdk inhibitors in human cancer. Adv Cancer Res *68*, 67-108.

Hanahan, D., and Weinberg, R.A. (2000). The hallmarks of cancer. Cell *100*, 57-70.

Haupt, Y., Maya, R., Kazaz, A., and Oren, M. (1997). Mdm2 promotes the rapid degradation of p53. Nature *387*, 296-299.

Hayman, A.R., Jones, S.J., Boyde, A., Foster, D., Colledge, W.H., Carlton, M.B., Evans, M.J., and Cox, T.M. (1996). Mice lacking tartrate-resistant acid phosphatase (Acp 5) have disrupted endochondral ossification and mild osteopetrosis. Development *122*, 3151-3162.

Henkel, G.W., McKercher, S.R., Yamamoto, H., Anderson, K.L., Oshima, R.G., and Maki, R.A. (1996). PU.1 but not ets-2 is essential for macrophage development from embryonic stem cells. Blood *88*, 2917-2926.

Hershey, C.L., and Fisher, D.E. (2004). Mitf and Tfe3: members of a b-HLH-ZIP transcription factor family essential for osteoclast development and function. Bone *34*, 689-696.

Hirai, H., and Sherr, C.J. (1996). Interaction of D-type cyclins with a novel myb-like transcription factor, DMP1. Mol Cell Biol *16*, 6457-6467.

Honda, R., Tanaka, H., and Yasuda, H. (1997). Oncoprotein MDM2 is a ubiquitin ligase E3 for tumor suppressor p53. FEBS Lett *420*, 25-27.

Ikeda, F., Nishimura, R., Matsubara, T., Tanaka, S., Inoue, J., Reddy, S.V., Hata, K., Yamashita, K., Hiraga, T., Watanabe, T.*, et al.* (2004). Critical roles of c-Jun signaling in regulation of NFAT family and RANKL-regulated osteoclast differentiation. J Clin Invest *114*, 475-484.

Inada, M., Wang, Y., Byrne, M.H., Rahman, M.U., Miyaura, C., Lopez-Otin, C., and Krane, S.M. (2004). Critical roles for collagenase-3 (Mmp13) in development of growth plate cartilage and in endochondral ossification. Proc Natl Acad Sci U S A *101*, 17192-17197.

Inagaki, A., Schoenmakers, S., and Baarends, W.M. DNA double strand break repair, chromosome synapsis and transcriptional silencing in meiosis. Epigenetics *5*, 255-266.

Inoue, K., Roussel, M.F., and Sherr, C.J. (1999). Induction of ARF tumor suppressor gene expression and cell cycle arrest by transcription factor DMP1. Proc Natl Acad Sci U S A *96*, 3993-3998.

Inoue, K., and Sherr, C.J. (1998). Gene expression and cell cycle arrest mediated by transcription factor DMP1 is antagonized by D-type cyclins through a cyclin-dependent-kinase-independent mechanism. Mol Cell Biol *18*, 1590-1600.

Insogna, K.L., Sahni, M., Grey, A.B., Tanaka, S., Horne, W.C., Neff, L., Mitnick, M., Levy, J.B., and Baron, R. (1997). Colony-stimulating factor-1 induces cytoskeletal reorganization and c-src-dependent tyrosine phosphorylation of selected cellular proteins in rodent osteoclasts. J Clin Invest *100*, 2476-2485.

Itahana, K., Bhat, K.P., Jin, A., Itahana, Y., Hawke, D., Kobayashi, R., and Zhang, Y. (2003). Tumor suppressor ARF degrades B23, a nucleolar protein involved in ribosome biogenesis and cell proliferation. Mol Cell *12*, 1151-1164.

Ito, M., and Yoshioka, M. (1999). Regression of the hyaloid vessels and pupillary membrane of the mouse. Anat Embryol (Berl) *200*, 403-411.

Jacobs, J.J., Kieboom, K., Marino, S., DePinho, R.A., and van Lohuizen, M. (1999). The oncogene and Polycomb-group gene bmi-1 regulates cell proliferation and senescence through the ink4a locus. Nature *397*, 164-168.

Jefferies, H.B., Fumagalli, S., Dennis, P.B., Reinhard, C., Pearson, R.B., and Thomas, G. (1997). Rapamycin suppresses 5'TOP mRNA translation through inhibition of p70s6k. EMBO J *16*, 3693-3704.

Jefferies, H.B., Reinhard, C., Kozma, S.C., and Thomas, G. (1994). Rapamycin selectively represses translation of the "polypyrimidine tract" mRNA family. Proc Natl Acad Sci U S A *91*, 4441-4445.

Jeno, P., Ballou, L.M., Novak-Hofer, I., and Thomas, G. (1988). Identification and characterization of a mitogen-activated S6 kinase. Proc Natl Acad Sci U S A *85*, 406-410.

Johnson, R.S., Spiegelman, B.M., and Papaioannou, V. (1992). Pleiotropic effects of a null mutation in the c-fos proto-oncogene. Cell *71*, 577-586.

Jones, S.N., Roe, A.E., Donehower, L.A., and Bradley, A. (1995). Rescue of embryonic lethality in Mdm2-deficient mice by absence of p53. Nature *378*, 206-208.

Kamijo, T., Bodner, S., van de Kamp, E., Randle, D.H., and Sherr, C.J. (1999). Tumor spectrum in ARF-deficient mice. Cancer Res *59*, 2217-2222.

Kamijo, T., Zindy, F., Roussel, M.F., Quelle, D.E., Downing, J.R., Ashmun, R.A., Grosveld, G., and Sherr, C.J. (1997). Tumor suppression at the mouse INK4a locus mediated by the alternative reading frame product p19ARF. Cell *91*, 649-659.

Kang, Y.J., Olson, M.O., and Busch, H. (1974). Phosphorylation of acid-soluble proteins in isolated nucleoli of Novikoff hepatoma ascites cells. Effects of divalent cations. J Biol Chem *249*, 5580-5585.

Kang, Y.J., Olson, M.O., Jones, C., and Busch, H. (1975). Nucleolar phosphoproteins of normal rat liver and Novikoff hepatoma ascites cells. Cancer Res *35*, 1470-1475.

Keith, C.T., and Schreiber, S.L. (1995). PIK-related kinases: DNA repair, recombination, and cell cycle checkpoints. Science *270*, 50-51.

Kim, H.H., Lee, D.E., Shin, J.N., Lee, Y.S., Jeon, Y.M., Chung, C.H., Ni, J., Kwon, B.S., and Lee, Z.H. (1999). Receptor activator of NF-kappaB recruits multiple TRAF family adaptors and activates c-Jun N-terminal kinase. FEBS Lett *443*, 297-302.

Kim, J.E., and Chen, J. (2000). Cytoplasmic-nuclear shuttling of FKBP12-rapamycin-associated protein is involved in rapamycin-sensitive signaling and translation initiation. Proc Natl Acad Sci U S A *97*, 14340-14345.

Kim, K., Kim, J.H., Lee, J., Jin, H.M., Lee, S.H., Fisher, D.E., Kook, H., Kim, K.K., Choi, Y., and Kim, N. (2005a). Nuclear factor of activated T cells c1 induces osteoclast-associated receptor gene expression during tumor necrosis factor-related activation-induced cytokine-mediated osteoclastogenesis. J Biol Chem *280*, 35209-35216.

Kim, Y., Sato, K., Asagiri, M., Morita, I., Soma, K., and Takayanagi, H. (2005b). Contribution of nuclear factor of activated T cells c1 to the transcriptional control of immunoreceptor osteoclast-associated receptor but not triggering receptor expressed by myeloid cells-2 during osteoclastogenesis. J Biol Chem *280*, 32905-32913.

Kirstein, B., Chambers, T.J., and Fuller, K. (2006). Secretion of tartrate-resistant acid phosphatase by osteoclasts correlates with resorptive behavior. J Cell Biochem *98*, 1085-1094.

Kiss, T. (2001). Small nucleolar RNA-guided post-transcriptional modification of cellular RNAs. EMBO J *20*, 3617-3622.

Kominami, K., Nagasaka, T., Cullings, H.M., Hoshizima, N., Sasamoto, H., Young, J., Leggett, B.A., Tanaka, N., and Matsubara, N. (2009). Methylation in p14(ARF) is frequently observed in colorectal cancer with low-level microsatellite instability. J Int Med Res *37*, 1038-1045.

Konishi, N., Nakamura, M., Kishi, M., Nishimine, M., Ishida, E., and Shimada, K. (2002). Heterogeneous methylation and deletion patterns of the INK4a/ARF locus within prostate carcinomas. Am J Pathol *160*, 1207-1214.

Korgaonkar, C., Hagen, J., Tompkins, V., Frazier, A.A., Allamargot, C., Quelle, F.W., and Quelle, D.E. (2005). Nucleophosmin (B23) targets ARF to nucleoli and inhibits its function. Mol Cell Biol *25*, 1258-1271.

Kornak, U., Kasper, D., Bosl, M.R., Kaiser, E., Schweizer, M., Schulz, A., Friedrich, W., Delling, G., and Jentsch, T.J. (2001). Loss of the ClC-7 chloride channel leads to osteopetrosis in mice and man. Cell *104*, 205-215.

Kosaki, N., Takaishi, H., Kamekura, S., Kimura, T., Okada, Y., Minqi, L., Amizuka, N., Chung, U.I., Nakamura, K., Kawaguchi, H*., et al.* (2007). Impaired bone fracture healing in matrix metalloproteinase-13 deficient mice. Biochem Biophys Res Commun *354*, 846-851.

Krane, S.M., and Inada, M. (2008). Matrix metalloproteinases and bone. Bone *43*, 7-18.

Kubbutat, M.H., Jones, S.N., and Vousden, K.H. (1997). Regulation of p53 stability by Mdm2. Nature *387*, 299-303.

Kuo, M.L., den Besten, W., Bertwistle, D., Roussel, M.F., and Sherr, C.J. (2004). N-terminal polyubiquitination and degradation of the Arf tumor suppressor. Genes Dev *18*, 1862-1874.

Kwon, O.H., Lee, C.K., Lee, Y.I., Paik, S.G., and Lee, H.J. (2005). The hematopoietic transcription factor PU.1 regulates RANK gene expression in myeloid progenitors. Biochem Biophys Res Commun *335*, 437-446.

Lacey, D.L., Timms, E., Tan, H.L., Kelley, M.J., Dunstan, C.R., Burgess, T., Elliott, R., Colombero, A., Elliott, G., Scully, S*., et al.* (1998). Osteoprotegerin ligand is a cytokine that regulates osteoclast differentiation and activation. Cell *93*, 165-176.

Laud, K., Marian, C., Avril, M.F., Barrois, M., Chompret, A., Goldstein, A.M., Tucker, M.A., Clark, P.A., Peters, G., Chaudru, V*., et al.* (2006). Comprehensive analysis of CDKN2A (p16INK4A/p14ARF) and CDKN2B genes in 53 melanoma index cases considered to be at heightened risk of melanoma. J Med Genet *43*, 39-47.

Li, J., Sarosi, I., Yan, X.Q., Morony, S., Capparelli, C., Tan, H.L., McCabe, S., Elliott, R., Scully, S., Van, G*., et al.* (2000). RANK is the intrinsic hematopoietic cell surface receptor that controls osteoclastogenesis and regulation of bone mass and calcium metabolism. Proc Natl Acad Sci U S A *97*, 1566-1571.

Lindahl, P., Johansson, B.R., Leveen, P., and Betsholtz, C. (1997). Pericyte loss and microaneurysm formation in PDGF-B-deficient mice. Science *277*, 242-245.

Lohrum, M.A., Ashcroft, M., Kubbutat, M.H., and Vousden, K.H. (2000). Identification of a cryptic nucleolar-localization signal in MDM2. Nat Cell Biol *2*, 179-181.

Luchin, A., Purdom, G., Murphy, K., Clark, M.Y., Angel, N., Cassady, A.I., Hume, D.A., and Ostrowski, M.C. (2000). The microphthalmia transcription factor regulates expression of the tartrate-resistant acid phosphatase gene during terminal differentiation of osteoclasts. J Bone Miner Res *15*, 451-460.

Luchin, A., Suchting, S., Merson, T., Rosol, T.J., Hume, D.A., Cassady, A.I., and Ostrowski, M.C. (2001). Genetic and physical interactions between Microphthalmia transcription factor and PU.1 are necessary for osteoclast gene expression and differentiation. J Biol Chem *276*, 36703-36710.

Maggi, L.B., Jr., Kuchenruether, M., Dadey, D.Y., Schwope, R.M., Grisendi, S., Townsend, R.R., Pandolfi, P.P., and Weber, J.D. (2008). Nucleophosmin serves as a rate-limiting nuclear export chaperone for the Mammalian ribosome. Mol Cell Biol *28*, 7050-7065.

Mahadevaiah, S.K., Turner, J.M., Baudat, F., Rogakou, E.P., de Boer, P., Blanco-Rodriguez, J., Jasin, M., Keeney, S., Bonner, W.M., and Burgoyne, P.S. (2001). Recombinational DNA double-strand breaks in mice precede synapsis. Nat Genet *27*, 271-276.

Marcotrigiano, J., Gingras, A.C., Sonenberg, N., and Burley, S.K. (1999). Cap-dependent translation initiation in eukaryotes is regulated by a molecular mimic of eIF4G. Mol Cell *3*, 707-716.

Margolis, D.S., Szivek, J.A., Lai, L.W., and Lien, Y.H. (2008). Phenotypic characteristics of bone in carbonic anhydrase II-deficient mice. Calcif Tissue Int *82*, 66-76.

Matsumoto, M., Kogawa, M., Wada, S., Takayanagi, H., Tsujimoto, M., Katayama, S., Hisatake, K., and Nogi, Y. (2004). Essential role of p38 mitogen-activated protein kinase in cathepsin K gene expression during osteoclastogenesis through association of NFATc1 and PU.1. J Biol Chem *279*, 45969-45979.

Matsuo, K., Galson, D.L., Zhao, C., Peng, L., Laplace, C., Wang, K.Z., Bachler, M.A., Amano, H., Aburatani, H., Ishikawa, H.*, et al.* (2004). Nuclear factor of activated T-cells (NFAT) rescues osteoclastogenesis in precursors lacking c-Fos. J Biol Chem *279*, 26475-26480.

McHugh, K.P., Hodivala-Dilke, K., Zheng, M.H., Namba, N., Lam, J., Novack, D., Feng, X., Ross, F.P., Hynes, R.O., and Teitelbaum, S.L. (2000). Mice lacking beta3 integrins are osteosclerotic because of dysfunctional osteoclasts. J Clin Invest *105*, 433-440.

McKeller, R.N., Fowler, J.L., Cunningham, J.J., Warner, N., Smeyne, R.J., Zindy, F., and Skapek, S.X. (2002). The Arf tumor suppressor gene promotes hyaloid vascular regression during mouse eye development. Proc Natl Acad Sci U S A *99*, 3848-3853.

Melendez, B., Malumbres, M., Perez de Castro, I., Santos, J., Pellicer, A., and Fernandez-Piqueras, J. (2000). Characterization of the murine p19(ARF) promoter CpG island and its methylation pattern in primary lymphomas. Carcinogenesis *21*, 817-821.

Miceli, A.P., Saporita, A.J., and Weber, J.D. (2011) Hyper-growth mTOR signals translationally activate the ARF tumor suppressor checkpoint. Mol Cell Biol. In Review.

Minkin, C. (1982). Bone acid phosphatase: tartrate-resistant acid phosphatase as a marker of osteoclast function. Calcif Tissue Int *34*, 285-290.

Momand, J., Zambetti, G.P., Olson, D.C., George, D., and Levine, A.J. (1992). The mdm-2 oncogene product forms a complex with the p53 protein and inhibits p53-mediated transactivation. Cell *69*, 1237-1245.

Montes de Oca Luna, R., Wagner, D.S., and Lozano, G. (1995). Rescue of early embryonic lethality in mdm2-deficient mice by deletion of p53. Nature *378*, 203-206.

Nakamura, M., Watanabe, T., Klangby, U., Asker, C., Wiman, K., Yonekawa, Y., Kleihues, P., and Ohgaki, H. (2001). p14ARF deletion and methylation in genetic pathways to glioblastomas. Brain Pathol *11*, 159-168.

Nishi, Y., Atley, L., Eyre, D.E., Edelson, J.G., Superti-Furga, A., Yasuda, T., Desnick, R.J., and Gelb, B.D. (1999). Determination of bone markers in pycnodysostosis: effects of cathepsin K deficiency on bone matrix degradation. J Bone Miner Res *14*, 1902-1908.

Nozawa, Y., Van Belzen, N., Van der Made, A.C., Dinjens, W.N., and Bosman, F.T. (1996). Expression of nucleophosmin/B23 in normal and neoplastic colorectal mucosa. J Pathol *178*, 48-52.

Olanich, M.E., Moss, B.L., Piwnica-Worms, D., Townsend, R.R., and Weber, J.D. Identification of FUSE-binding protein 1 as a regulatory mRNA-binding protein that represses nucleophosmin translation. Oncogene *30*, 77-86.

Oliner, J.D., Pietenpol, J.A., Thiagalingam, S., Gyuris, J., Kinzler, K.W., and Vogelstein, B. (1993). Oncoprotein MDM2 conceals the activation domain of tumour suppressor p53. Nature *362*, 857-860.

Ozenne, P., Eymin, B., Brambilla, E., and Gazzeri, S. The ARF tumor suppressor: structure, functions and status in cancer. Int J Cancer *127*, 2239-2247.

Palmero, I., Pantoja, C., and Serrano, M. (1998). p19ARF links the tumour suppressor p53 to Ras. Nature *395*, 125-126.

Partington, G.A., Fuller, K., Chambers, T.J., and Pondel, M. (2004). Mitf-PU.1 interactions with the tartrate-resistant acid phosphatase gene promoter during osteoclast differentiation. Bone *34*, 237-245.

Pasmant, E., Laurendeau, I., Heron, D., Vidaud, M., Vidaud, D., and Bieche, I. (2007). Characterization of a germ-line deletion, including the entire INK4/ARF locus, in a melanoma-neural system tumor family: identification of ANRIL, an antisense noncoding RNA whose expression coclusters with ARF. Cancer Res *67*, 3963-3969.

Pelletier, C.L., Maggi, L.B., Jr., Brady, S.N., Scheidenhelm, D.K., Gutmann, D.H., and Weber, J.D. (2007). TSC1 sets the rate of ribosome export and protein synthesis through nucleophosmin translation. Cancer Res *67*, 1609-1617.

Pich, A., Chiusa, L., and Margaria, E. (2000). Prognostic relevance of AgNORs in tumor pathology. Micron *31*, 133-141.

Qi, Y., Gregory, M.A., Li, Z., Brousal, J.P., West, K., and Hann, S.R. (2004). p19ARF directly and differentially controls the functions of c-Myc independently of p53. Nature *431*, 712-717.

Quelle, D.E., Zindy, F., Ashmun, R.A., and Sherr, C.J. (1995). Alternative reading frames of the INK4a tumor suppressor gene encode two unrelated proteins capable of inducing cell cycle arrest. Cell *83*, 993-1000.

Randerson-Moor, J.A., Harland, M., Williams, S., Cuthbert-Heavens, D., Sheridan, E., Aveyard, J., Sibley, K., Whitaker, L., Knowles, M., Bishop, J.N.*, et al.* (2001). A germline deletion of p14(ARF) but not CDKN2A in a melanoma-neural system tumour syndrome family. Hum Mol Genet *10*, 55-62.

Rauch, D.A., Hurchla, M.A., Harding, J.C., Deng, H., Shea, L.K., Eagleton, M.C., Niewiesk, S., Lairmore, M.D., Piwnica-Worms, D., Rosol, T.J.*, et al.* The ARF tumor suppressor regulates bone remodeling and osteosarcoma development in mice. PLoS One *5*, e15755.

Ringshausen, I., O'Shea, C.C., Finch, A.J., Swigart, L.B., and Evan, G.I. (2006). Mdm2 is critically and continuously required to suppress lethal p53 activity in vivo. Cancer Cell *10*, 501-514.

Rizos, H., Puig, S., Badenas, C., Malvehy, J., Darmanian, A.P., Jimenez, L., Mila, M., and Kefford, R.F. (2001). A melanoma-associated germline mutation in exon 1beta inactivates p14ARF. Oncogene *20*, 5543-5547.

Rizos, H., Woodruff, S., and Kefford, R.F. (2005). p14ARF interacts with the SUMO-conjugating enzyme Ubc9 and promotes the sumoylation of its binding partners. Cell Cycle *4*, 597-603.

Robertson, K.D., and Jones, P.A. (1998). The human ARF cell cycle regulatory gene promoter is a CpG island which can be silenced by DNA methylation and down-regulated by wild-type p53. Mol Cell Biol *18*, 6457-6473.

Roth, J., Dobbelstein, M., Freedman, D.A., Shenk, T., and Levine, A.J. (1998). Nucleo-cytoplasmic shuttling of the hdm2 oncoprotein regulates the levels of the p53 protein via a pathway used by the human immunodeficiency virus rev protein. EMBO J *17*, 554-564.

Ruggero, D., and Pandolfi, P.P. (2003). Does the ribosome translate cancer? Nat Rev Cancer *3*, 179-192.

Ruvinsky, I., and Meyuhas, O. (2006). Ribosomal protein S6 phosphorylation: from protein synthesis to cell size. Trends Biochem Sci *31*, 342-348.

Sabatini, D.M., Pierchala, B.A., Barrow, R.K., Schell, M.J., and Snyder, S.H. (1995). The rapamycin and FKBP12 target (RAFT) displays phosphatidylinositol 4-kinase activity. J Biol Chem *270*, 20875-20878.

Sabers, C.J., Martin, M.M., Brunn, G.J., Williams, J.M., Dumont, F.J., Wiederrecht, G., and Abraham, R.T. (1995). Isolation of a protein target of the FKBP12-rapamycin complex in mammalian cells. J Biol Chem *270*, 815-822.

Saftig, P., Hunziker, E., Wehmeyer, O., Jones, S., Boyde, A., Rommerskirch, W., Moritz, J.D., Schu, P., and von Figura, K. (1998). Impaired osteoclastic bone resorption leads to osteopetrosis in cathepsin-K-deficient mice. Proc Natl Acad Sci U S A *95*, 13453-13458.

Savkur, R.S., and Olson, M.O. (1998). Preferential cleavage in pre-ribosomal RNA byprotein B23 endoribonuclease. Nucleic Acids Res *26*, 4508-4515.

Schlesinger, P.H., Blair, H.C., Teitelbaum, S.L., and Edwards, J.C. (1997). Characterization of the osteoclast ruffled border chloride channel and its role in bone resorption. J Biol Chem *272*, 18636-18643.

Scimeca, J.C., Franchi, A., Trojani, C., Parrinello, H., Grosgeorge, J., Robert, C., Jaillon, O., Poirier, C., Gaudray, P., and Carle, G.F. (2000). The gene encoding the mouse homologue of the human osteoclast-specific 116-kDa V-ATPase subunit bears a deletion in osteosclerotic (oc/oc) mutants. Bone *26*, 207-213.

Scott, E.W., Simon, M.C., Anastasi, J., and Singh, H. (1994). Requirement of transcription factor PU.1 in the development of multiple hematopoietic lineages. Science *265*, 1573-1577.

Sehgal, S.N. (2003). Sirolimus: its discovery, biological properties, and mechanism of action. Transplant Proc *35*, 7S-14S.

Serrano, M., Hannon, G.J., and Beach, D. (1993). A new regulatory motif in cell-cycle control causing specific inhibition of cyclin D/CDK4. Nature *366*, 704-707.

Sharpless, N.E. (2005). INK4a/ARF: a multifunctional tumor suppressor locus. Mutat Res *576*, 22-38.

Sharpless, N.E., Ramsey, M.R., Balasubramanian, P., Castrillon, D.H., and DePinho, R.A. (2004). The differential impact of p16(INK4a) or p19(ARF) deficiency on cell growth and tumorigenesis. Oncogene *23*, 379-385.

Sherr, C.J. (1996). Cancer cell cycles. Science *274*, 1672-1677.

Sherr, C.J. (2000). The Pezcoller lecture: cancer cell cycles revisited. Cancer Res *60*, 3689-3695.

Sherr, C.J. (2001). The INK4a/ARF network in tumour suppression. Nat Rev Mol Cell Biol *2*, 731-737.

Sherr, C.J. (2006). Divorcing ARF and p53: an unsettled case. Nat Rev Cancer *6*, 663-673.

Sherr, C.J., Rettenmier, C.W., and Roussel, M.F. (1988). Macrophage colony-stimulating factor, CSF-1, and its proto-oncogene-encoded receptor. Cold Spring Harb Symp Quant Biol *53 Pt 1*, 521-530.

Sherr, C.J., and Weber, J.D. (2000). The ARF/p53 pathway. Curr Opin Genet Dev *10*, 94-99.

Shields, L.B., Gercel-Taylor, C., Yashar, C.M., Wan, T.C., Katsanis, W.A., Spinnato, J.A., and Taylor, D.D. (1997). Induction of immune responses to ovarian tumor antigens by multiparity. J Soc Gynecol Investig *4*, 298-304.

Silva, R.L., Thornton, J.D., Martin, A.C., Rehg, J.E., Bertwistle, D., Zindy, F., and Skapek, S.X. (2005). Arf-dependent regulation of Pdgf signaling in perivascular cells in the developing mouse eye. EMBO J *24*, 2803-2814.

Singh, H., DeKoter, R.P., and Walsh, J.C. (1999). PU.1, a shared transcriptional regulator of lymphoid and myeloid cell fates. Cold Spring Harb Symp Quant Biol *64*, 13-20.

Skaar, T.C., Prasad, S.C., Sharareh, S., Lippman, M.E., Brunner, N., and Clarke, R. (1998). Two-dimensional gel electrophoresis analyses identify nucleophosmin as an estrogen regulated protein associated with acquired estrogen-independence in human breast cancer cells. J Steroid Biochem Mol Biol *67*, 391-402.

Sly, W.S., and Hu, P.Y. (1995). Human carbonic anhydrases and carbonic anhydrase deficiencies. Annu Rev Biochem *64*, 375-401.

Soriano, P., Montgomery, C., Geske, R., and Bradley, A. (1991). Targeted disruption of the c-src proto-oncogene leads to osteopetrosis in mice. Cell *64*, 693-702.

Sreeramaneni, R., Chaudhry, A., McMahon, M., Sherr, C.J., and Inoue, K. (2005). Ras-Raf-Arf signaling critically depends on the Dmp1 transcription factor. Mol Cell Biol *25*, 220-232.

Stickens, D., Behonick, D.J., Ortega, N., Heyer, B., Hartenstein, B., Yu, Y., Fosang, A.J., Schorpp-Kistner, M., Angel, P., and Werb, Z. (2004). Altered endochondral bone development in matrix metalloproteinase 13-deficient mice. Development *131*, 5883-5895.

Stott, F.J., Bates, S., James, M.C., McConnell, B.B., Starborg, M., Brookes, S., Palmero, I., Ryan, K., Hara, E., Vousden, K.H.*, et al.* (1998). The alternative product from the human CDKN2A locus, p14(ARF), participates in a regulatory feedback loop with p53 and MDM2. EMBO J *17*, 5001-5014.

Subong, E.N., Shue, M.J., Epstein, J.I., Briggman, J.V., Chan, P.K., and Partin, A.W. (1999). Monoclonal antibody to prostate cancer nuclear matrix protein (PRO:4-216) recognizes nucleophosmin/B23. Prostate *39*, 298-304.

Sugimoto, M., Kuo, M.L., Roussel, M.F., and Sherr, C.J. (2003). Nucleolar Arf tumor suppressor inhibits ribosomal RNA processing. Mol Cell *11*, 415-424.

Suter, A., Everts, V., Boyde, A., Jones, S.J., Lullmann-Rauch, R., Hartmann, D., Hayman, A.R., Cox, T.M., Evans, M.J., Meister, T.*, et al.* (2001). Overlapping functions of lysosomal acid phosphatase (LAP) and tartrate-resistant acid phosphatase (Acp5) revealed by doubly deficient mice. Development *128*, 4899-4910.

Takayanagi, H., Kim, S., Koga, T., Nishina, H., Isshiki, M., Yoshida, H., Saiura, A., Isobe, M., Yokochi, T., Inoue, J.*, et al.* (2002). Induction and activation of the transcription factor NFATc1 (NFAT2) integrate RANKL signaling in terminal differentiation of osteoclasts. Dev Cell *3*, 889-901.

Tanaka, M., Sasaki, H., Kino, I., Sugimura, T., and Terada, M. (1992). Genes preferentially expressed in embryo stomach are predominantly expressed in gastric cancer. Cancer Res *52*, 3372-3377.

Tanaka, S., Takahashi, N., Udagawa, N., Tamura, T., Akatsu, T., Stanley, E.R., Kurokawa, T., and Suda, T. (1993). Macrophage colony-stimulating factor is indispensable for both proliferation and differentiation of osteoclast progenitors. J Clin Invest *91*, 257-263.

Tao, W., and Levine, A.J. (1999). P19(ARF) stabilizes p53 by blocking nucleo-cytoplasmic shuttling of Mdm2. Proc Natl Acad Sci U S A *96*, 6937-6941.

Teitelbaum, S.L., and Ross, F.P. (2003). Genetic regulation of osteoclast development and function. Nat Rev Genet *4*, 638-649.

Terada, N., Patel, H.R., Takase, K., Kohno, K., Nairn, A.C., and Gelfand, E.W. (1994). Rapamycin selectively inhibits translation of mRNAs encoding elongation factors and ribosomal proteins. Proc Natl Acad Sci U S A *91*, 11477-11481.

Thanos, D., and Maniatis, T. (1995). NF-kappa B: a lesson in family values. Cell *80*, 529-532.

Thesingh, C.W., and Scherft, J.P. (1985). Fusion disability of embryonic osteoclast precursor cells and macrophages in the microphthalmic osteopetrotic mouse. Bone *6*, 43-52.

Tondravi, M.M., McKercher, S.R., Anderson, K., Erdmann, J.M., Quiroz, M., Maki, R., and Teitelbaum, S.L. (1997). Osteopetrosis in mice lacking haematopoietic transcription factor PU.1. Nature *386*, 81-84.

Tsui, K.H., Cheng, A.J., Chang, P.L., Pan, T.L., and Yung, B.Y. (2004). Association of nucleophosmin/B23 mRNA expression with clinical outcome in patients with bladder carcinoma. Urology *64*, 839-844.

Udagawa, N., Takahashi, N., Akatsu, T., Tanaka, H., Sasaki, T., Nishihara, T., Koga, T., Martin, T.J., and Suda, T. (1990). Origin of osteoclasts: mature monocytes and macrophages are capable of differentiating into osteoclasts under a suitable microenvironment prepared by bone marrow-derived stromal cells. Proc Natl Acad Sci U S A *87*, 7260-7264.

Vassilev, L.T., Vu, B.T., Graves, B., Carvajal, D., Podlaski, F., Filipovic, Z., Kong, N., Kammlott, U., Lukacs, C., Klein, C*., et al.* (2004). In vivo activation of the p53 pathway by small-molecule antagonists of MDM2. Science *303*, 844-848.

Vu, T.H., Shipley, J.M., Bergers, G., Berger, J.E., Helms, J.A., Hanahan, D., Shapiro, S.D., Senior, R.M., and Werb, Z. (1998). MMP-9/gelatinase B is a key regulator of growth plate angiogenesis and apoptosis of hypertrophic chondrocytes. Cell *93*, 411-422.

Wagner, E.F., and Eferl, R. (2005). Fos/AP-1 proteins in bone and the immune system. Immunol Rev *208*, 126-140.

Wang, H., Wang, L., Erdjument-Bromage, H., Vidal, M., Tempst, P., Jones, R.S., and Zhang, Y. (2004). Role of histone H2A ubiquitination in Polycomb silencing. Nature *431*, 873-878.

Wang, Z.Q., Ovitt, C., Grigoriadis, A.E., Mohle-Steinlein, U., Ruther, U., and Wagner, E.F. (1992). Bone and haematopoietic defects in mice lacking c-fos. Nature *360*, 741-745.

Weber, J.D., Jeffers, J.R., Rehg, J.E., Randle, D.H., Lozano, G., Roussel, M.F., Sherr, C.J., and Zambetti, G.P. (2000). p53-independent functions of the p19(ARF) tumor suppressor. Genes Dev *14*, 2358-2365.

Weber, J.D., Taylor, L.J., Roussel, M.F., Sherr, C.J., and Bar-Sagi, D. (1999). Nucleolar Arf sequesters Mdm2 and activates p53. Nat Cell Biol *1*, 20-26.

Woo, K.M., Kim, H.M., and Ko, J.S. (2002). Macrophage colony-stimulating factor promotes the survival of osteoclast precursors by up-regulating Bcl-X(L). Exp Mol Med *34*, 340-346.

Yao, G.Q., Sun, B.H., Weir, E.C., and Insogna, K.L. (2002). A role for cell-surface CSF-1 in osteoblast-mediated osteoclastogenesis. Calcif Tissue Int *70*, 339-346.

Yasuda, H., Shima, N., Nakagawa, N., Yamaguchi, K., Kinosaki, M., Mochizuki, S., Tomoyasu, A., Yano, K., Goto, M., Murakami, A*., et al.* (1998). Osteoclast differentiation factor is a ligand for osteoprotegerin/osteoclastogenesis-inhibitory factor and is identical to TRANCE/RANKL. Proc Natl Acad Sci U S A *95*, 3597-3602.

Yoshida, H., Hayashi, S., Kunisada, T., Ogawa, M., Nishikawa, S., Okamura, H., Sudo, T., and Shultz, L.D. (1990). The murine mutation osteopetrosis is in the coding region of the macrophage colony stimulating factor gene. Nature *345*, 442-444.

Young, N.P., and Jacks, T. Tissue-specific p19Arf regulation dictates the response to oncogenic K-ras. Proc Natl Acad Sci U S A *107*, 10184-10189.

Yu, Y., Maggi, L.B., Jr., Brady, S.N., Apicelli, A.J., Dai, M.S., Lu, H., and Weber, J.D. (2006). Nucleophosmin is essential for ribosomal protein L5 nuclear export. Mol Cell Biol *26*, 3798-3809.

Yun, J.P., Chew, E.C., Liew, C.T., Chan, J.Y., Jin, M.L., Ding, M.X., Fai, Y.H., Li, H.K., Liang, X.M., and Wu, Q.L. (2003). Nucleophosmin/B23 is a proliferate shuttle protein associated with nuclear matrix. J Cell Biochem *90*, 1140-1148.

Zemliakova, V.V., Strel'nikov, V.V., Zborovskaia, I.B., Balukova, O.V., Maiorova, O.A., Vasil'ev, E.V., Zaletaev, D.V., and Nemtsova, M.V. (2004). [Abnormal methylation of p16/CDKN2A AND p14/ARF genes GpG Islands in non-small cell lung cancer and in acute lymphoblastic leukemia]. Mol Biol (Mosk) *38*, 966-972.

Zheng, S., Chen, P., McMillan, A., Lafuente, A., Lafuente, M.J., Ballesta, A., Trias, M., and Wiencke, J.K. (2000). Correlations of partial and extensive methylation at the p14(ARF) locus with reduced mRNA expression in colorectal cancer cell lines and clinicopathological features in primary tumors. Carcinogenesis *21*, 2057-2064.

Zhu, M., Provis, J.M., and Penfold, P.L. (1999). The human hyaloid system: cellular phenotypes and inter-relationships. Exp Eye Res *68*, 553-563.

Zindy, F., Eischen, C.M., Randle, D.H., Kamijo, T., Cleveland, J.L., Sherr, C.J., and Roussel, M.F. (1998). Myc signaling via the ARF tumor suppressor regulates p53-dependent apoptosis and immortalization. Genes Dev *12*, 2424-2433.

Zindy, F., Williams, R.T., Baudino, T.A., Rehg, J.E., Skapek, S.X., Cleveland, J.L., Roussel, M.F., and Sherr, C.J. (2003). Arf tumor suppressor promoter monitors latent oncogenic signals in vivo. Proc Natl Acad Sci U S A *100*, 15930-15935.

Chapter 2

Cathepsin K-Cre Causes Unexpected Germline Deletion of Genes in Mice

2.1 Abstract

Cathepsin K-driven Cre is reported to be active solely in osteoclasts and is the most relevant tool for generating osteoclast-specific gene loss. We generated *Ctsk*$^{Cre/+}$; *ROSA*$^{+}$ mice and found Cre activity present in gametes, resulting in germline deletion of genes upon breeding with floxed-gene mice. Together with our finding that *Ctsk*$^{Cre/+}$ mice display enhanced estrogen levels, these results raise concerns regarding *in vivo* bone phenotypes created using *Ctsk*$^{Cre/+}$ mice.

2.2 Introduction and Results

Cathepsin K is a lysosomal cysteine protease of the papain family that is secreted by osteoclasts during bone resorption and functions as the primary protease in the degradation of type I collagen (Georges et al., 2009; Troen, 2004; Zaidi et al., 2001). In partially replacing the *Ctsk* locus with *Cre*, one allele of *Ctsk* is lost; however, $Ctsk^{+/-}$ mice are capable of maintaining normal bone turnover (Saftig et al., 1998). During mouse development, Cathepsin K expression is highest in musculoskeletal tissues and predominantly expressed in osteoclasts (Rantakokko et al., 1996). Furthermore, expression of Cre mRNA in $Ctsk^{Cre/+}$ mice was demonstrated to be unique to bone, with Cre activity evident only in osteoclasts (Nakamura et al., 2007).

In lieu of generating our own osteoclast-specific genetic mouse models, we first sought to confirm that Cre activity was unique to osteoclasts in $Ctsk^{Cre/+}$ mice. Thus, we crossed $Ctsk^{Cre/+}$ mice with $Rosa^{+}$ reporter mice. Ovary and testis tissues from $Rosa^{+}$; $Ctsk^{Cre/+}$ mice were analyzed for Cre activity by LacZ staining. In ovaries of $Ctsk^{Cre/+};Rosa^{+}$ mice, Cre activity was primarily detected in the oocytes and granulosa cells, whereas Cre activity was not detected in $Ctsk^{+/+};Rosa^{+}$ female mice (Figure 2.1a). In testes, abundant staining was evident in spermatozoa, which are the haploid and mature gametes. Again, Cre activity was not detected in $Ctsk^{+/+};Rosa^{+}$ male mice (Figure 2.1b). This data demonstrates that Cathepsin K-driven Cre activity is present in gametes of both female and male mice. Of note, only one *Cre* allele was necessary for DNA excision at the *Rosa* locus. Given this data, we investigated the presence of Cre and Cathepsin K mRNAs in ovary and testis tissues. We isolated ovary and testis RNA and quantified Cathepsin K and Cre mRNA by qRT-PCR. In ovaries of 10-week-old wild-

type mice, we detected Cathepsin K mRNA. Cathepsin K mRNA decreased as *Ctsk* was replaced by *Cre*. Accordingly, we detected increasing amounts of Cre mRNA as Cathepsin K mRNA decreased (Figure 2.2a,b). Similar results for Cathepsin K mRNA were obtained using testes RNA from 8-week-old mice, albeit at much lower levels relative to that observed in ovaries. Importantly, we again detected a dose-dependent decrease in Cathepsin K mRNA as Cre mRNA levels increased in testes (Figure 2.2a,b). Given the presence of Cathepsin K mRNA in ovaries, we analyzed ovary tissues from 16-week-old mice for the presence of Cathepsin K by immunohistochemistry (IHC). Our results indicate that Cathepsin K is expressed at the protein level in ovaries and is primarily localized to oocytes within the developing follicles (Figure 2.2c). Furthermore, we noted that follicles expressing Cathepsin K were primarily those in the early stages of maturation. As a control, adjacent tissue sections were stained with or without primary antibody. Sections incubated without antibody were negative for Cathepsin K in positive areas of the adjacent section that was incubated with primary antibody (Figure 2.2c). These results indicate that Cathepsin K is present in mouse ovaries and may be expressed at a specific stage during follicle development.

To determine if $Ctsk^{Cre/+}$ mice would produce germline loss of a floxed gene, we crossed $Ctsk^{Cre/+}$ mice with mice containing floxed *exon1β* of the ARF tumor suppressor (Gromley et al., 2009). A primer set used to detect the presence of the 5' loxP site in tail DNA of $Arf^{fl/fl}$ mice was unable to amplify a product, suggesting the loss of template (Figure 2.3). We next confirmed the presence of DNA using control primers. Again, the results suggest that although DNA is clearly present in all samples, the primers we used to detect the 5' loxP site are unable to recognize a template. We therefore reasoned that

exon1β of *Arf* was not present in the tail DNA. To test this, we used two different primers sets that each contained a forward and reverse complementary sequence to a region of DNA outside of the loxP sites (Figure 2.3). Both sets of primers resulted in products that suggested the loss of exon1β (Figure 2.3). All results were repeated using DNA generated from ear tissue (data not shown). To confirm germline *Arf* loss, we exploited the fact that the testis is the only tissue in which others and we have been able to detect ARF protein by IHC (Gromley et al., 2009). Testes from mice, in which *exon1β* of *Arf* had seemingly been excised, were analyzed by IHC for ARF protein expression. While we detected ARF in wild-type mice, we were unable to detect ARF protein expression in a mouse showing loss of *exon1β* at the DNA level (Figure 2.4a). These results imply that one copy of *Cre* under the control of the *Ctsk* promoter is sufficient to cause non-specific recombination and result in germline *Arf* loss. Germline deletion of *Arf* in the mouse results in a 100% penetrant spontaneous tumor formation phenotype. To confirm germline *Arf* loss, we followed $Ctsk^{Cre/+}$; $Arf^{fl/fl}$ mice whose genotype indicated a loss of *Arf* to determine if they would develop spontaneous tumors reminiscent of germline *Arf*-null animals. All mice (100% penetrant) displayed a tumor type with the onset and tumor type comparable to those published for traditional *Arf*-/- mice (Kamijo et al., 1999) (Figure 2.4b,c). This data demonstrates that crossing mice containing a floxed gene with $Ctsk^{Cre/+}$ mice can result in germline loss of the floxed gene. Finally, given that we observed Cathepsin K expression in ovaries, we assessed whether loss of *Ctsk* in $Ctsk^{Cre/Cre}$ mice would alter serum estrogen levels. We examined the levels of estrogen (as measured by serum estradiol) in wild-type and $Ctsk^{Cre/Cre}$ ($Ctsk^{-/-}$) mice. In the absence of *Ctsk*, estrogen

levels doubled that observed in wild-type mice (Figure 2.5), implying that Cathepsin K counteracts the production and/or release of estrogen into the blood of female mice.

2.3 Discussion

Together, our results demonstrate that Cathepsin K is expressed in gametes and this expression can result in germline excision of a floxed allele when using $Ctsk^{Cre/+}$ mice. Within the ovary, we observed Cathepsin K protein expression primarily in oocytes. Data from Chiu *et al*. showing expression of Cathepsin K mRNA in mouse ovaries supports this finding (Chiu et al., 2004). Expression of Cathepsin K has also been noted in human ovary samples (Bromme and Okamoto, 1995). While there is no published role for Cathepsin K in ovaries, our data showing that Cathepsin K may be expressed during early stages of oocyte development suggests a possible role for Cathepsin K during oocyte maturation. Moreover, other Cathepsins have also been shown to be expressed during specific stages of follicle development in teleosts (Fabra and Cerda, 2004). In testis, Cre activity was noted within seminiferous tubules and was largely localized to mature spermatozoa. To support this finding, when creating transgenic mice that express Cre driven by the *Ctsk* promoter, Chiu *et al.* published the expression of Cre expression in the testis of multiple mouse lines (Chiu et al., 2004).

Upon crossing $Ctsk^{Cre/+}$ mice with $Arf^{fl/fl}$ mice, we generated germline *Arf* loss as demonstrated by PCR, IHC for ARF in testis, and disease phenotypes that mimic traditional *Arf*-null mice (Kamijo et al., 1999). These findings place into question previous data that has been generated using mice containing *Cre* driven by the *Ctsk* promoter to create osteoclast-specific knockouts (Chiu et al., 2004; Nakamura et al., 2007). We are not suggesting that all animal models with *Cre* under the control the *Ctsk* promoter will result in a genomic knockout as neither every follicle nor seminiferous tubules was positive for Cre activity. However, our data clearly indicate that careful

testing is necessary when using this mouse model to ensure that the intended gene excision has occurred only in osteoclasts and that results are correctly interpreted. It is especially important to consider a genotyping result in which both alleles appear to be floxed (based on a tail DNA sample); it is possible that this result reflects one floxed allele and one null allele (Figure 2.6). Finally, our results indicate that loss of Cathepsin K results in significantly increased circulating levels of estradiol, a well-studied regulator of bone physiology (Manolagas et al., 2002). Given that estrogen suppresses osteoclast activity while enhancing osteoblast activity, enhanced estrogen upon loss of *Cathepsin K* in ovaries may inadvertently affect the bone phenotype of an intended conditional knockout mouse.

2.4 Methods

Generation of $Ctsk^{Cre/+}$;$Rosa^{+}$ and $Ctsk^{Cre/+}$;$Arf^{fl/fl}$ mice.

All animals were used in protocols that were reviewed and approved by the Washington University Animal Studies Committee. $Ctsk^{Cre/+}$ mice and the $Rosa^{+}$ reporter mice have been described previously (Nakamura et al., 2007; Soriano, 1999). *Cathepsin K-Cre* "knockin" heterozygous mice ($Ctsk^{Cre/+}$; maintained on a C57BL/6 background) were crossed with mice heterozygous for an *R26R* allele, where a constitutively active chromosomal gene was manipulated to insert the *lacZ* gene such that the β-galactosidase protein is produced only following the removal of a "stuffer" fragment flanked by loxP sites ($Rosa^{+}$; maintained on a C57BL/6 background) to generate $Ctsk^{Cre/+}$; $Rosa^{+}$ mice. $Ctsk^{+/+}$; $Rosa^{+}$ mice served as controls. $Ctsk^{Cre/+}$ mice were also crossed with mice homozygous for a floxed allele of *Arf* where exon1β is flanked by loxP sites ($Arf^{fl/fl}$; maintained on a mixed background of C57BL/6 and 129SvJae, a kind gift from C. Sherr, St. Jude Children's Research Hospital) to generate $Ctsk^{Cre/+}$; $Arf^{fl/+}$. Subsequent rounds of matings of these offspring eventually yielded $Ctsk^{Cre/+}$; $Arf^{fl/fl}$ mice. Cohorts of these mice as well as other siblings consisting of various combinations of Cre and floxed *Arf* alleles were viable and fertile and also used for breeding in our studies. Tail and/or ear snips were used to prepare DNA for PCR-based genotyping as previously described (Truett et al., 2000). *Ctsk* wild-type and *Cre*-knockin alleles were detected using primers Ctsk-P1 5'-TTATTCCTTCCGCCAGGATG-3', Ctsk-P2 5'-TTGCTGTTATACTGCTTCTG-3' and Ctsk-P3 5'-TAGTTTTTACTGCCAGACCG-3'. When used together in a PCR reaction, a wild-type allele generates a 135bp fragment whereas the presence of *Cre* produces a

300bp fragment. *Arf* wild-type and floxed alleles were determined by using primers SpeLxF-30 5'-TTGCTACTTTACTGCAGCCAGACCACTAGG-3' and SpeLxR-30 5'-CTCGGAGATTGAGAAAGCGGGAAGTCAAGC-3' in which the wild-type allele generates a 260bp product and the floxed allele generates a 360bp product. The presence of the *R26R* allele was assessed by amplification of a 320bp fragment using primers R26Rfwd 5'-AAAGTCGCTCTGAGTTGTTAT-3' and R26Rrev 5'-GCGAAGAGTTTGTCCTCAACC-3'. See Figure 2.3a for a list of primers and product sizes used to determine *Arf* recombination.

Tissue harvest and histology.

Testis and ovary tissues were taken from mice that were cardiac perfused with formalin, then fixed using a rapid microwave fixation technique (Lu et al., 2007). Fixed tissues were PBS washed then processed through graded alcohols and xylenes then embedded in paraffin. 5-µm tissue sections were immunostained. Alternatively, frozen testis and ovary tissues were prepared from sucrose-perfused mice, embedded in OCT over liquid nitrogen, sectioned at 5-µm and LacZ stained.

Immunostaining.

All sections were deparaffinized, rehydrated, washed in PBS, and blocked with serum-free Protein block (Dako) for 30min at room temperature. All immunostaining required antigen retrieval which was performed in a food steamer using a 1X Reveal decloaker buffer (pH 6.0, Biocare Medical). Antibodies for the following markers were diluted in Antibody diluents (Dako) and applied overnight at 4°C: rat anto-$p19^{ARF}$ (1:400,

Abcam) and rabbit anti-Cathepsin K (1:200, Abcam). A secondary antibody conjugated to Alexa Fluor 488 was incubated on tissue sections for 1hr at room temperature (1:300, Invitrogen). Nuclei were counterstained using *SlowFade* Gold Antifade reagent with 4',6-diamidino-2-phenylindole (DAPI) (Invitrogen).

Quantitative real-time PCR.

Ovary and testis tissues were isolated, flash-frozen in liquid nitrogen, and homogenized in RNA-Solv (Omega Bio-Tek). The SuperScript III first-strand synthesis system (Invitrogen) was used to generate first strand cDNA. Real-time PCR was performed with iQ SYBR Green Supermix (Bio-Rad) on an iCycler thermal cycler (Bio-Rad).

LacZ staining.

Frozen sections were air-dried for 30min at room temperature, then fixed in 2% paraformaldehyde/0.125% glutaraldehyde in 1x PBS pH 7.4 for 5min. Sections were then washed sequentially in 2mM $MgCl_2$ /PBS and 2mM $MgCl_2$, 0.02% Nonidet P40, 0.01% deoxycholate in PBS. Tissue sections were then washed briefly in LacZ staining buffer (5mM potassium ferrocyanide, 5mM potassium ferricyanide, 2mM $MgCl_2$, 1xPBS) and incubated in LacZ staining buffer supplemented with 1mg/ml X-Gal overnight at 37^{o}C with gentle shaking. Tissue sections were washed in diH_2O briefly and nuclei were counterstained with Nuclear Fast Red (Dako).

Microscopy and imaging.

Gross pathological images were captured using a Sony Cyber-shot 12.1 megapixel digital camera equipped with a Carl Zeiss 5x optical zoom wide (28mm) lens. Microscopy images for histology were obtained with a BX61 microscope (Olympus America), using the following objectives: UPlan Apochromatic 20X/NA 0.70 and UPlan Apochromatic 40X/NA 0.85. Tissue sections stained with LacZ were mounted with Krystalon (EMD) and coverslipped. Histological microscopy images were obtained with a DP70 color Bayer mosaic digital camera, Peltier device cooled to -10^{o}C (Olympus America). These images were captured with MicroSuite Biological Suite version 5 software (Olympus Soft Imaging Solutions) and resized and formatted with Adobe Photoshop CS3 software (Adobe Systems Incorporated). Fluorescence microscopy images were obtained with an Eclipse 90i microscope (Nikon) using the following objectives: Plan Apochromatic 10x/NA 0.45, Plan Apochromatic 20x/NA 0.75, and Plan Apochromatic Oil 100x/NA 1.40. Tissue sections for fluorescence microscopy images were mounted with *SlowFade* Gold Antifade reagent with DAPI (Invitrogen), coverslipped, and images were obtained using a CoolSnap HQ^{2} monochrome digital camera, Peltier cooled to -30^{o}C (Photometrics). Fluorescence images were captured with MetaMorph version 7.6 software, (MDS Analytical Technologies) and resized and formatted with Adobe Photoshop CS3 software (Adobe Systems Incorporated).

Estradiol Analysis.

Serum estradiol was measured using the Estradiol EIA Kit (Cayman Chemical). The developed color intensity is inversely proportional to the amount of free hormone in each sample and was quantified using an iMARK microplate reader (Bio-Rad).

Statistical analysis.

Data were analyzed using Excel (Microsoft Office). Results are expressed as the mean ±SD, and statistical significance was determined using a two-tailed t-test.

Acknowledgements

The authors would like to thank the members of the Weber laboratory for their advice and technical assistance and Steve Teitelbaum, Katherine Weilbaecher, Loren Michel, Mark Sands, Roberta Faccio, and Michelle Hurchla for insightful comments and reagents. This work was supported by NIH grant CA120436 and an Era of Hope Scholar Award in Breast Cancer Research (BC007304) to J.D.W.

Author Contributions

C.L.W., R.D.K., L.B.M., and J.D.W. designed experiments. C.L.W., R.D.K., M.L.B., and C.L. performed the experiments. C.L.W., R.D.K., L.B.M., and J.D.W. analyzed the data. C.L.W. and J.D.W. wrote the manuscript.

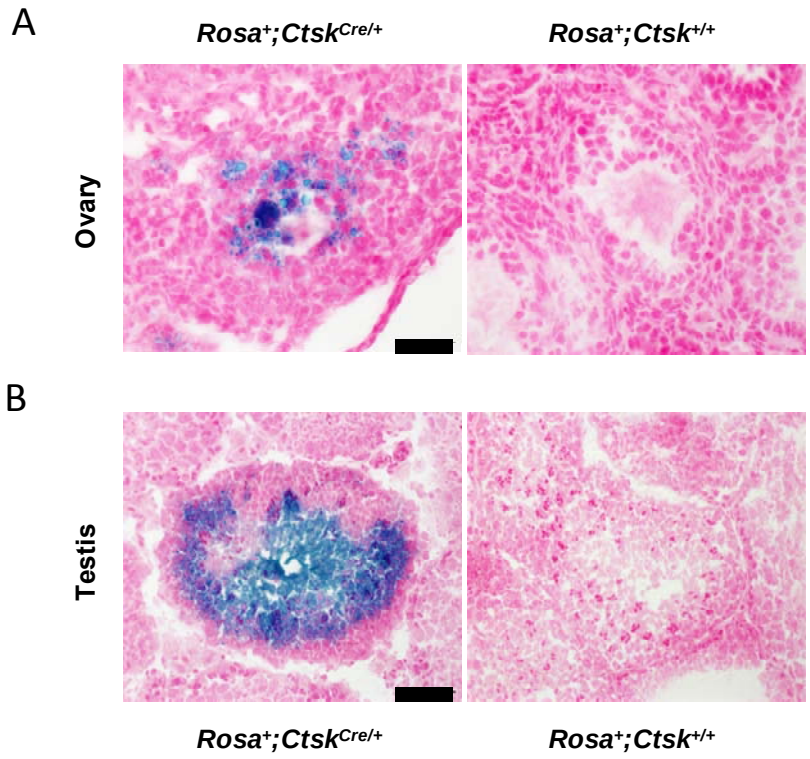

Figure 2.1.

Cre activity is present in the gametes of *Ctsk*$^{Cre/+}$ mice. Reproductive organs of indicated genotypes were analyzed for Cre activity by LacZ staining. (A) In ovaries of *Rosa*$^{+}$; *Ctsk*$^{Cre/+}$ mice, Cre activity was detected in oocytes and cells surrounding the developing oocytes (left panel). Controls were negative for LacZ staining (right panel). Scale bar = 50μM. (B) In testes of *Rosa*$^{+}$; *Ctsk*$^{Cre/+}$ mice, Cre activity was detected primarily in spermatozoa (left panel). Controls were negative for LacZ staining (right panel). Scale bar = 100μM.

A

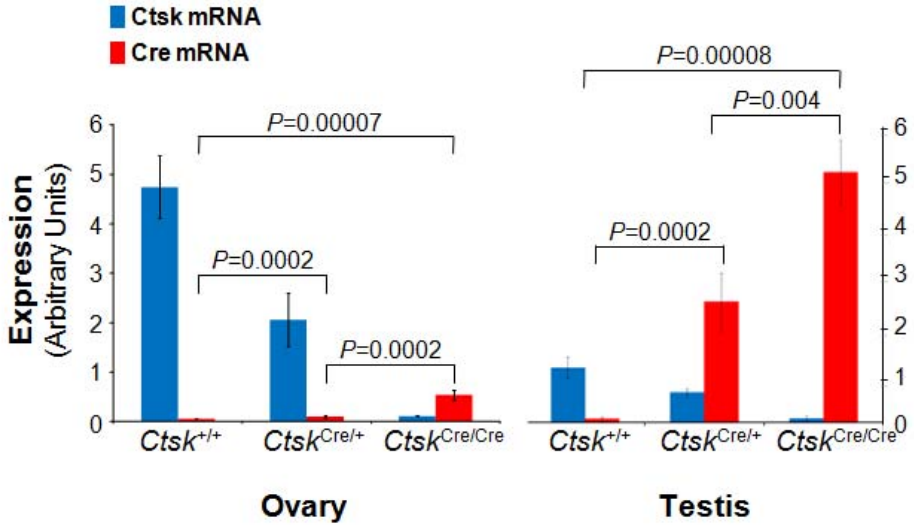
Ctsk mRNA
Cre mRNA
Expression
(Arbitrary Units)
P=0.00007
P=0.0002
P=0.0002
P=0.00008
P=0.004
P=0.0002
Ctsk+/+
CtskCre/+
CtskCre/Cre
Ctsk+/+
CtskCre/+
CtskCre/Cre
Ovary
Testis

B

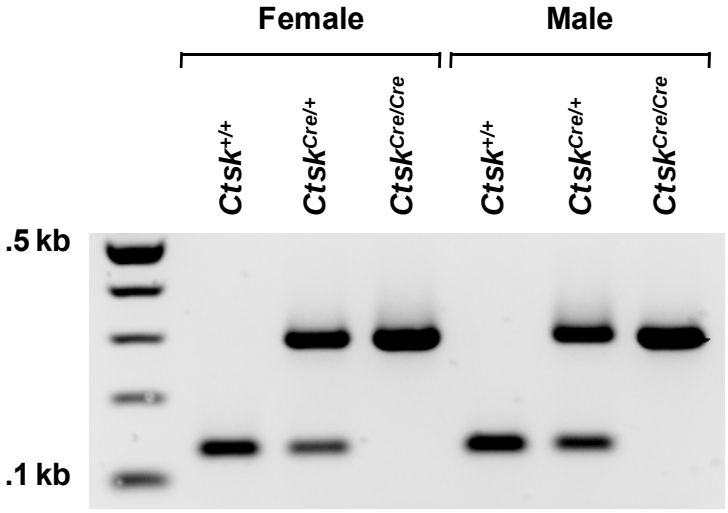
Female
Male
Ctsk+/+
CtskCre/+
CtskCre/Cre
Ctsk+/+
CtskCre/+
CtskCre/Cre
.5 kb
.1 kb

C

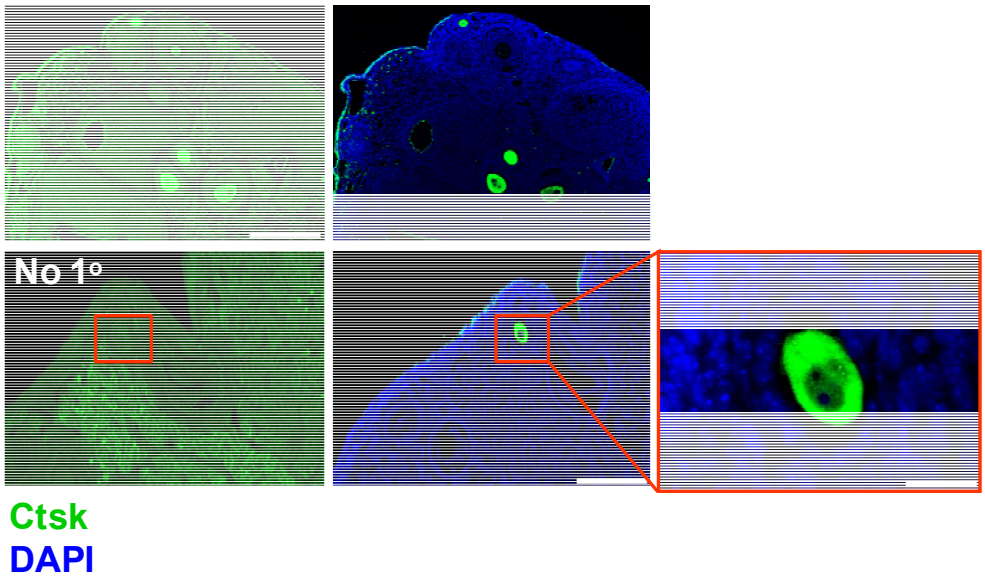

Figure 2.2.

Cathepsin K and Cre are detected in ovary and testis tissues. (A) Quantitative RT-PCR was used to quantify the presence of Cathepsin K mRNA (blue) and Cre mRNA (red) in ovary (left) and testis (right) for all indicated genotypes (n=3). Histone 3.3 was used as a control. Data are represented as means ±SD. A two-tailed t-test was used to generate indicated p values. (B) DNA was extracted from the tails of mice used for quantitative RT-PCR analysis to verify their genotypes. The top bands indicate the presence of Cre. The bottom band is indicative of a wild-type Cathepsin K allele. (C) Ovaries from WT mice analyzed by IHC for Cathepsin K. Top panels, scale bar = 200μM. Bottom, left panel shows staining without primary antibody. An adjacent section

to the control (bottom, middle) was incubated with primary antibody (scale bar = 100μM). Red box indicates positively-stained oocyte (bottom, right scale bar = 20μM).

A

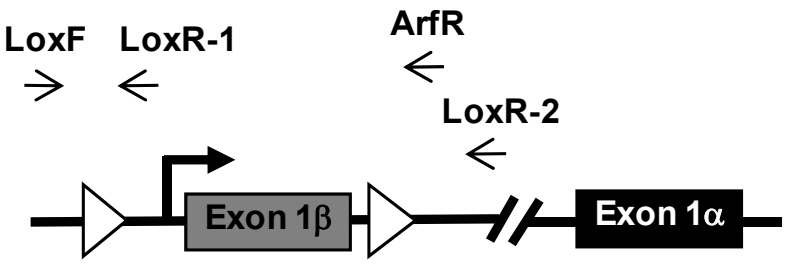

	Product Size		
Primer Pair	**WT**	**Floxed**	**KO**
LoxF/LoxR-1	262 bp	362 bp	N.A.
LoxF/ArfR	1651 bp	1851 bp	298 bp
LoxF/LoxR-2	1798 bp	1998 bp	445 bp

B

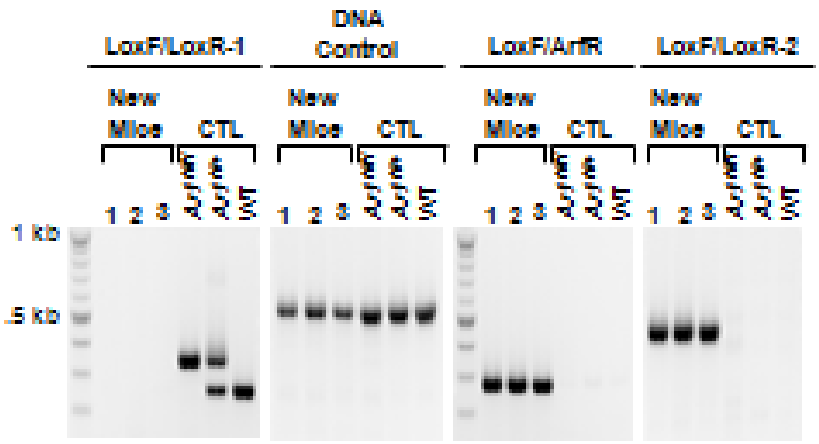

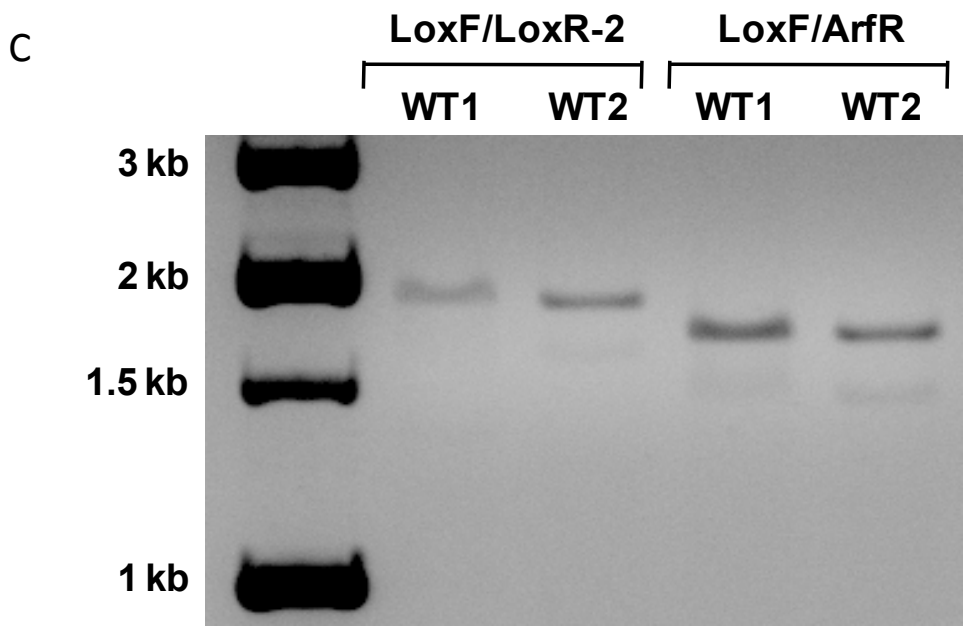

Figure 2.3.

Crossing *Arf*$^{fl/fl}$ mice with *Ctsk*$^{Cre/+}$ mice results in germline *Arf* loss. (A) Three sets of primer pairs were designed to detect the presence of floxed *exon 1beta*, which is unique to *Arf*. Controls are mice that were never crossed with *Ctsk*$^{Cre/+}$ mice. (B) PCR products were not detected upon genotyping new mice for the presence of the 5' loxP site using the first set of primers: LoxF/LoxR-1 (far left panel). This cannot be attributed to an absence of DNA as control primers detect DNA in all lanes (left middle panel). Two sets of primer pairs were used to detect the presence of *exon 1beta*. LoxF/ArfR results in a product size of 298bp in new mice, indicating a loss of *exon1*β (left middle panel).

LoxF/LoxR-2 results in a product size of 445bp when genotyping new mice, indicating a loss of *exon1*β (far right panel). (C) Primer sets used to detect the presence of *exon 1beta* in wild-type mice give a product of 1798bp (LoxF/LoxR-2, left) or 1651bp (LoxF/ArfR, right).

A

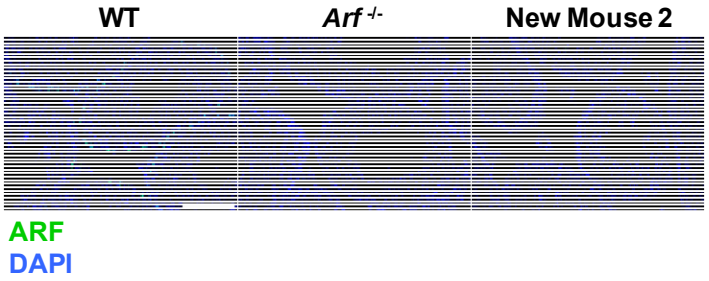
WT
Arf -/-
New Mouse 2
ARF
DAPI

B

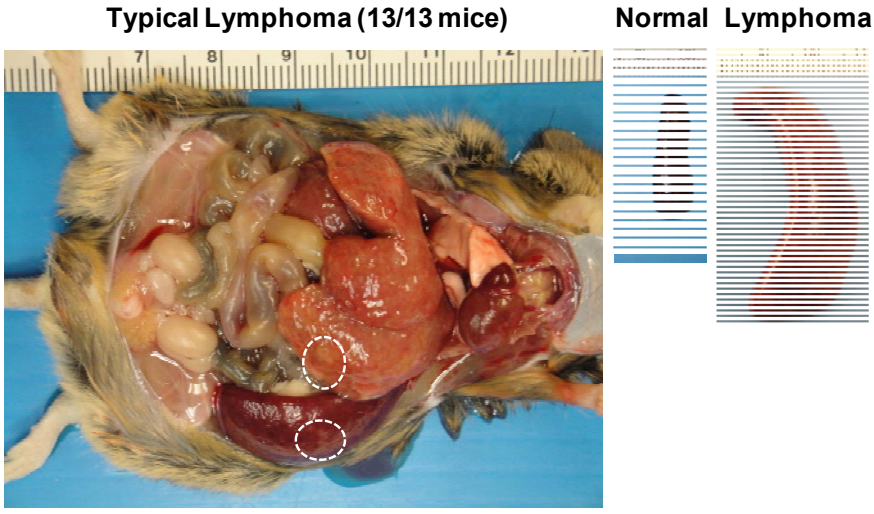
Typical Lymphoma (13/13 mice)
Normal
Lymphoma

C


Typical Fibrosarcoma (1/13 mice)

Figure 2.4.

Crossing *Arf* $^{fl/fl}$ mice with *Ctsk*$^{Cre/+}$ results in germline *Arf* loss. (A) Immunofluorescent staining for ARF in testis tissues indicates the loss of exon 1β at the protein level (scale bar = 100μM). (B,C) *Ctsk*$^{Cre/+}$; *Arf*$^{fl/fl}$ mice phenocopy traditional *Arf*$^{-/-}$ mice, displaying both (B) lymphomas and (C) fibrosarcomas.

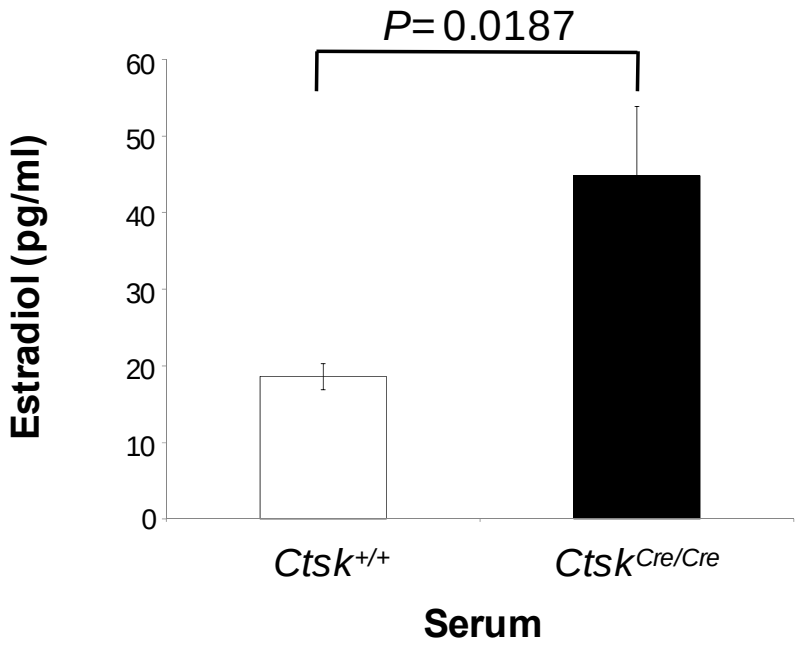

Figure 2.5.

Homozygous loss of *Cathepsin K* enhances serum estradiol levels. Serum from *Ctsk*$^{+/+}$ (wild-type, n=3) and *Ctsk*$^{Cre/Cre}$ (*Ctsk* $^{-/-}$, n=3) mice was analyzed for estradiol. Data are represented as means ±SD and p value was generated using a two-tailed t-test.

A

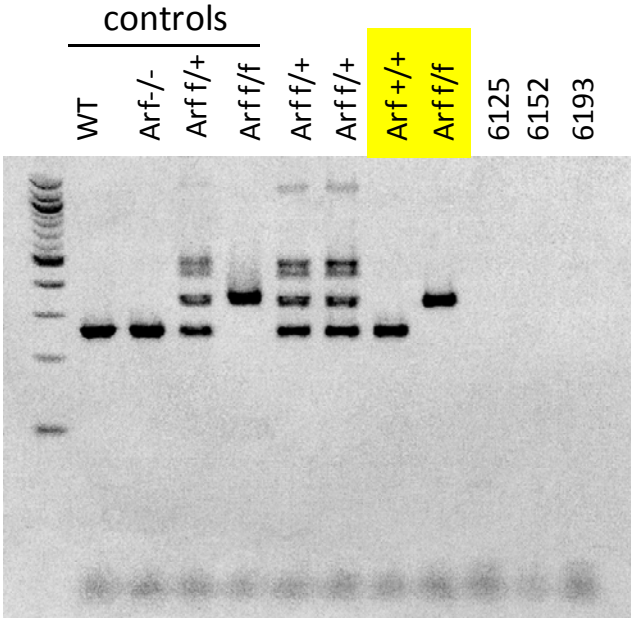
controls
WT
Arf-/-
Arf f/+
Arf f/f
Arf f/+
Arf f/+
Arf +/+
Arf f/f
6125
6152
6193

B

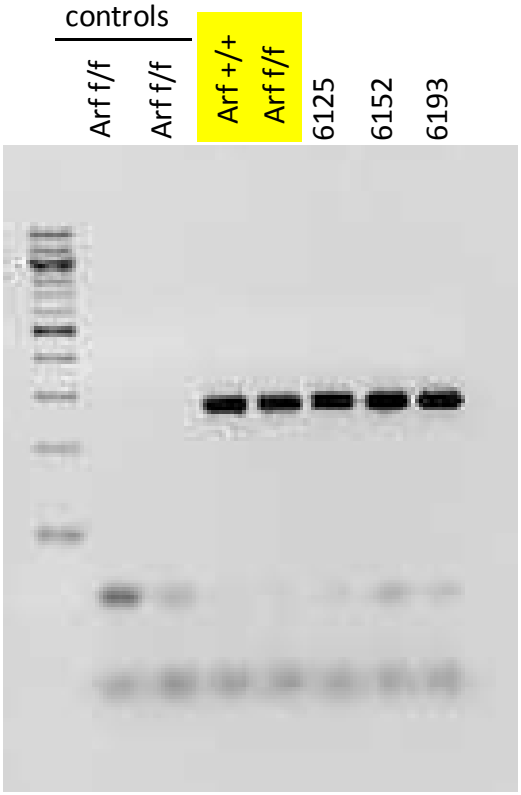
controls
Arf f/f
Arf f/f
Arf +/+
Arf f/f
6125
6152
6193

Figure 2.6.

Genotyping results can be misinterpreted when breeding floxed mice with *Ctsk*$^{Cre/+}$ mice. (A) DNA was extracted from tails of mice and genotyped for the presence of the exon 1β loxP site. The presence of a loxP site results in a 362bp band. In the absence of loxP (i.e. WT *Arf*), the band is 262bp (refer to Figure 2.3a for map). Controls are mice that were not bred with *Ctsk*$^{Cre/+}$ mice. Mice of interest are highlighted in yellow. Note that left mouse of interest appears to be *Arf*$^{+/+}$ and right mouse of interest appears to be *Arf*$^{fl/fl}$. (B) DNA from mice of interest are genotyped to detect the presence of exon 1β using LoxF/ArfR primers, which generate a band of 298bp if exon 1β is absent (refer to Figure 2.3a for map). Genotyping results indicate that exon 1β is absent on at least one allele. Thus, the mice of interest are actually *Arf*$^{+/-}$(left) and *Arf*$^{fl/-}$ (right).

2.6 References

Bromme, D., and Okamoto, K. (1995). Human cathepsin O2, a novel cysteine protease highly expressed in osteoclastomas and ovary molecular cloning, sequencing and tissue distribution. Biol Chem Hoppe Seyler *376*, 379-384.

Chiu, W.S., McManus, J.F., Notini, A.J., Cassady, A.I., Zajac, J.D., and Davey, R.A. (2004). Transgenic mice that express Cre recombinase in osteoclasts. Genesis *39*, 178-185.

Fabra, M., and Cerda, J. (2004). Ovarian cysteine proteinases in the teleost Fundulus heteroclitus: molecular cloning and gene expression during vitellogenesis and oocyte maturation. Mol Reprod Dev *67*, 282-294.

Georges, S., Ruiz Velasco, C., Trichet, V., Fortun, Y., Heymann, D., and Padrines, M. (2009). Proteases and bone remodelling. Cytokine Growth Factor Rev *20*, 29-41.

Gromley, A., Churchman, M.L., Zindy, F., and Sherr, C.J. (2009). Transient expression of the Arf tumor suppressor during male germ cell and eye development in Arf-Cre reporter mice. Proc Natl Acad Sci U S A *106*, 6285-6290.

Kamijo, T., Bodner, S., van de Kamp, E., Randle, D.H., and Sherr, C.J. (1999). Tumor spectrum in ARF-deficient mice. Cancer Res *59*, 2217-2222.

Lu, Z.H., Wright, J.D., Belt, B., Cardiff, R.D., and Arbeit, J.M. (2007). Hypoxia-inducible factor-1 facilitates cervical cancer progression in human papillomavirus type 16 transgenic mice. Am J Pathol *171*, 667-681.

Manolagas, S.C., Kousteni, S., and Jilka, R.L. (2002). Sex steroids and bone. Recent Prog Horm Res *57*, 385-409.

Nakamura, T., Imai, Y., Matsumoto, T., Sato, S., Takeuchi, K., Igarashi, K., Harada, Y., Azuma, Y., Krust, A., Yamamoto, Y*., et al.* (2007). Estrogen prevents bone loss via estrogen receptor alpha and induction of Fas ligand in osteoclasts. Cell *130*, 811-823.

Rantakokko, J., Aro, H.T., Savontaus, M., and Vuorio, E. (1996). Mouse cathepsin K: cDNA cloning and predominant expression of the gene in osteoclasts, and in some hypertrophying chondrocytes during mouse development. FEBS Lett *393*, 307-313.

Saftig, P., Hunziker, E., Wehmeyer, O., Jones, S., Boyde, A., Rommerskirch, W., Moritz, J.D., Schu, P., and von Figura, K. (1998). Impaired osteoclastic bone resorption leads to osteopetrosis in cathepsin-K-deficient mice. Proc Natl Acad Sci U S A *95*, 13453-13458.

Soriano, P. (1999). Generalized lacZ expression with the ROSA26 Cre reporter strain. Nat Genet *21*, 70-71.

Troen, B.R. (2004). The role of cathepsin K in normal bone resorption. Drug News Perspect *17*, 19-28.

Truett, G.E., Heeger, P., Mynatt, R.L., Truett, A.A., Walker, J.A., and Warman, M.L. (2000). Preparation of PCR-quality mouse genomic DNA with hot sodium hydroxide and tris (HotSHOT). Biotechniques *29*, 52, 54.

Zaidi, M., Troen, B., Moonga, B.S., and Abe, E. (2001). Cathepsin K, osteoclastic resorption, and osteoporosis therapy. J Bone Miner Res *16*, 1747-1749.

Chapter 3

The Role of ARF in Osteoclasts

3.1 Abstract

The ARF tumor suppressor is upregulated upon oncogenic stress and can halt proliferation in both p53-dependent and -independent mechanisms. With a focus on p53-independent ARF tumor suppression, we have previously demonstrated that basal ARF can suppress ribosome biogenesis, in part through the negative regulation of nucleophosmin, to ultimately suppress protein synthesis . Importantly, these findings were demonstrated using dividing mouse embryonic fibroblasts. Given that protein synthesis and the cell cycle are coordinately controlled, we questioned whether basal ARF regulates protein synthesis in a proliferation-independent context. Here we use the osteoclast as a model to study post-mitotic growth in a physiologically-relevant setting where protein synthesis is necessary for proper function.

Our results show that *Arf* loss enhances osteoclastogenesis *in vitro* as demonstrated by increased OC number and size, protein markers of osteoclastogenesis, and increased bone resorption relative to wild-type osteoclasts. Notably, enhanced osteoclastogenesis upon *Arf* loss is independent of both proliferation and p53. Furthermore, we demonstrated that ARF and NPM colocalize in wild-type osteoclasts, suggesting that ARF may be stiffening protein synthesis to maintain either osteoclastogenesis, osteoclast function, or both. Subsequent data revealed enhanced protein synthesis and ribosome activity during osteoclastogenesis upon *Arf*$^{-/-}$ loss relative to wild-type. To determine if ARF regulation of osteoclastogenesis has an impact on bone resorption *in vivo*, we generated radiation chimeras and challenged them with RANKL. We found that *Arf* loss results in elevated bone resorption as determined by a decrease in trabecular bone volume and bone mineral density. We confirmed that the increase in bone

resorption is due, at least in part, to increased osteoclastogenesis *in vivo*. This data collectively suggests that ARF regulates proliferation-independent cell growth, and is a function that is physiologically-relevant both *in vitro* and *in vivo*.

3.2 Introduction

The locus encoding the ARF tumor suppressor is unique in that it also encodes the $p16^{INK4a}$ tumor suppressor protein. In fact, these two tumor suppressor share two of their three exons and thus significant homology at the DNA and mRNA level. However, the first exon of *Arf* (exon1β) is distinctive and splices into the shared exons 2 and 3 such that *Arf* is translated in an alternative reading frame (hence the ARF moniker) (Quelle et al., 1995; Sherr, 2000). Given the arrangement of these two potent tumor suppressors, it is important that the cell tightly regulate this locus. Under normal conditions, the locus is repressed by polycomb repressive complexes (Aguilo et al.). However, in a state of oncogenic stress, the locus is turned on to regulated cell growth and proliferation.

ARF and INK4a are also distinctive in their mechanisms of tumor suppression. INK4a inhibits the cyclin D-dependent kinases, Cdk4 and Cdk6, from phosphorylating the retinoblastoma (Rb) tumor suppressor. In a hypophosphorylated state, Rb remains bound to E2F transcription factors, which prohibit them from transcriptionally instructing the cell to enter S phase (Serrano et al., 1993; Sharpless, 2005; Sherr, 1996). The ARF tumor suppressor is classically known to bind and sequester MDM2 in the nucleolus (Weber et al., 1999). This prevents MDM2 from interacting with p53, which is known to result in the shuttling of p53 into the cytoplasm, and act as an E3 ligase in the ubiquitination and targeting of p53 for proteasomal degradation (Haupt et al., 1997; Honda et al., 1997; Kubbutat et al., 1997; Roth et al., 1998). Interestingly, it was subsequently demonstrated that ARF overexpression can arrest *p53/Mdm2-null* and *Arf/p53/Mdm2-null* (designated triple knock-out or TKO) mouse embryonic fibroblasts (MEFs) (Weber et al., 2000a). Moreover, TKO mice develop a wider spectrum of tumors

and at a greater frequency compared to mice lacking both *p53* and *Mdm2* or *p53* alone (Weber et al., 2000a). These data were the first to genetically demonstrate that ARF can act as a tumor suppressor independently of its ability to regulate p53 activity. Since this study, a flurry of work has amounted to a list of around 30 ARF-interacting proteins that are believed to be important for ARF's p53-independent tumor-suppressive functions (Sherr, 2006). Among this list is nucleophosmin (NPM), which is known to be important for growth and development in mice (Grisendi et al., 2005) and has been attributed a variety of roles in cancer progression (Bernard et al., 2003; Brady et al., 2009; Grisendi et al., 2006; Nozawa et al., 1996; Shields et al., 1997; Skaar et al., 1998; Subong et al., 1999; Tanaka et al., 1992). NPM is one of the most characterized ARF-interacting proteins. It is well-known for its ability to shuttle between the nucleus and cytoplasm (Kang et al., 1974; Kang et al., 1975). In doing so, NPM transports key components of the ribosomal machinery to the cytoplasm for translation (Maggi et al., 2008; Yu et al., 2006). In fact, NPM is known to be a rate-limiting factor for protein translation as its loss results in decreased protein output and a build-up of ribosomes at the interior perimeter of the nucleus (Maggi et al., 2008). Importantly, ARF has been shown to counteract the nucleocytoplasmic shutting of NPM and, in this manner, acts as a p53-independent tumor suppressor (Brady et al., 2004).

The importance of ARF as a tumor suppressor is evident given that mice in which exon 1β has been specifically deleted begin developing tumors as early as 8 weeks of age (Kamijo et al., 1999). After one year, 80% of the mice succumb to spontaneous tumor development, namely sarcomas and lymphoid malignancies. $Arf^{+/-}$ mice also develop tumors, albeit after a longer latency relative to $Arf^{-/-}$ mice (Kamijo et al., 1999). In

humans, the locus encoding *Arf* is the second most commonly mutated locus (Hainaut et al., 1997; Hall and Peters, 1996). While it is often difficult to determine the individual roles of the multiple tumor suppressor encoded by the locus in human cancer, there are specific cases in which only *Arf* is affected. For example, deletion or mutation of *Arf* has been reported in glioblastoma patients, melanoma patients, and a family with melanoma-neural system tumor syndrome (Laud et al., 2006; Nakamura et al., 2001; Randerson-Moor et al., 2001; Rizos et al., 2001). Furthermore, the *Arf* promoter is known to be methylated and consequently silenced in many human cancers (Furonaka et al., 2004; Kominami et al., 2009; Konishi et al., 2002; Melendez et al., 2000; Zemliakova et al., 2004; Zheng et al., 2000).

As previously mentioned, normal conditions require that ARF levels be kept low, and thus ARF is nearly undetectable in the absence of oncogenic stress. Still, various functions have recently been ascribed to these basal levels of ARF. One of the first described roles of basal ARF was initiated based on the observation that $Arf^{-/-}$ mice have eyes that are slightly smaller than their wild-type counterparts (Kamijo et al., 1999; Kamijo et al., 1997; McKeller et al., 2002). Studies have since demonstrated that the hyaloid vascular system (HVS) in the vitreous of the eye fails to regress in the absence of *Arf* (McKeller et al., 2002). Using $Arf^{Gfp/+}$ mice to more closely examine the localization of ARF within the developing eye, it was determined that ARF was expressed in mural cells expressing platelet-derived growth factor receptor β (Pdgfrβ) (Silva et al., 2005). In the absence of *Arf*, these cells abnormally proliferate, which causes the persistent HVS and ultimately leads to blindness in $Arf^{-/-}$ mice (Gromley et al., 2009; Silva et al., 2005). Notably, $p53^{-/-}$ mice have normal vision (McKeller et al., 2002), and thus the role of basal

ARF in eye development is independent of its ability to regulate p53 activity. The use of $Arf^{Gfp/+}$ mice also revealed the expression of ARF in male spermatogonia, which are the cells that line the basement membrane of each seminiferous tubule and differentiate into mature spermatozoa as they progress through meiosis I and meiosis II moving toward the lumen of the tubule (Cole et al.; Gromley et al., 2009). In the absence of *Arf*, spermatogonia have heightened levels of apoptosis, which limited data suggests is the result of an increase in phosphorylated histone H2AX (Churchman et al.). Ultimately, the enhanced apoptosis during germ cell development upon *Arf* loss results in reduced sperm number compared to that in wild-type mice (Churchman et al.; Cole et al.). While the apoptosis of these cells in p53-dependent, ARF's regulation of H2AX phosphorylation is independent of p53 (Churchman et al.).

Basal ARF has also been shown to regulate osteoblastogenesis and osteoblast activity. Osteoblasts are the bone-forming cells of the skeleton. Thus, the role of ARF in osteoblasts is especially important given that our work here has focused on the role of ARF in osteoclastogenesis and the regulation of bone resorption *in vivo*. In the presence of osteogenic media *in vitro*, $Arf^{-/-}$ stromal cells exhibit enhanced osteoblastogenesis compared to wild-type stromal cells (Rauch et al.). This finding can, at least partially, be attributed to an increase in the proliferation of osteoblast precursor cells (unpublished communicated data). ARF's ability to regulate osteoblastogenesis is also relevant *in vivo* as long bones from $Arf^{-/-}$ mice have heightened levels of osteoblast differentiation markers, which correlates to increased bone formation (Rauch et al.). Furthermore, $Arf^{-/-}$ mice display an overall increase in trabecular bone volume and bone mineral density when assessed by microCT (Rauch et al.).

Given the nucleolar localization of ARF and its previously reported roles in regulating the nucleocytoplasmic shuttling of NPM, our lab has recently examined the role of basal ARF in regulating nucleolar structure and function to limit protein synthesis in mouse embryonic fibroblasts (MEFs). We have shown that *Arf* loss results in an increase in both the size and number of AgNORs, which is indicative of abnormal nucleolar function (Apicelli et al., 2008). Given that nucleoli house the proteins required for the initial steps in ribosome biogenesis, Apicelli and colleagues examined protein synthesis upon basal *Arf* loss beginning with the transcription of ribosomal DNA (rDNA). Data suggest that *Arf* loss not only enhances the transcription of rDNA but also the processing of the newly transcribed 47S transcript into intermediate precursors that lead to the final 5.8S, 18S, and 28S subunits, both of which are functions that have previously been ascribed to ARF (Apicelli et al., 2008; Ayrault et al., 2006; Ayrault et al., 2004; Qi et al., 2004; Sugimoto et al., 2003). Furthermore, in accordance with ARF's ability to bind and restrain NPM, loss of basal *Arf* exacerbated the export of ribosomes from the nucleus to the cytoplasm (Apicelli et al., 2008). Ultimately, the increases in ribosomal biogenesis upon *Arf* loss resulted in enhanced protein synthesis relative to that observed in wild-type MEFs (Apicelli et al., 2008). In an effort to translate these findings into a physiologically-relevant cell model with a requirement for protein synthesis, Apicelli and colleagues initiated the study of basal ARF function in osteoclasts. The data show that *Arf* loss appears to enhance overall osteoclastogenesis after 3 days of treatment with M-CSF and RANKL . In the absence of *Arf*, there were a greater number of TRAP-positive osteoclasts with more than five nuclei (Apicelli et al., 2008). *Arf* loss also appears to enhance the function of osteoclasts *in vitro* as wild-type bone marrow

macrophages (BMMs) allowed to differentiated one day longer than *Arf*$^{-/-}$ BMMs in osteoclastogenic media still did not exhibit as much TRAP activity as the *Arf*$^{-/-}$ osteoclasts (Apicelli et al., 2008). These differences translate into what is observed *in vivo*, where serum TRAP levels are elevated in the absence of *Arf.* This change could not be attributed to an increase in the number of macrophages upon *Arf* loss as assessed by BrdU incorporation *in vitro* (Apicelli et al., 2008). Here, we expanded upon these initial findings to definitively determine if basal ARF regulates osteoclasts and whether this regulation is relevant *in vivo*. Additionally, we aimed to determine the mechanism through which ARF acts in this post-mitotic setting.

After 5 days of culturing bone marrow macrophages (BMMs) in the presence of M-CSF and RANKL, we quantified an increase in both the size and number of mature osteoclasts in absence of *Arf*. Enhanced osteoclastogenesis was also confirmed by TRAP and Cathepsin K protein levels and pit staining. Importantly, we could not attribute the difference between wild-type and *Arf*-null osteoclasts to enhanced proliferation either before (as previously shown) or after the addition of RANKL. Furthermore, this is a p53-independent function of ARF as BMMs isolated from *p53*-null mice did not phenocopy those from *Arf*-null mice when differentiated *in vitro*. Instead, *p53*$^{-/-}$ osteoclasts closely resembled wild-type osteoclasts, which is in accordance with previously published findings (Wang et al., 2006). Given the known roles of ARF in regulating protein synthesis, we questioned whether ARF might be regulating osteoclastogenesis by limiting protein synthesis during differentiation. Our data demonstrate that *Arf* loss results in enhanced protein production, especially in pre-OCs (day 3 of differentiation) and mature OCs (day 5 of differentiation). In part, this appears to be due to increased ribosome

output upon *Arf* loss in pre-OCs. Finally, we wanted to know if our *in vitro* results would translate to increased bone resorption upon *Arf* loss *in vivo*. We generated radiation chimeras, in which wild-type mice either received wild-type or $Arf^{-/-}$ bone marrow. Our results demonstrate that *Arf* loss causes a significant increase in bone resorption and bone mineral density compared to mice with wild-type osteoclasts. Taken together, these results point towards a physiologically-relevant role of basal ARF in regulating proliferation- and p53-independent cell growth.

3.3 Methods

Mice

Arf$^{-/-}$ mice were maintained on a 129X1/SvJ x C57BL/6 background. Age-matched wild-type controls on the same background were used except where noted. All mice were housed in a pathogen-free animal facility, fed standard chow *ad libitum*, and treated following animal protocols approved by the Washington University Animal Studies Committee.

Osteoclast culture

Whole bone marrow was isolated from the femurs and tibias of wild-type, *Arf*$^{-/-}$, and *p53*$^{-/-}$ mice. Macrophages were grown in α-minimal essential medium (α-MEM) containing 10% fetal bovine serum (FBS) and CMG14-12 culture supernatant (1/10 vol) as a source of M-CSF. Osteoclasts were generated from bone marrow macrophages using CMG14-12 supernatant (1/100 vol or 1/50 vol) and recombinant GST-RANKL (50ng/mL). To assess for RANKL hypersensitivity, all wells were identically treated except for the indicated amounts of RANKL (12.5, 25, 50, or 100 ng/mL). In 48-well tissue culture dishes, BMMs were plated at 1.5 X 10^4 cells per well. Osteoclasts were fixed and visualized by histochemical staining for tartrate-resistance acid phosphatase according to the manufacturer's protocol (Sigma).

quantitative RT-PCR, and Immunoblotting

RNA and protein were isolated from all cells using the illustra^{TM} triplePrep kit (GE Healthcare) as described in the manufacturer's protocol. For qRT-PCR, first-strand

cDNA was prepared using the SuperScript III first-strand synthesis system (Invitrogen). Real-time PCR was performed with iQ SYBR Green Supermix (Bio-Rad) according to the manufacturer's protocol. Primer sequences TRAP forward: 5'-CAGCTCCCTAGAAGATGGATTCAT-3' and reverse: 5'-GTCAGGAGTGGGAGCCATATG-3' and Cathepsin K forward: 5'-ATGTGGGTGTTCAAGTTTCTGC-3' and reverse: 5'-CCACAAGATTCTGGGGACTC-3' Protein was eluted in 7M Urea and further diluted to 3M Urea such that protein concentration could be quantified by Bradford assays. Antibodies used included rabbit anti-Cathepsin K (Abcam) and goat anti-TRAP (Santa Cruz).

Proliferation analysis

Macrophages were cultured in the absence of RANKL or in the presence of 50ng/mL RANKL for 24h on glass coverslips in 24-well plates. Cells were labeled with bromodeoxyuridine (BrdU) for 24h, fixed, and then stained with DAPI and an antibody against BrdU. BrdU-positive cells were blindly counted for each experiment.

Apoptosis analysis

Macrophages were seeded at 5000 cells/well in 96-well dishes and differentiated in the presence of M-CSF and 50ng/mL RANKL. Cell death was assessed by cell death detectio ELISA^{PLUS} kit (Roche Applied Sciences), which detects cytoplasmic histone-associated DNA fragmentation. Absorbance was measured at 405nm.

In vitro bone resorption

Bone marrow macrophages from either wild-type or *Arf*$^{-/-}$ mice were differentiated *in vitro* on bovine bone slices in the presence of M-CSF and 50ng/mL RANKL. After 8 days in the presence of osteoclastogenic media, cells were removed from bone by mechanical agitation. Bone slices were then incubated with peroxidase-conjugated wheat germ agglutinin (Sigma) followed by 3,3-diaminobenzidine (Sigma) to visualize areas of bone Resorptive area was blindly quantified by determining the average of four fields from each bone slice.

Immunofluorescence

Wild-type bone marrow macrophages were cultured in the presence of M-CSF and 50ng/mL RANKL for 6 days on glass coverslips in 24-well plates. Cells were then fixed with ice-cold methanol:acetone (1:1 vol) and stained with rat anti-ARF and rabbit anti-NPM followed by FITC-conjugated anti-rabbit and rhodamine-conjugated anti-rat. Nuclei were visualized with DAPI.

^{35}S-methionine incorporation assays

Bone marrow macrophages were plated in 6-well dishes in the presence of only M-CSF (BMMs) or M-CSF and 50ng/mL RANKL (pre-OCs and OCs). All cells were starved of methionine and cysteine for 30min prior to labeling at the appropriate time point during differentiation (3 days post-RANKL for pre-OC and 5 days post-RANKL for OCs). Following starvation, cells were pulsed with 150 μCi of ^{35}S-mehtionine for the indicated times (2, 4, or 8 hours). The first time point (t=0) was harvested immediately

after the pulse. Following the pulse, cells were washed with cold phosphate-buffered saline and then lysed with 1% Triton X-100 buffer. Protein was precipitated from cell lysates using 10% tricholoroacetic acid and pellets were analyzed by liquid scintillation counting to quantify the incorporated counts per million.

Ribosome fractionation

3 x 10^6 cells per condition were treated with 50ug/mL cycloheximide for 10min. Cells were then mechanically lifted and lysed. Cytoplasmic fractions were separated by centrifugation and layered over a continuous sucrose gradient. Gradients were fractionated and RNA absorbance was monitored at 254nm.

Histology

Bones were isolated within 24h following the final dose of RANKL and fixed in formalin overnight. Fixed bones were then decalcified for 14 days in 14% EDTA and subsequently dehydrated in increasing amounts of EtOH. Paraffin-embedded sections were stained for tartrate-resistant acid phosphatase and quantified using Bioquant Osteo (Bioquant Image Analysis).

AgNOR staining

Bone marrow macrophages were seeded on glass coverslips and assessed for AgNORs at the indicated times according to a modified protocol that was originally presented by Aubele et al. (Aubele et al., 1994). Briefly, cells were first fixed in 2%

glutaraldehyde and then 3:1 ethanol-acetic acid solution. Cells were subsequently stained using a 0.33% formic acid-33.3% silver nitrate solution in 0.66% gelatin and then mounted on slides using Vectashield. AgNOR numbers were blindly quantified.

Generation of radiation chimeras

7 week-old wild-type mice on a 129X1/SvJ x C57BL/6 background were lethally irradiate (1000 rads). After 24 hours, 1 x 10^6 donor whole bone marrow cells (either from wild-type or *Arf*$^{-/-}$ mice) were intravenously transferred into the tails of recipient mice. Hematopoietic reconstitution with the donor genotype was confirmed by PCR of peripheral blood.

viva CT analysis

Tibias were scanned from the proximal epiphysis to the tibia-fibula junction by *in vivo* microCT (VivaCT 40, Scanco Medical, calibrated at regular intervals by single individual).We assessed bone parameters by blindly contouring 30 sections below the growth plate of each tibia to exclude cortical bone. For all measurements, a threshold of 180 (on a 0-1000 scale) was maintained.

3.4 Results

Arf loss accelerates osteoclastogenesis in vitro

To definitively determine whether *Arf* loss was affecting osteoclastogenesis *in vitro*, we first isolated bone marrow macrophages (BMMs) from WT and $Arf^{-/-}$ mice. After five days in the presence of M-CSF (1/100 vol) and 50ng/mL RANKL, we confirmed that the osteoclasts were either WT or *Arf*-null by PCR (Figure 3.1a) and Western analysis (Figure 3.1b). The cells were TRAP-stained for quantification (Figure 3.2a), and we observed an increase in the number of TRAP-positive multinucleated osteoclasts (Figure 3.2b), indicating that *Arf* loss enhances osteoclastogenesis *in vitro*. The total area quantified was also greater in the absence of *Arf* (Figure 3.2c), indicating that $Arf^{-/-}$ osteoclasts are larger than their wild-type counterparts (Figure 3.2d). Furthermore, when differentiating BMMs under various concentrations of RANKL, we found that loss of *Arf* permitted osteoclastogenesis even in the presence of very low RANKL concentrations (Figure 3.3a). Furthermore, in these osteoclast differentiation experiments, *Arf* loss resulted in an increase in the number, area covered by osteoclasts, and osteoclast size at all concentrations of RANKL relative to wild-type cells (Figure 3.3b-d). During differentiation, we noted that osteoclasts were forming much earlier in the absence of *Arf* (observation not quantified). To affirm this observation, we isolated cells on each day during osteoclastogenesis for five days and assessed both the mRNA and proteins levels of two well-characterized markers of osteoclastogenesis: tartrate-resistant acid phosphatase (TRAP) and Cathepsin K (Zhao et al., 2007). Interestingly, the mRNA levels did not appear any earlier in the absence of *Arf*, but they were significantly

increased in the absence of *Arf* relative to wild-type (Figure 3.4), which suggests that *Arf* loss may also enhance osteoclast function in addition to exacerbating osteoclastogenesis. The protein levels of both Cathepsin K and TRAP support accelerated osteoclastogenesis in the absence of *Arf.* Cathepsin K protein levels were 19-fold greater by 4 days post-RANKL and 31-fold greater by day 5 compared to the levels on day 3 in WT cells. In comparison, $Arf^{-/-}$ cells had an 8-fold increase in Cathepsin K on day 3 compared to WT day 3 and by 4 days post-RANKL, the $Arf^{-/-}$ cells already exhibited levels of Cathepsin K (30-fold) that were comparable to that of day 5 WT cells (Figure 3.5). Similarly, TRAP levels observed after 5 days post-RANKL in WT cells were comparable to those seen only 4 days post-RANKL treatment in $Arf^{-/-}$ cells (Figure 3.5). Taken together, this data suggests that loss of *Arf* enhances osteoclastogenesis *in vitro*, resulting in both increased number and size of osteoclasts. It is possible that *Arf* loss results in increased osteoclast size as a result of enhanced fusion of mononuclear precursors. To evaluate this, we counted the number of nuclei per cell in WT and $Arf^{-/-}$ osteoclasts. Blinded quantification results suggest that there is no difference in the numbers of nuclei between WT and $Arf^{-/-}$ osteoclasts, implying that enhanced fusion does not explain the increase in size upon *Arf* loss (Figure 3.6). As I will discuss later in this section, the increased size may be a result of enhanced protein synthesis during osteoclastogenesis as a result of *Arf* loss. Finally, to determine whether the increased osteoclastogenesis in $Arf^{-/-}$cells results in more bone resorption *in vitro*, WT and $Arf^{-/-}$ macrophages were differentiated on bovine bone slices in the presence of M-CSF and RANKL for 8 days. The bone slices were then analyzed for resorption by staining and quantifying pit area (Figure 3.7a). After 8 days, less than 5% of the bone slices were covered in pits when plated with WT BMMs. However, we

found that *Arf* loss results in approximately 25% of the bone slice being covered with pits (Figure 3.7b). This data compliments our previous results suggesting that *Arf* loss results in enhanced osteoclastogenesis. More importantly, it suggests that while *Arf* loss accelerates osteoclastogenesis, differentiation still proceeds properly and results in active and functional osteoclasts *in vitro*.

Enhanced osteoclastogenesis: analyzing proliferation, apoptosis, and p53

To determine if *Arf* loss results in increased osteoclast number and size as a result of enhanced precursor proliferation, we quantified BrdU-positive nuclei before and after the addition of RANKL. In accordance with previously published data analyzing the proliferation of BMMs upon *Arf* loss (Apicelli et al., 2008), we did not observe an increase in proliferation in $Arf^{-/-}$ cells relative to WT (Figure 3.8a). As a control, we also assessed proliferation on days 3 and 4 of osteoclastogenesis. As expected, our results show that there is very little proliferation occurring by day 3 of osteoclastogenesis (Figure 3.8b). An increase in either osteoclast number or size could also be a result of decreased apoptosis. To assess whether *Arf* loss alters apoptosis *in vitro*, we examined cells 4, 5, 6, and 7 days after RANKL treatment as this is the timeframe in which we typically observe cell death. Apoptosis was quantified by an ELISA assessing histone-associated DNA fragmentation. On days 4, 5, and 6, we observed slight decreases in apoptosis in $Arf^{-/-}$ cells relative to WT. The most striking difference was observed on day 7; *Arf* loss significantly decreases the levels of fragmented DNA nearly 2-fold compared to that observed in WT osteoclasts (Figure 3.9). These data suggest that *Arf* loss results in a decrease in apoptosis during osteoclastogenesis *in vitro*. This result may, at least

partially, explain why we observe enhanced osteoclast number and/or size upon *Arf* loss. Finally, given the well-characterized p53-dependent role of ARF tumor suppression, we wanted to know if enhanced osteoclastogenesis upon *Arf* loss is dependent upon p53. We hypothesized that if *Arf* loss results in enhanced osteoclastogenesis as a result of decreased p53 activity, then $p53^{-/-}$ cells will phenocopy $Arf^{-/-}$ cells. Therefore, we isolated bone marrow macrophages from $p53^{-/-}$ mice and differentiated them alongside $Arf^{-/-}$ macrophages. As we expected, *Arf* loss resulted in enhanced osteoclast number compared to WT cells. However, *p53* loss had no affect on the number of osteoclasts as they were comparable to WT (Figure 3.10).

Protein synthesis upon Arf loss during osteoclastogenesis

As previously mentioned, it is possible that *Arf* loss results in increased osteoclast number and size as a result of enhanced protein synthesis. Given that we have observed enhanced protein synthesis following *Arf* loss in mitotic cells, we wanted to determine if $Arf^{-/-}$ cells exhibit elevated levels of protein synthesis during osteoclastogenesis. We began addressing this question by determining whether ARF colocalizes with nucleophosmin (NPM) in WT osteoclasts, as previous reports show that ARF's ability to interact with NPM plays a significant role in controlling protein synthesis. In Figure 3.11, we demonstrate that ARF and NPM do, in fact, colocalize in WT osteoclasts. Therefore, we moved forward by measuring the incorporation of ^{35}S-methionine into newly-synthesized proteins. In macrophages, we observed no differences in protein synthesis (except at t=4h) between wild-type and $Arf^{-/-}$ cells (Figure 3.12a). However, in both pre-osteoclasts and osteoclasts, protein synthesis was significantly enhanced upon *Arf* loss

relative to WT cells (Figure 3.12b,c). In mature osteoclasts (day 5), *Arf* loss approximately doubled the amount of protein synthesis by 8 hours post-^{35}S pulse (Figure 3.12c). In pre-osteoclasts, we again measured nearly a 2-fold increase in protein synthesis by 8 hours post-^{35}S pulse (Figure 3.12b). Furthermore, we noted that the overall highest levels of protein synthesis, regardless of genotype, were occurring during the pre-osteoclast stage of differentiation (day 3) (Figure 3.12b). Therefore, we decided to focus our attention on the differences between WT and *Arf*$^{-/-}$ pre-osteoclasts when assessing ribosome output. The relative amount of actively-translating ribosomes was measured by freezing mRNAs onto actively-translating ribosomes with cycloheximide treatment, separating pre-osteoclast cytosolic fractions over a sucrose gradient, and reading the amount of RNA at an absorbance of 254nm. Using this technique, the actively-translating ribosomes or polysomes, appear on the far right of the trace. As shown in Figure 3.13, we noted a slightly larger pool of polysomes in *Arf*$^{-/-}$ pre-osteoclasts relative to WT pre-osteoclasts. To verify the significance of this slight change in the two profiles, we report the ribosome profiles between WT cells on a pure B6 background and *Arf*$^{-/-}$ cells on a mixed B6/129 background. Previous data from our lab has shown that even a change in the genetic background can dramatically alter the ribosome profiles in mice of the same genotype (unpublished data). Our profiles demonstrate that there is no difference in ribosome output between WT (B6) and *Arf*$^{-/-}$ (B6/129) BMMs (Figure 3.14a), pre-osteoclasts (Figure 3.14b), and osteoclasts (Figure 3.14c), indicating that the difference we observed in Figure 3.13 is biologically meaningful. Taken together, the data suggests that we are, at least in part, observing enhanced levels of protein synthesis upon *Arf* loss as a result of an increased pool of actively-translating polysomes. More

importantly, this data supports the idea that *Arf* loss enhances osteoclastogenesis as a result of elevated protein synthesis. Finally, we have previously made a correlation between an increase in the number of AgNORs and enhanced protein synthesis upon *Arf* loss in mitotic mouse embryonic fibroblasts (Apicelli et al., 2008). Therefore, we wanted to determine if the number of AgNORs per nucleus is increased upon *Arf* loss during osteoclastogenesis. Results show that *Arf* loss does not alter the number of AgNORs in BMMs (Figure 3.15a), pre-osteoclasts (Figure 3.15b), and osteoclasts (Figure 3.15c) relative to WT cells.

Examining the effects of osteoclast Arf loss in vivo

Finally, we wanted to determine if the effects we had observed upon *Arf* loss *in vitro* translated to differences in bone resorption *in vivo*. Initially, we planned to create an osteoclast-specific knockout of *Arf* by breeding $Arf^{fl/fl}$ and $Ctsk^{Cre/+}$ mice. However, our breedings resulted in germline loss of *Arf* (see Chapter 2). As an alternative approach, we generated radiation chimeras by lethally irradiating WT mice and subsequently transplanting them with WT or $Arf^{-/-}$ bone marrow. This allowed us to examine $Arf^{-/-}$ osteoclasts in the presence of WT osteoblasts, which was necessary given the previously published data demonstrating that germline *Arf* loss enhances osteoblastogenesis and osteoblast activity *in vivo* resulting in an overall increase in bone volume (Rauch et al.). Three weeks following the transplant, bone resorption was assessed by vivaCT (Figure 3.16). Initial vivaCT results showed no difference in bone volume between mice that received WT bone marrow and mice that received $Arf^{-/-}$ bone marrow (Figure 3.17). We therefore decided to challenge our radiation chimeras by injecting them with RANKL to

stimulate bone resorption. Our method of RANKL injection was based on a recent study demonstrating that three consecutive daily doses of various concentrations of RANKL was enough to cause significant bone resorption (Tomimori et al., 2009). To confirm this method, we first injected WT mice with either PBS or 2mg/kg RANKL for three consecutive days. The mice were imaged before beginning the series of injections and 1.5h following the final injection to assess bone loss. Our data demonstrate that three consecutive daily doses of 2mg/kg RANKL causes nearly 50 % bone loss (Figure 3.18). Ultimately, we decided to challenge our radiation chimeras with three consecutive daily doses of 1mg/kg RANKL and imaged them before the series of RANKL injections and 1.5h following the final injection as outlined in Figure 3.19. Representative 3D images of reconstructed tibias before and after RANKL stimulation are shown in Figure 3.20a. These images demonstrate that mice with $Arf^{-/-}$ osteoclasts resorb more bone compared to mice with WT osteoclasts. The difference in trabecular bone volume (reported as bone volume/total volume) following RANKL stimulation between mice that received a WT transplant and mice that received an $Arf^{-/-}$ transplant was blindly quantified based on vivaCT images of tibias. The data show that *Arf* loss results in a significant decrease in bone volume relative to WT, suggesting that *Arf* loss in osteoclasts enhances bone resorption upon RANKL stimulation *in vivo* (Figure 3.20b). Furthermore, *Arf* loss causes a corresponding decrease in trabecular number following RANKL stimulation, which is indicative of enhanced bone resorption (Figure 3.20c). An increase in trabecular number is often correlated with a decrease in trabecular spacing given that the more bone within a defined area, the less space there is between the bones. Our results follow this logic and demonstrate a significant increase in trabecular spacing in mice that received an $Arf^{-/-}$

transplant relative to mice that received a WT transplant (Figure 3.20d). Finally, vivaCT analysis indicates that there is a significant decrease in bone mineral density in the absence of *Arf* (Figure 3.20e). To determine if there are more osteoclasts in mice receiving an $Arf^{-/-}$ transplant, tibias of mice were removed and TRAP-stained following the final vivaCT scan. The number of osteoclasts in a defined area of the tibias was blindly quantified. Our data show that *Arf* loss significantly increases the number of osteoclasts *in vivo*, which supports our *in vitro* results (Figure 3.21). As a whole, our *in vivo* data suggests that *Arf* loss enhances bone resorption due, at least in part, to an increase in osteoclast number.

3.5 Discussion

ARF has long been appreciated as a protein that is upregulated in response to oncogenic stress (Sherr, 2001). Upon induction, ARF is known to impede the ability of MDM2 to negatively regulate the p53 tumor suppressor (Weber et al., 1999), a function originally thought to be the sole mechanism of ARF tumor suppression. However, we now know that ARF also suppresses tumorigenesis by mechanisms that are independent of its ability to regulate p53 (Weber et al., 2000a). In fact, there are nearly 30 purported ARF-interacting proteins that may well be playing a role in advancing cell growth and/or proliferation, and it will be exciting to see future results that further define the significance of their interactions with ARF (Sherr, 2006). Our lab has focused on the ARF-interacting protein, nucleophosmin (NPM). We have demonstrated that ARF's ability to impede the nucleocytoplasmic shuttling of NPM is also a means by which cell cycle progression in limited (Brady et al., 2004). NPM is necessary for the export of newly transcribed and processed ribosomes to the cytoplasm for translation (Maggi et al., 2008; Yu et al., 2006). Thus, ARF is able to limit the growth of a cell by prohibiting the transport of ribosomes from the nucleus to the cytoplasm in a p53-independent manner. Given that cell growth (i.e. protein synthesis) is necessary to maintain proper cell division, our lab questioned whether ARF also regulates cell growth in non-dividing cells. We hypothesized that the ability to limit protein synthesis might be more of a teleological role of ARF even though it is more commonly recognized as a tumor suppressor.

In parallel to questioning the role of ARF in non-dividing cells, a number of reports were surfacing that outlined roles for basal ARF. These included studies

demonstrating ARF's p53-independent role in limiting the proliferation of mural cells within the developing eye and ARF's p53-independent role in regulating the survival of spermatocytes during male germ cell development in mice (Churchman et al.; Gromley et al., 2009; McKeller et al., 2002; Silva et al., 2005). The importance of basal ARF in regulating these two functions is underscored by the fact that *Arf*$^{-/-}$ mice are blind and males have a low sperm count. Given our previous work showing that ARF acts a tumor suppressor by inhibiting NPM and thus protein synthesis, we were first interested in determining whether basal ARF can also regulated these functions. We have since demonstrated that basal ARF limits ribosomal DNA (rDNA) transcription, rRNA processing, and ribosomal export to the cytoplasm via NPM to ultimately maintain a proper rate of protein synthesis in dividing cells (Apicelli et al., 2008). Given this finding, we were poised to answer the following question: does basal ARF regulate protein synthesis in non-dividing cells?

Here, we used osteoclasts as a model because they are fully differentiated, non-dividing cells. In route to becoming mature and functional, osteoclasts are signaled to upregulated the production of proteins required for bone degradation, implying a requirement for protein synthesis even as they near maturation (Teitelbaum and Ross, 2003). *In vitro*, osteoclasts can be differentiation from bone marrow macrophages. In this study, we demonstrate that bone marrow macrophages derived from *Arf*$^{-/-}$ mice and allowed to differentiate *in vitro* result in the production of more and bigger osteoclasts when plated at the same density as wild-type macrophages, a finding that is supported by previous studies using slightly different concentrations of osteoclastogenic cytokines and an alternative approach to quantification (Apicelli et al., 2008). We further show in this

report that enhanced osteoclastogenesis upon *Arf* loss is complimented by the premature appearance of two proteins important that are necessary for proper osteoclast function: tartrate-resistant acid phosphatase (TRAP) and Cathepsin K. In fact, in the absence of either TRAP or Cathepsin K, mice are osteopetrotic, emphasizing their functional importance (Hayman et al., 1996; Saftig et al., 1998). Interestingly, while mRNA levels of TRAP and Cathepsin K are elevated during osteoclastogenesis, they do not appear any earlier during differentiation in the absence of *Arf*. This suggests that ARF may be regulating the timing of translation of these proteins. To support this hypothesis, we have demonstrated that *Arf* loss results in increased protein synthesis during osteoclastogenesis (observed in BMMs, pre-osteoclasts, and osteoclasts). This is, at least in part, due to elevated amounts of actively-translating ribosomes in pre-osteoclasts upon *Arf* loss. By isolating the mRNAs from the polysomes of pre-osteoclasts, we plan to determine whether *Arf* loss alters the amount of TRAP and Cathepsin K mRNA translation at a specific time point during osteoclastogenesis.

Our *in vitro* data also suggests that enhanced osteoclastogenesis upon *Arf* loss is independent of ARF's ability to regulate p53. This finding is supported by a previous report suggesting that osteoclastogenesis is only enhanced by *p53* loss *in vivo* due to the coupling of osteoblast and osteoclasts (Wang et al., 2006). Specifically, it has been reported that p53 regulates the osteoblast transcription factor osterix (Wang et al., 2006). Osterix is important for the upregulation of M-CSF transcription, a cytokine known to be important for cell proliferation and survival during osteoclastogenesis. However, *in vitro* studies have shown that the effects of *p53* on osteoclastogenesis are not cell autonomous (Wang et al., 2006); in fact, we found that $p53^{-/-}$ osteoclasts appear no different than wild-

type osteoclasts *in vitro*. This finding follows the other functions that have been reported for basal ARF in that they are all p53-independent and suggests that ARF only exerts its p53-dependent functions in the presence of oncogenic stress. We also show that ARF's ability to limit osteoclastogenesis is independent of proliferation. While we initiated this study knowing that any observed effects of *Arf* loss on the function of mature osteoclasts would intrinsically be independent of proliferation, given that mature osteoclasts do not divide, it remained unclear whether enhanced osteoclastogenesis in the absence of *Arf* was due in part to increased proliferation of osteoclast precursors. Of the proliferation experiments we show here, the most important in this regard is the finding that there is no difference in proliferation of osteoclast precursors following the addition of RANKL. This data suggests that we do not see enhanced numbers of osteoclasts on day 5 of osteoclastogenesis as a result of enhanced precursor proliferation after seeding the cells for differentiation. In contrast, we did observe a decrease in apoptosis in the absence of *Arf*, which was most prominent on day 7 of osteoclastogenesis, suggesting that *Arf* loss extends the lifespan of osteoclasts *in vitro*. It is possible that the small, yet significant, changes in apoptosis on days 3 and 4 of osteoclastogenesis contribute to the enhanced numbers of mature osteoclasts on day 5 as well as the increases we have observed in protein synthesis on days 3 and 5 of osteoclastogenesis. However, it is unlikely that the observed differences in apoptosis completely explain enhanced osteoclastogenesis or protein output given that the levels of apoptosis are very low on days 3 and 4 of osteoclastogenesis relative to day 7. To confirm this, we will need to assess protein synthesis and day 5 osteoclast numbers after lifting and reseeding equal numbers of osteoclast precursors on day 3 of osteoclastogenesis. Finally, it will be important to

determine whether *Arf* loss enhances the function of osteoclasts on a per cell basis, and we are currently designing experiments to assess this *in vitro* by quantifying actin rings and bone resorption of osteoclasts that have been lifted and reseeded as pre-osteoclasts.

Finally, we have now demonstrated that *Arf* loss in osteoclasts results in increased bone resorption *in vivo*. Given that basal ARF has also been demonstrated to limit osteoblastogenesis and osteoblast activity *in vivo* (Rauch et al.), we assessed the effects of *in vivo Arf* loss in osteoclasts in the context of wild-type osteoblasts by generating radiation chimeras. The radiation chimeras have allowed us to assess cell autonomous effects of *Arf* loss in osteoclasts in the sense that we can exclude any effects due to the coupling of osteoblasts and osteoclasts. Furthermore, we have observed an increase in the number of osteoclasts present in mice that received bone marrow transplants from $Arf^{-/-}$ mice relative to those that received bone marrow from wild-type mice. This *in vivo* data supports the enhanced osteoclastogenesis and increased osteoclast number that we have observed *in vitro*. Taken together, our *in vivo* data suggests that the effects of *Arf* loss during osteoclastogenesis we observed *in vitro* are physiologically-relevant.

These findings represent a new role for basal ARF in regulating osteoclastogenesis. More importantly, they are the first to demonstrate a role for basal ARF in regulating cell growth in a p53-independent and proliferation-independent context. It will be important to determine whether this function of ARF in osteoclastogenesis is relevant in other cell types and is representative of a teleological role for ARF. In terms of tumorigenesis, it also suggests that basal ARF may be limiting protein synthesis and, upon induction by oncogenic stress, shifts its focus to regulating p53 activity. Our lab has previously demonstrated that ARF preferentially binds to

MDM2 over NPM (Brady et al., 2004). Moreover, ARF uses the same resides to interact with both MDM2 and NPM (Brady et al., 2004; Weber et al., 2000b). With that in mind, it remains to be determined how, in the absence of oncogenic stress, such low levels of ARF are regulating protein synthesis if at least a partial pool of ARF is bound by MDM2. This might partially be explained by recent studies suggesting that ARF can regulate the sumoylation of NPM (Kuo et al., 2008; Tago et al., 2005) . It is possible such a modification controls the activity of NPM rather than needing ARF to constantly be bound to NPM . Alternatively, the cell might somehow signal ARF to focus its attention on protein synthesis regulation under normal conditions and restrain MDM2 during oncogenic stress. Furthermore, the role of basal ARF in regulating protein synthesis could conceivably be important in preventing tumorigenesis in the face of oncogenic stimulation. We would hypothesize that a cell with unrestrained protein synthesis becomes more transformable over time as it increases its levels of unwarranted proteins, and our lab is currently designing experiments to test this possibility both *in vitro* and *in vivo*.

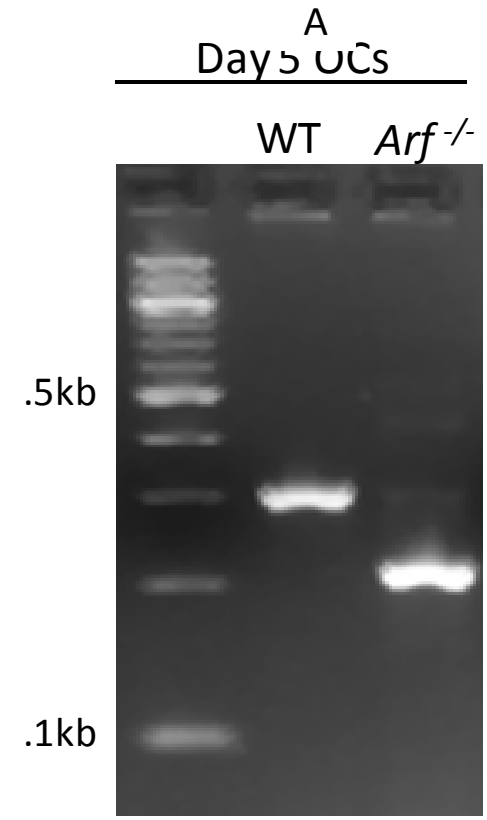
A
Day 5 OCs
WT
Arf -/-
.5kb
.1kb

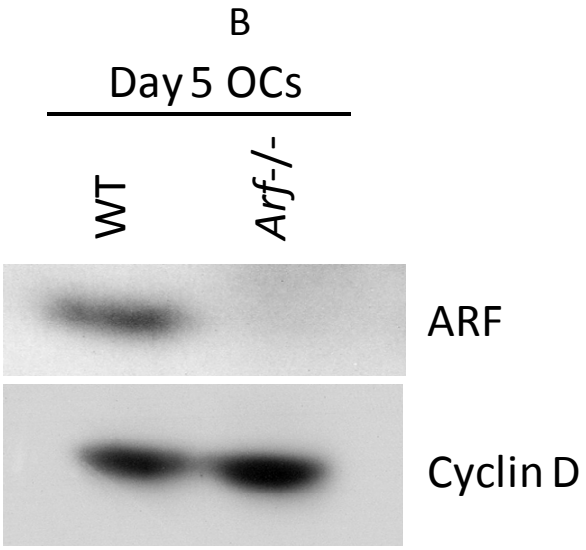
B
Day 5 OCs
WT
Arf-/-
ARF
Cyclin D

Figure 3.1.

Genotyping and immunoblotting confirm the presence of ARF in wild-type osteoclasts. Bone marrow macrophages (BMMs) were isolated from wild-type and *Arf*$^{-/-}$ mice and differentiated *in vitro* in the presence of M-CSF and RANKL for 5 days. Both DNA and protein were isolated from day 5 osteoclasts. (A) The absence of exon1β by genotyping confirms that mature OCs are void of *Arf*. (B). Day 5 OCs derived from wild-type and *Arf*$^{-/-}$ BMMs immunoblotted for ARF. Cyclin D is loading control.

A

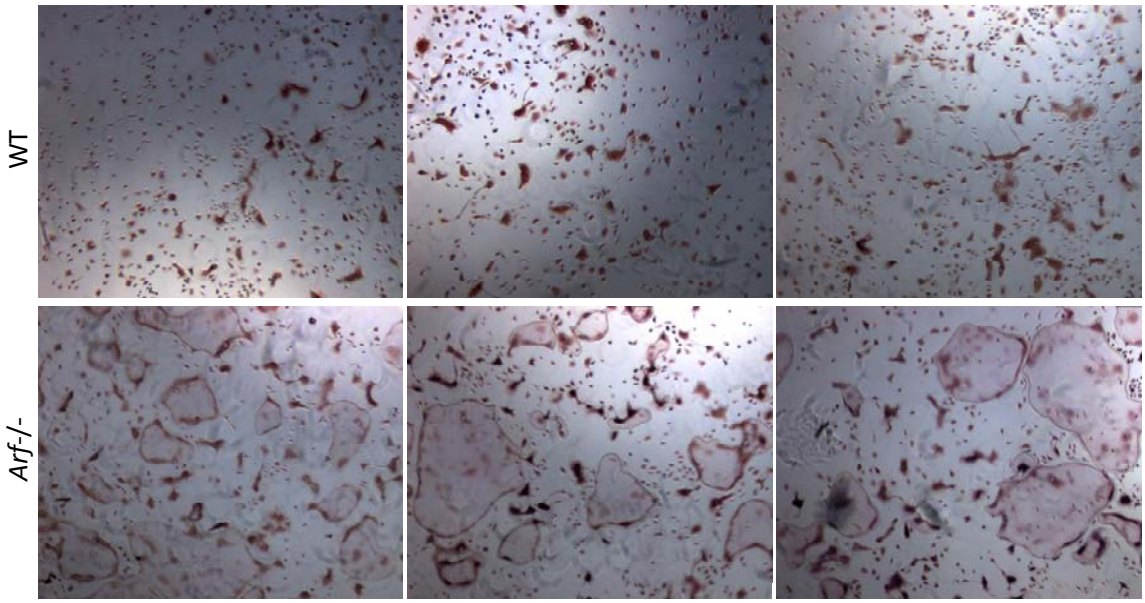

B

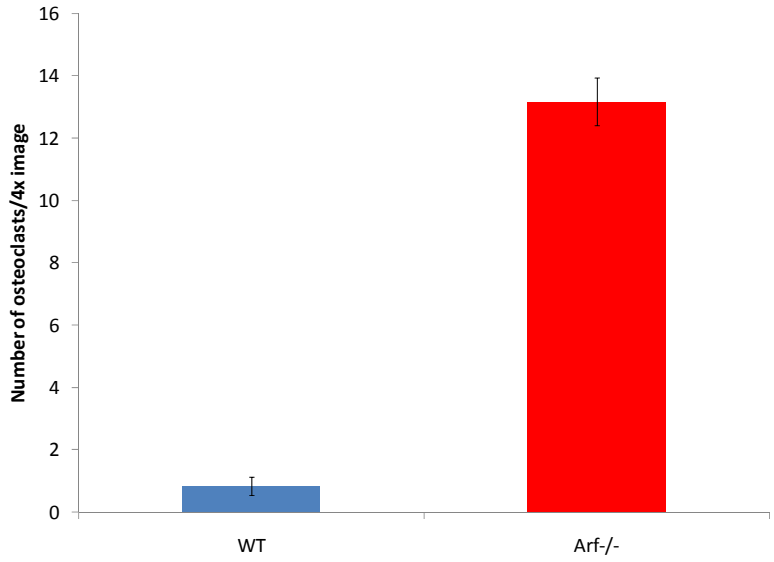

C

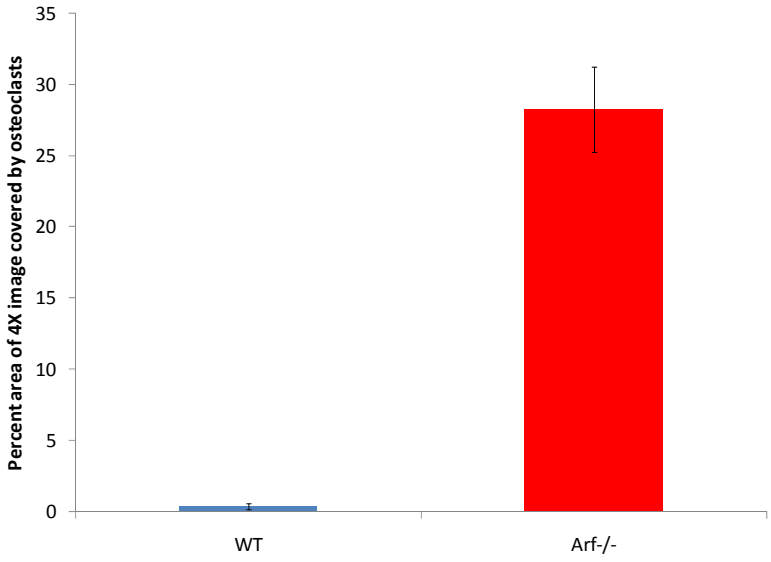
Percent area of 4X image covered by osteoclasts
35
30
25
20
15
10
5
0
WT
Arf-/-

D

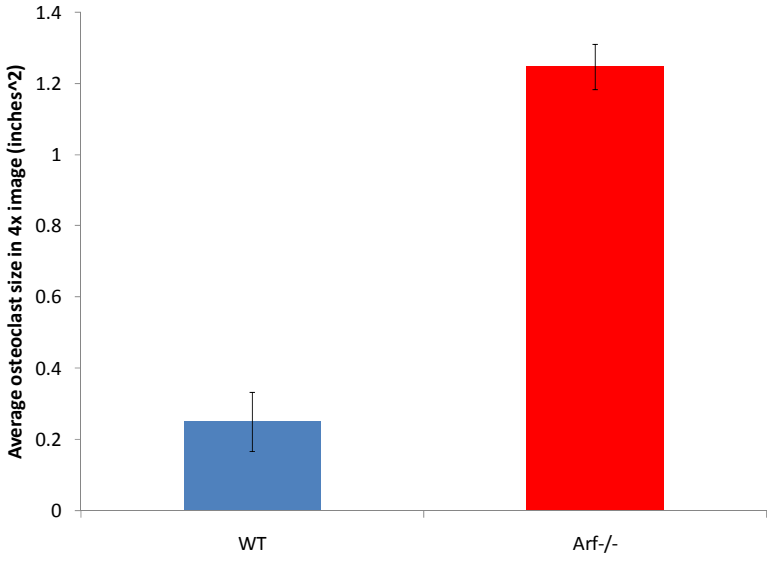
Average osteoclast size in 4x image (inches^2)
1.4
1.2
1
0.8
0.6
0.4
0.2
0
WT
Arf-/-

Figure 3.2.

***Arf* loss enhances osteoclastogenesis *in vitro*.** Bone marrow macrophages were isolated from either wild-type or *Arf*-null mice. Equal numbers of macrophages were plated in 48-well dishes in the presence of M-CSF (1/100 vol) and RANKL. After 5 days in the presence of osteoclastogenic media, cells were fixed and TRAP-stained. WT = blue bars and $Arf^{-/-}$ = red bars (A). Three representative 4X images from both wild-type and $Arf^{-/-}$ day 5 TRAP-stained osteoclasts. (B) Multinucleated TRAP-positive osteoclasts were blindly counted in three fields of each well and averaged. There are significantly more osteoclasts present in the absence of *Arf* ($p \leq 0.05$). (C) Three fields in each well of TRAP-stained multinucleated osteoclasts were blindly assessed for the percent area covered by osteoclasts and averaged. The absence of *Arf* results in a significantly greater area covered by osteoclasts relative to wild-type ($p \leq 0.05$). (D) Average osteoclast size was determined by dividing the total area covered by osteoclasts by the total number of osteoclasts in that field (inches^2). The absence of *Arf* results in significantly larger osteoclasts relative to wild-type ($p \leq 0.05$).

A

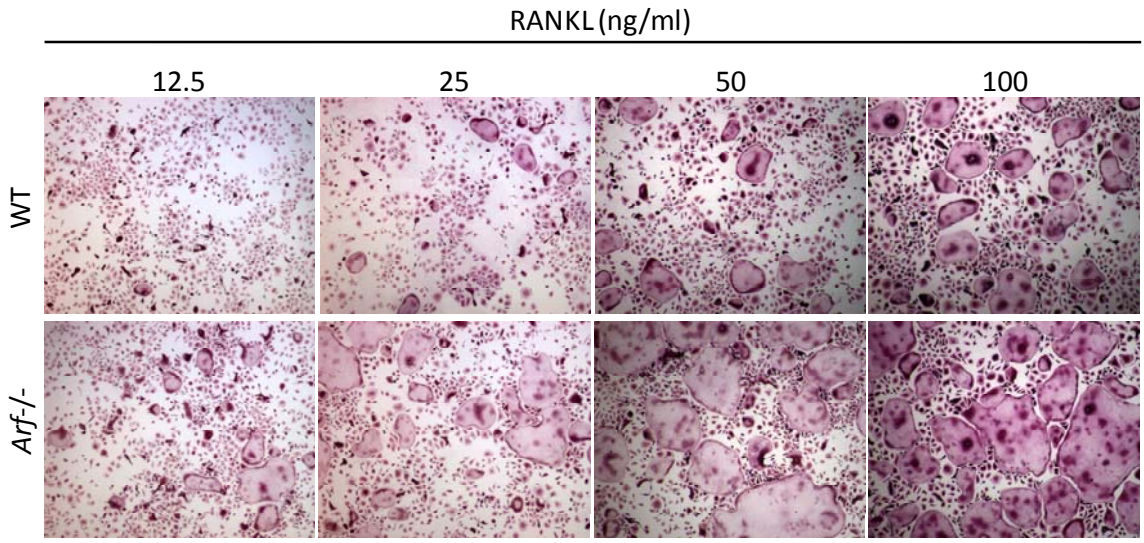

B

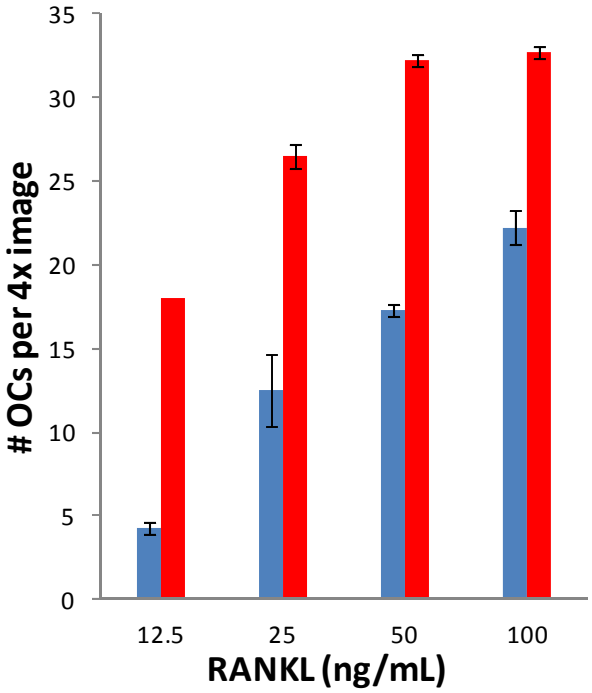
35
30
25
20
15
10
5
0
OCs per 4x image
12.5
25
50
100
RANKL (ng/mL)

C

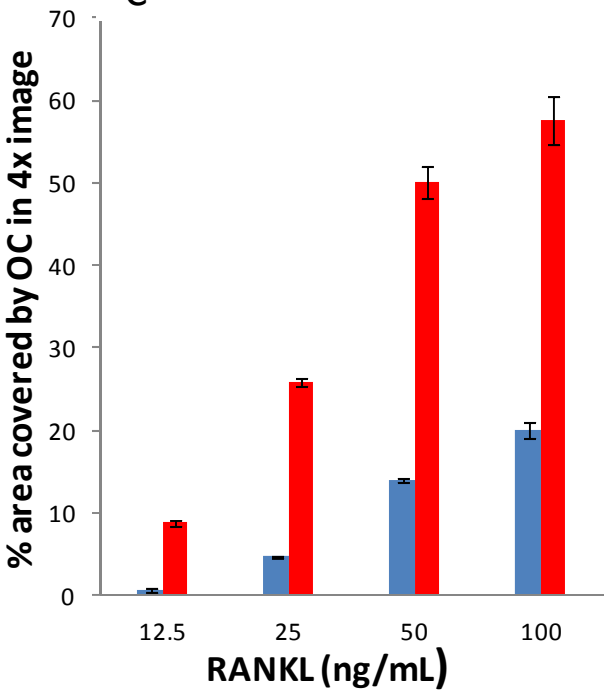
70
60
50
40
30
20
10
0
% area covered by OC in 4x image
12.5
25
50
100
RANKL (ng/mL)

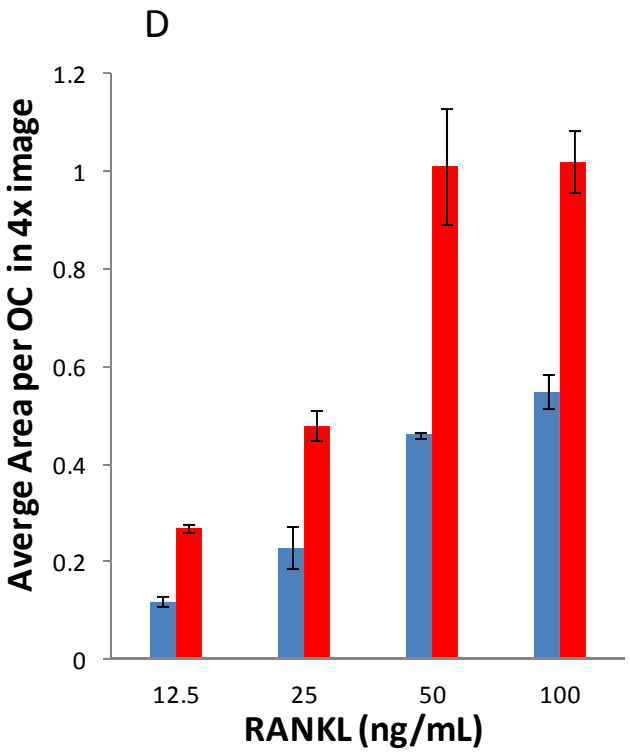

Figure 3.3

***Arf*-null macrophages are hypersensitive to RANKL.** Bone marrow macrophages were isolated from either wild-type or *Arf*-null mice. Equal numbers of macrophages were plated in 48-well dishes in the presence of M-CSF and varying concentrations of RANKL. After 5 days in the presence of osteoclastogenic media, cells were fixed and TRAP-stained. WT = blue bars and $Arf^{-/-}$ = red bars (A) Representative 4X images of wild-type and *Arf*-null cells under each tested concentration of RANKL. (B) Multinucleated TRAP-positive osteoclasts were blindly counted in three fields of each well. At all concentrations of RANKL, there are significantly more osteoclasts present in the absence of *Arf* ($p \leq 0.05$ at all concentrations). (C) Three fields in each well of TRAP-stained multinucleated osteoclasts were blindly assessed for the percent area covered by osteoclasts. At all concentrations of RANKL, the absence of *Arf* results in a

significantly greater area covered by osteoclasts relative to wild-type ($p \leq 0.05$ at all concentrations). (D) Average osteoclast size was determined by dividing the total area covered by osteoclasts by the total number of osteoclasts in that field (inches^2). At all concentrations of RANKL, the absence of *Arf* results in significantly larger osteoclasts relative to wild-type ($p \leq 0.05$ at all concentrations).

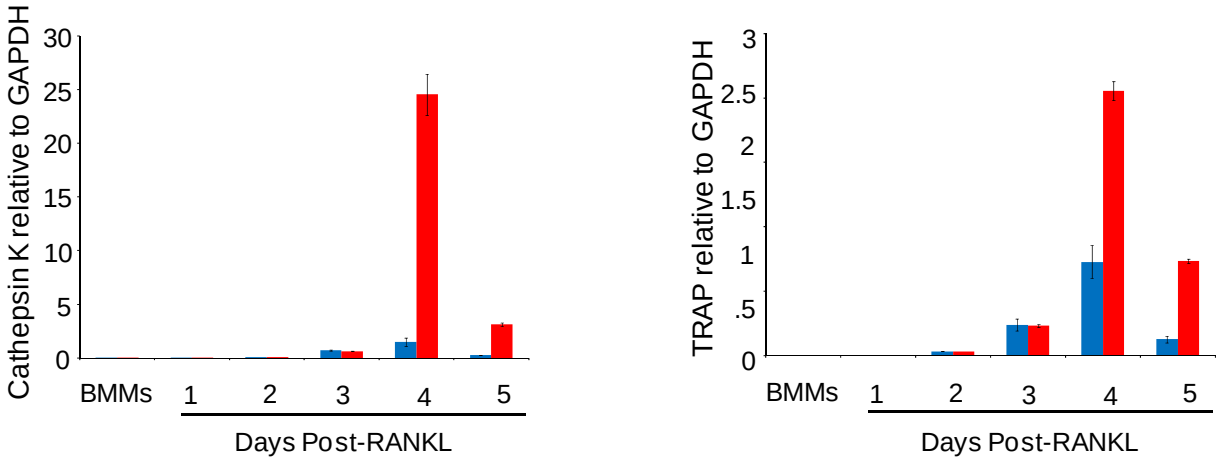

Figure 3.4.

***Arf* loss results in increased levels of Cathepsin K and TRAP mRNA during osteoclastogenesis.** Bone marrow macrophages from either wild-type or *Arf*$^{-/-}$ mice were differentiated *in vitro* with M-CSF and 50ng/mL RANKL. RNA was isolated from bone marrow macrophages (before RANKL addition) and each day after the addition of RANKL for 5 days. Equal amounts of RNA were used to generate cDNA by reverse transcription. Equal amounts of cDNA were used to assess the levels of Cathepsin K mRNA (left figure) and TRAP mRNA (right figure) by quantitative RT-PCR. WT = blue bars, *Arf*$^{-/-}$ = red bars. On days 4 and 5 (post-RANKL), loss of *Arf* significantly increases the amount of both Cathepsin K mRNA (left) and TRAP mRNA (right) ($p \leq 0.05$ on days 4 and 5 only).

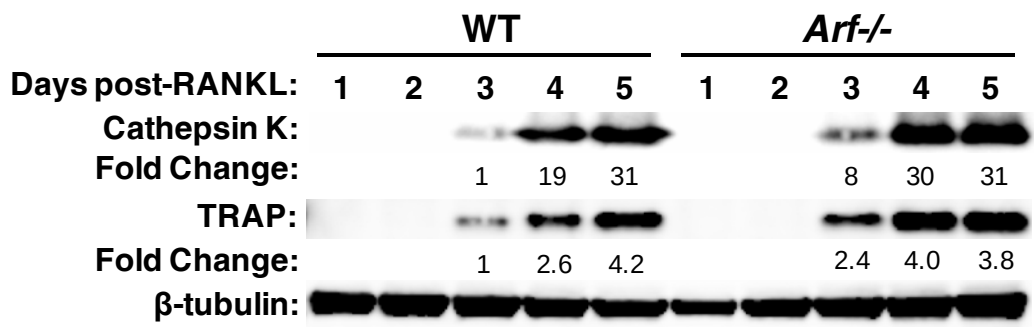

Figure 3.5.

***Arf* loss results in increased protein levels of Cathepsin K and TRAP during osteoclastogenesis.** Bone marrow macrophages from either wild-type or *Arf*$^{-/-}$ mice were differentiated *in vitro* with M-CSF and 50ng/mL RANKL. Total protein was isolated each day after the addition of RANKL for 5 days. Equal amounts of protein were separated by SDS-PAGE. Membranes were probed for Cathepsin K, TRAP, and β-tubulin (control). Protein bands were quantified by densitometry. Levels of Cathepsin K were first normalized to β-tubulin and fold changed was subsequently assessed calculating the fold change for each day relative to WT day 3. Levels of TRAP were first normalized to β-tubulin and fold changed was subsequently assessed calculating the fold change for each day relative to WT day 3.

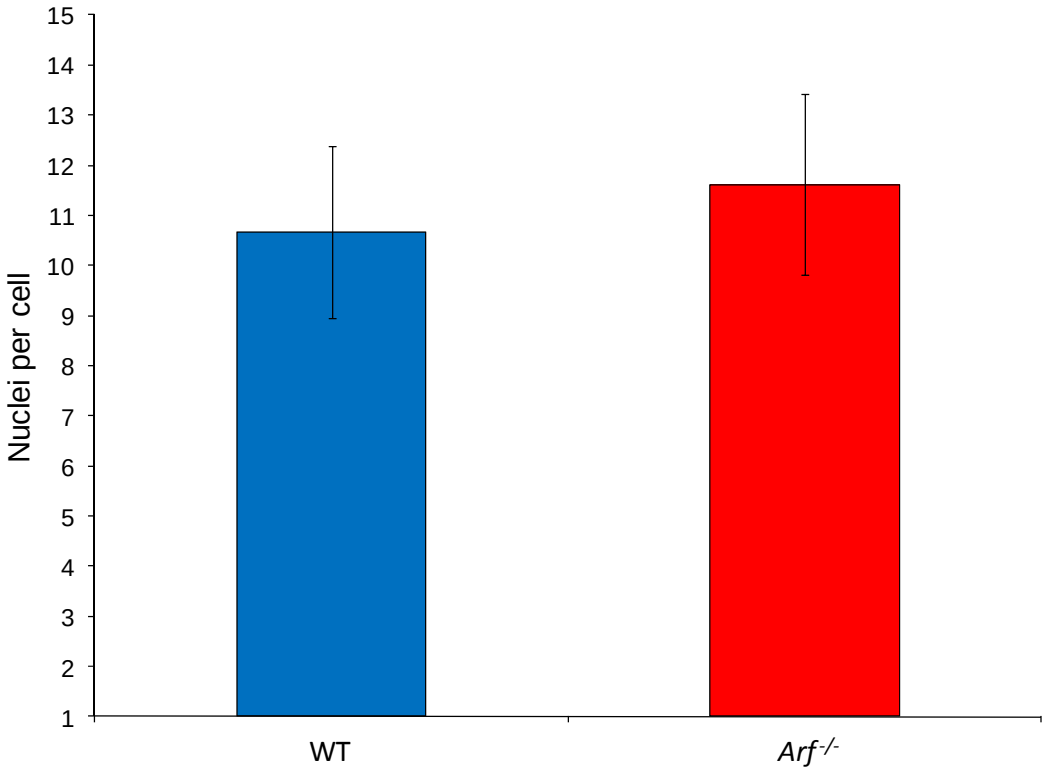

Figure 3.6.

Enhanced fusion during osteoclastogenesis does not explain the increase in osteoclast size upon *Arf* loss. Bone marrow macrophages from either wild-type or *Arf*$^{-/-}$ mice were differentiated *in vitro* on glass coverslips in the presence of M-CSF and 50ng/mL RANKL. After 6 days in the presence of osteoclastogenic media, cells were fixed and stained with DAPI to demarcate nuclei. Nuclei numbers were blindly counted in 100 osteoclasts of each genotype. WT = blue bars, *Arf*$^{-/-}$ = red bars. Difference is not statistically significant.

A

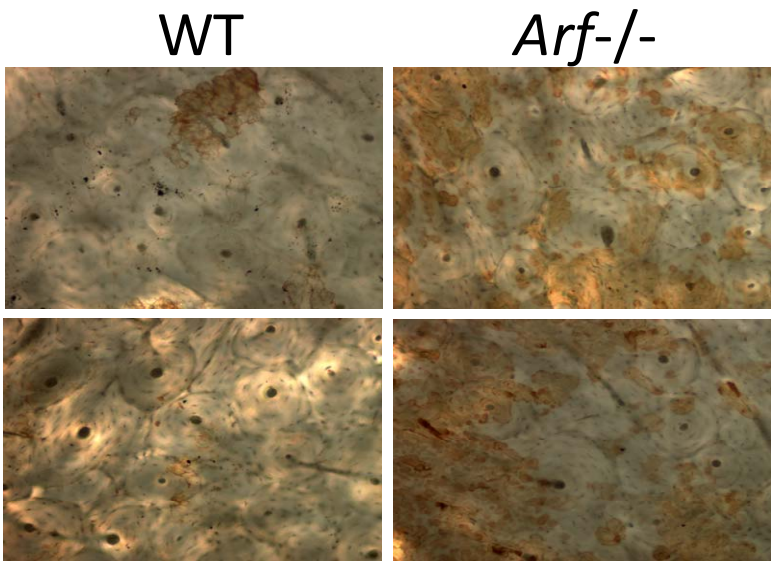

B

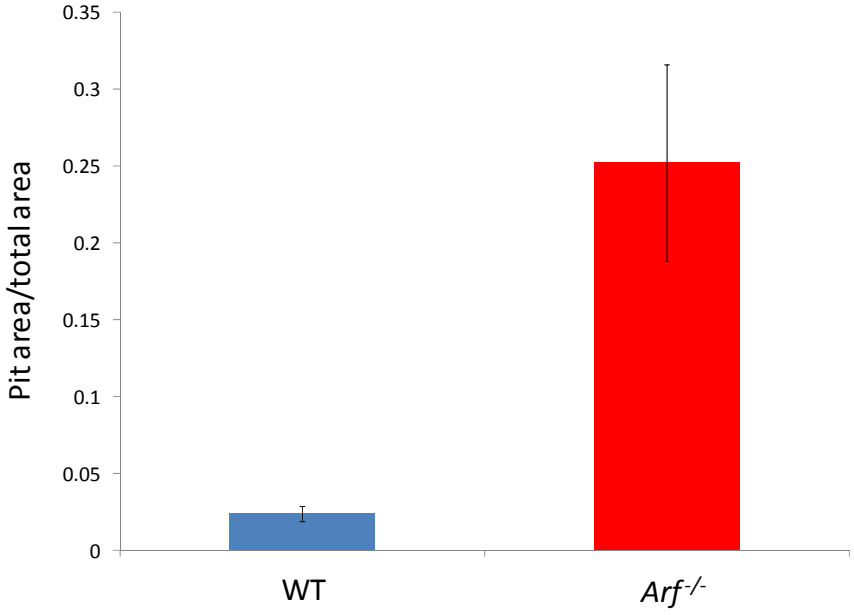

Figure 3.7.

***Arf* loss increases bone resorption by osteoclasts *in vitro*.** Bone marrow macrophages from either wild-type or *Arf*$^{-/-}$ mice were differentiated *in vitro* on bovine bone slices in the presence of M-CSF and 50ng/mL RANKL. After 8 days in the presence of osteoclastogenic media, cell were removed and bone slices were incubated with peroxidase-conjugated wheat germ agglutinin followed by 3,3-diaminobenzidine to visualize areas of bone resorption. (A) Two representaive fields from each genotype (dark brown indicates areas of bone resorption) (B) Resorptive area (pits) were blindly quantified by determining the average of four fields from each bone slice. Difference is statistically significant ($p \leq 0.05$).

A

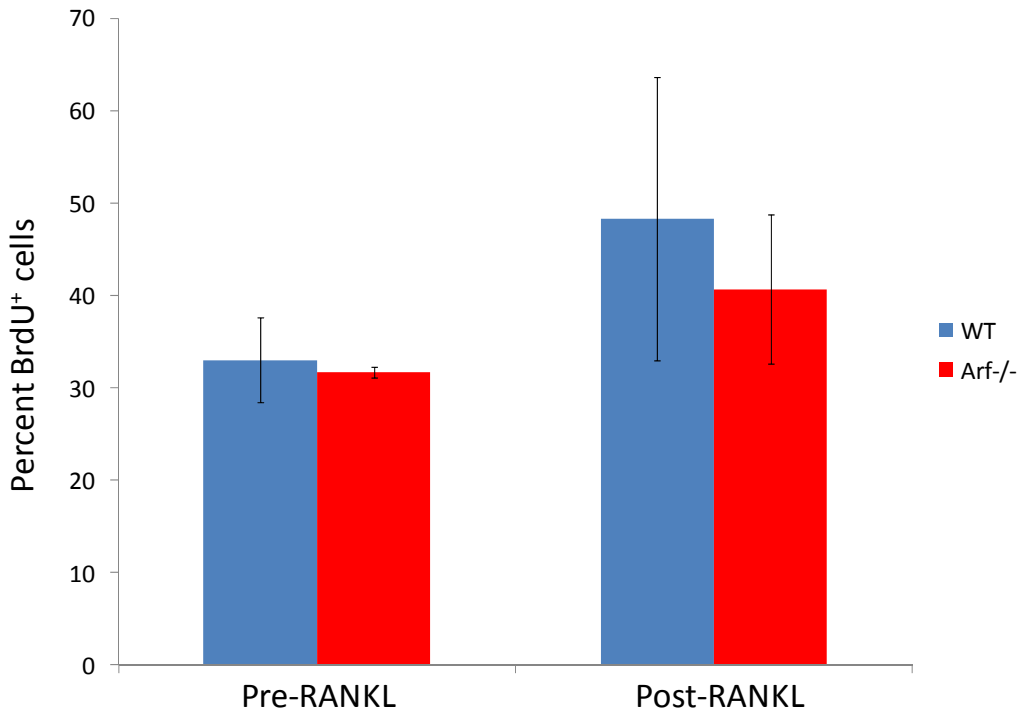
70
60
50
40
30
20
10
0
Percent BrdU+ cells
Pre-RANKL
Post-RANKL
WT
Arf-/-

B

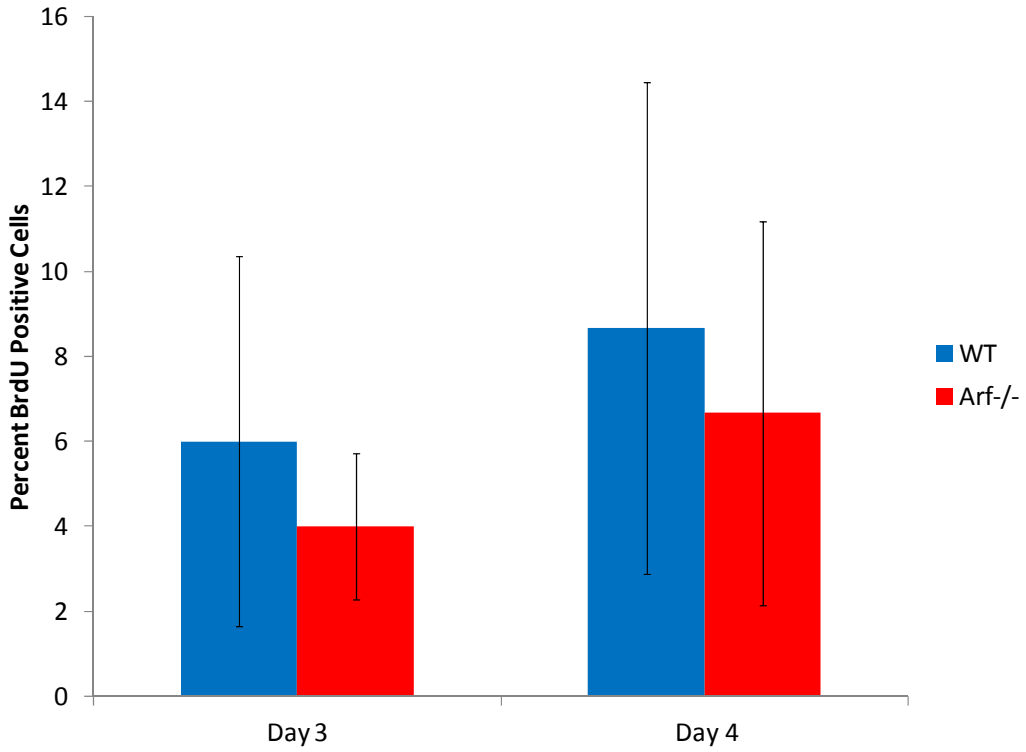
16
14
12
10
8
6
4
2
0
Percent BrdU Positive Cells
Day 3
Day 4
WT
Arf-/-

Figure 3.8.

Proliferation of osteoclast precursors in not enhanced upon *Arf* loss. Bone marrow macrophages from either wild-type or *Arf*$^{-/-}$ mice were differentiated *in vitro* on glass coverslips either in the presence of M-CSF (BMMs) or M-CSF and 50ng/mL RANKL (osteoclasts). Cells were incubated for 24h with BrdU to assess proliferation. (A) Cells were fixed as macrophages (pre-RANKL) and 24h after RANKL addition (post-RANKL). (B) Cells were fixed 3 and 4 days post-RANKL as proliferation controls. All fixed cells were then incubated with an antibody recognizing BrdU and DAPI to demarcate nuclei. At least100 nuclei were blindly assessed for BrdU for each genotype and at each time point. WT = blue bars, *Arf*$^{-/-}$ = red bars. All differences are not statistically significant.

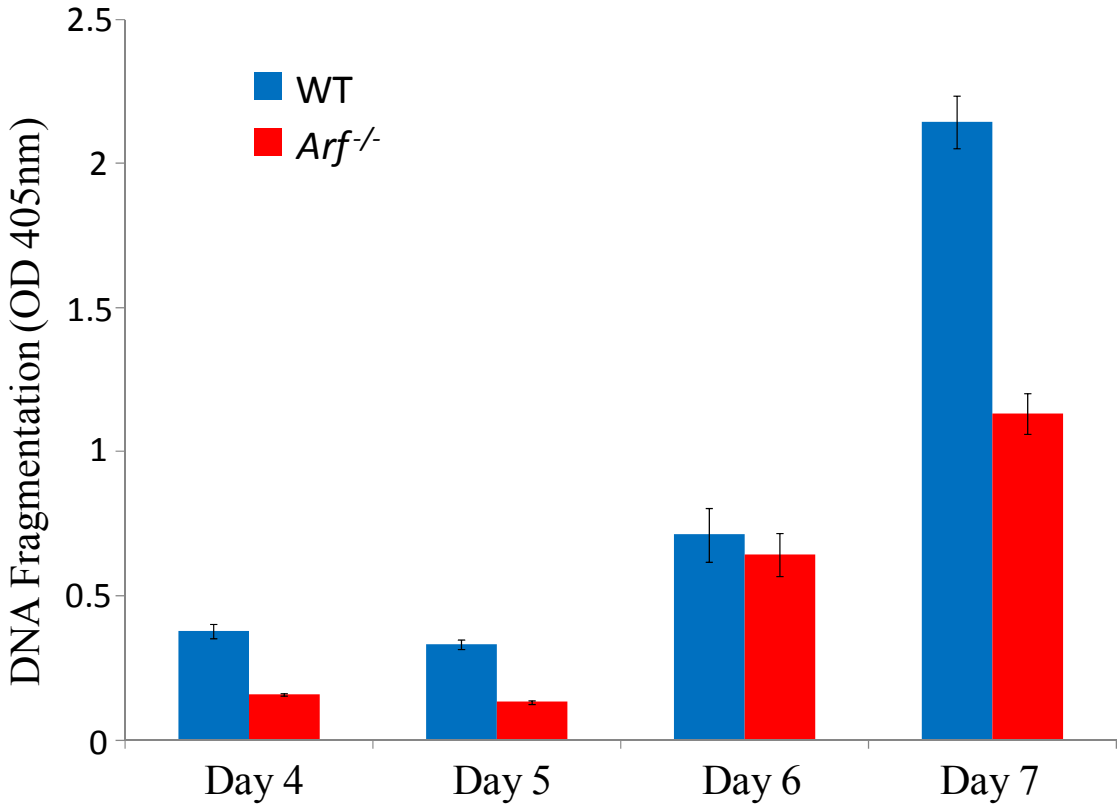

Figure 3.9.

***Arf* loss extends the lifespan of osteoclasts *in* vitro.** Bone marrow macrophages from either wild-type or *Arf*$^{-/-}$ mice were seeded at 5000 cells/well in 96-well dishes and differentiated in the presence of M-CSF and 50ng/mL RANKL. On days 4, 5, 6, and 7 after the addition of RANKL, cell death was assessed by an ELISA, which detects cytoplasmic histone-associated DNA fragmentation Absorbance was measured at 405nm. WT = blue bars and *Arf*$^{-/-}$ = red bars. *Arf* loss results in a statistically significant

decrease in apoptosis on days 4, 5, and 7 ($p \leq 0.05$). The difference observed on day 6 is not statistically significant.

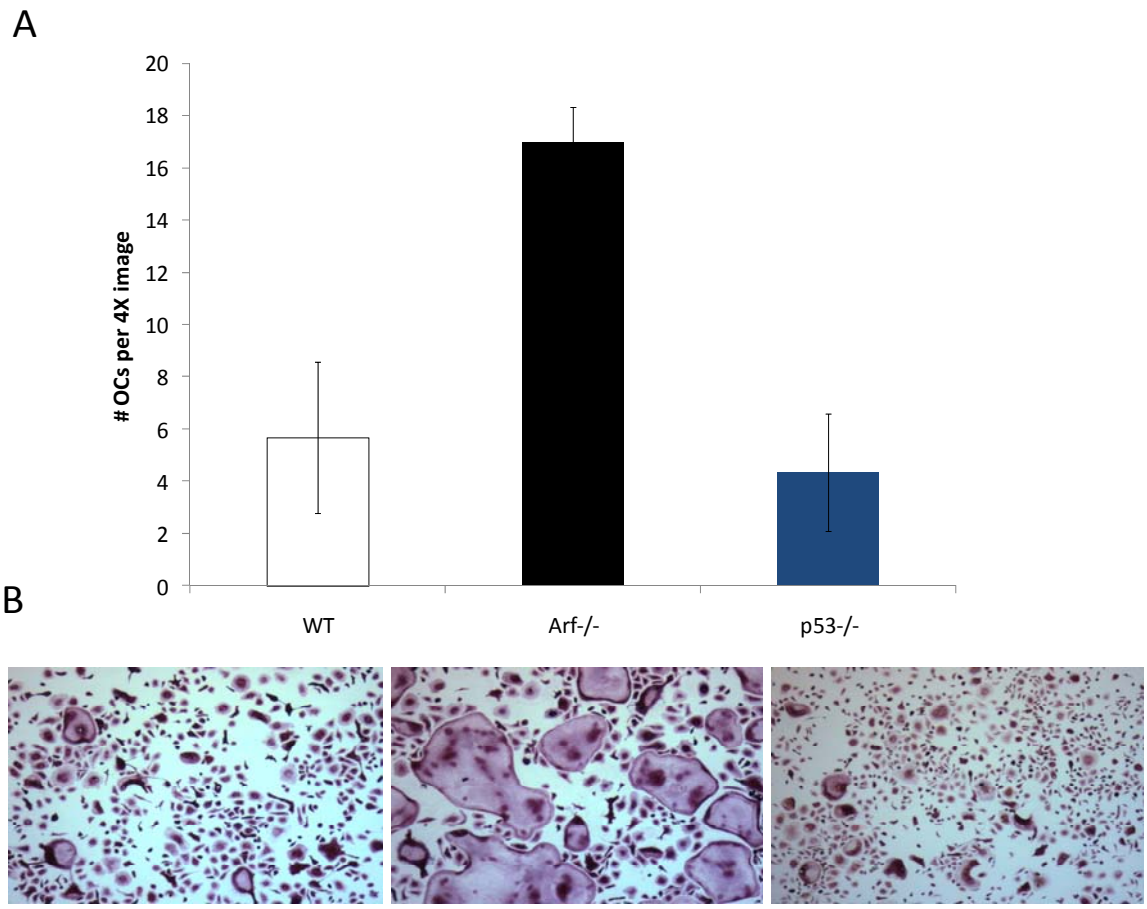

Figure 3.10.

***p53* loss does not phenocopy *Arf* loss during osteoclastogenesis *in vitro*.** Bone marrow macrophages from either wild-type, *Arf*$^{-/-}$, or *p53*$^{-/-}$ mice were differentiated in 48-well dishes in the presence of M-CSF and 50ng/mL RANKL. After 5 days in the presence of osteoclastogenic media, cells were fixed and TRAP-stained. (A) Osteoclast number was blindly quantified by counting TRAP-positive multinucleated cells in two fields of each well at a 4X magnification. The two fields were averaged for each well and reported as number of osteoclasts per 4X image. There were significantly more osteoclasts derived

from *Arf*$^{-/-}$ macrophages relative to both wild-type and *p53*$^{-/-}$ ($p \leq 0.05$). The difference in osteoclast number between wild-type and *p53*$^{-/-}$ is not statistically significant. (B) Representative TRAP-stained 4X images are shown below their respective genotypes.

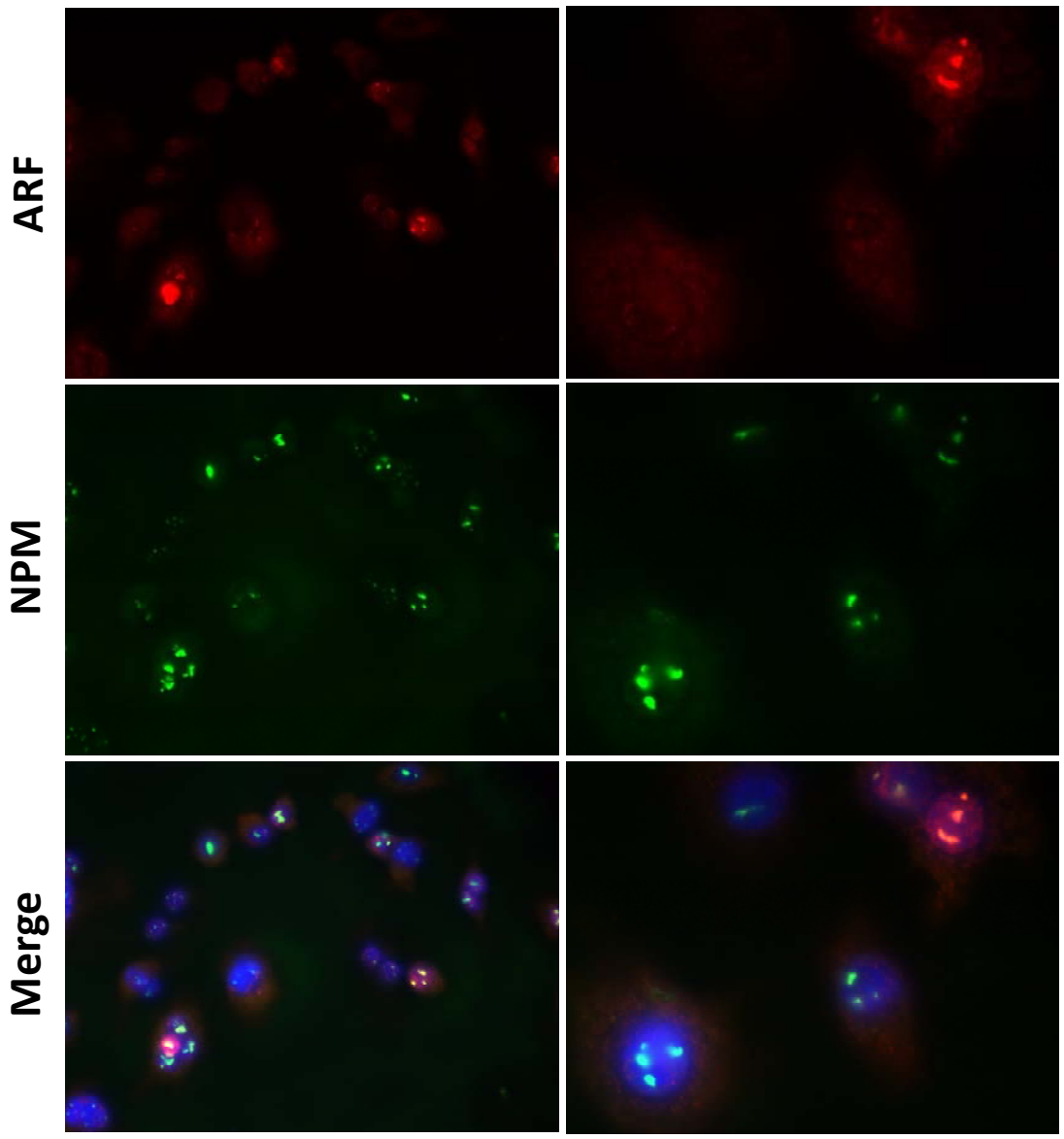

Figure 3.11.

ARF colocalizes with NPM in nucleoli of wild-type osteoclasts. Bone marrow macrophages from either wild-type mice were differentiated *in vitro* on glass coverslips in the presence of M-CSF and 50ng/mL RANKL. After 6 days in the presence of osteoclastogenic media, cells were fixed and stained for ARF and NPM followed by FITC- and rhodamine-conjugated secondary antibodies. DAPI was used to demarcate

nuclei. ARF is visualized in red channel (top images). NPM is visualized in green channel (middle images). Merged images (bottom) represent the red, green, and blue channels.

A

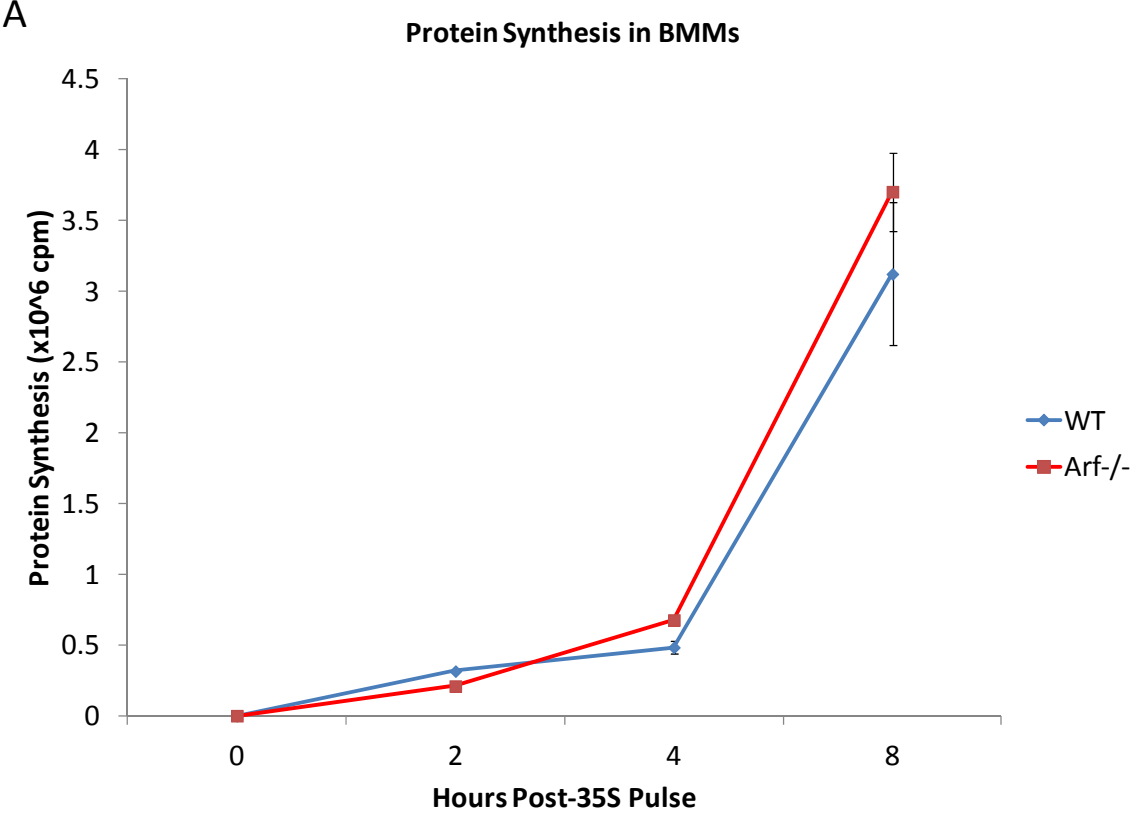
Protein Synthesis in BMMs
Protein Synthesis (x10^6 cpm)
4.5
4
3.5
3
2.5
2
1.5
1
0.5
0
0
2
4
8
Hours Post-35S Pulse
WT
Arf-/-

B

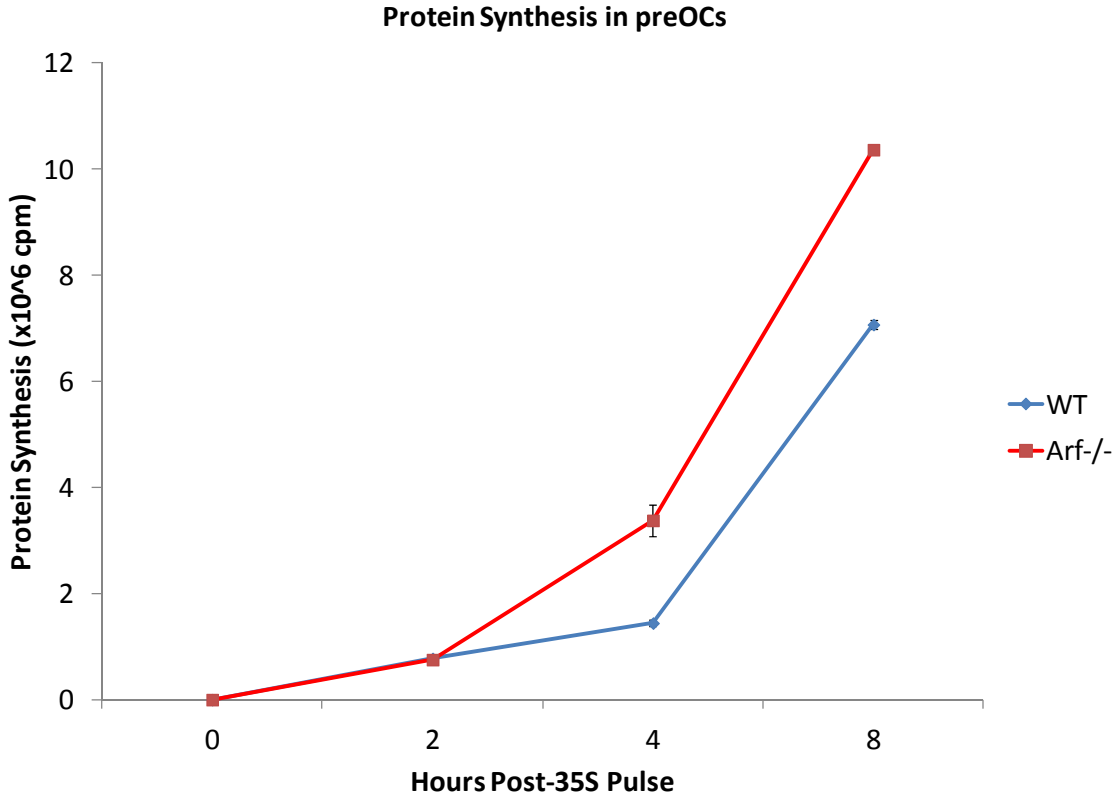
Protein Synthesis in preOCs
Protein Synthesis (x10^6 cpm)
12
10
8
6
4
2
0
0
2
4
8
Hours Post-35S Pulse
WT
Arf-/-

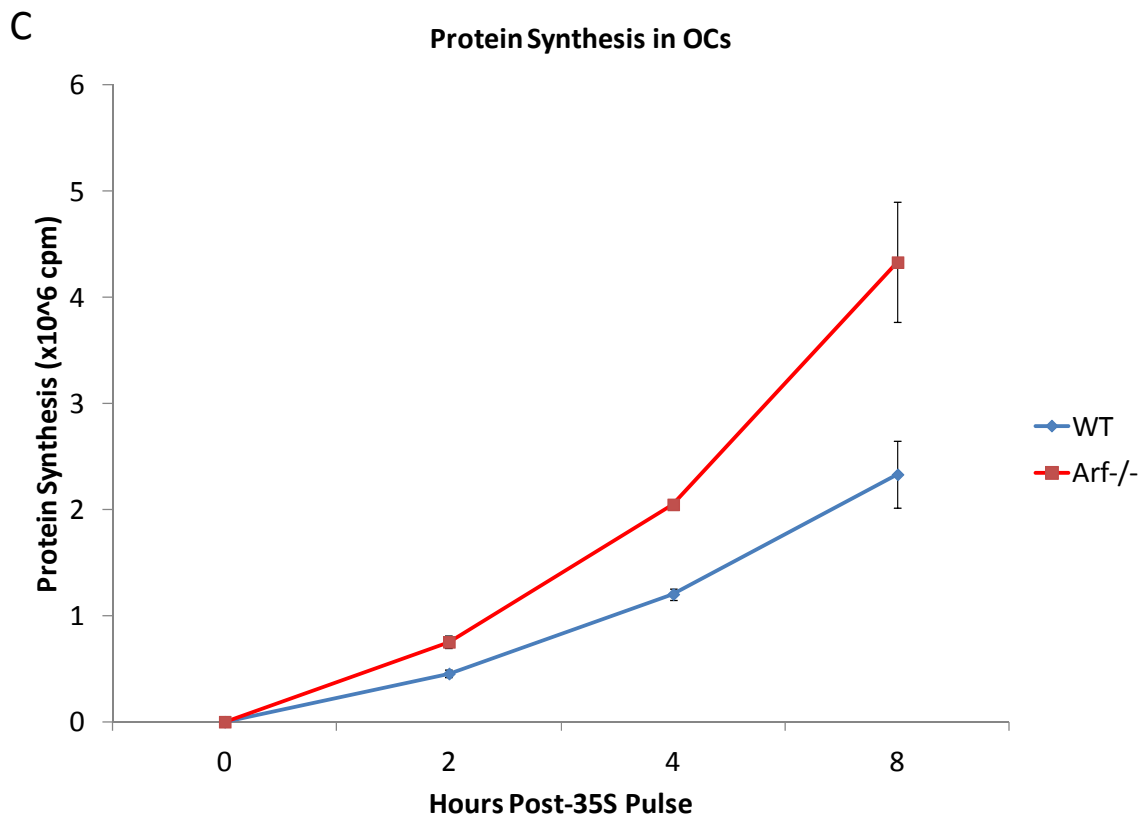

Figure 3.12.

Loss of *Arf* results in enhanced protein synthesis during osteoclastogenesis. Bone marrow macrophages from either wild-type or *Arf*$^{-/-}$ mice were plated in 6-well dishes in the presence of only M-CSF (BMMs) or M-CSF and 50ng/mL RANKL (pre-OCs and OCs). All cells were starved of methionine and cysteine for 30min prior to labeling at the appropriate time point during differentiation (3 days post-RANKL for pre-OC and 5 days post-RANKL for OCs). Following starvation, cells were pulsed with 150 μCi of ^{35}S-mehtionine for the indicated times (2, 4, or 8 hours). The first time point (t=0) was harvested immediately after the pulse. Following the pulse, cells were washed with cold phosphate-buffered saline and then lysed with 1% Triton X-100 buffer. Protein was precipitated from cell lysates using 10% tricholoroacetic acid and pellets were analyzed by liquid scintillation counting to quantify the incorporated counts per million. WT =

blue, *Arf*$^{-/-}$ = red. (A) Protein synthesis in bone marrow macrophages (*Arf*$^{-/-}$ only statistically higher than wild-type at t = 4h, $p \leq 0.05$). (B) Protein synthesis in pre-osteoclasts (*Arf*$^{-/-}$ statistically higher than wild-type at t = 4h and t = 8h, $p \leq 0.05$). (C) Protein synthesis in osteoclasts (*Arf*$^{-/-}$ statistically higher than wild-type at t = 2, t = 4h, and t = 8, $p \leq 0.05$).

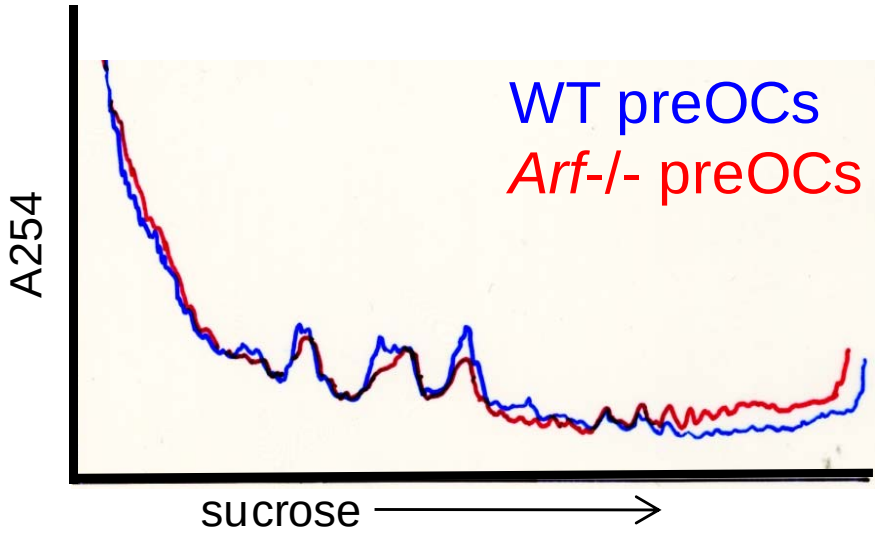

Figure 3.13.

Loss of *Arf* results in enhanced ribosome output in pre-osteoclasts. Bone marrow macrophages from either wild-type or *Arf*$^{-/-}$ mice were differentiated in 100mm dishes for 3 days in the presence of M-CSF and 50ng/mL RANKL. Cells were then treated with 50ug/mL cycloheximide to freeze actively-translating ribosomes onto mRNAs. 3 x 10^6 cells were lysed and cytosolic fractions were separated by centrifugation over a continuous sucrose gradient. RNA absorbance was continuously monitored at 254nm to detect ribosomal subunits. WT = blue bars, *Arf*$^{-/-}$ = red bars.

A

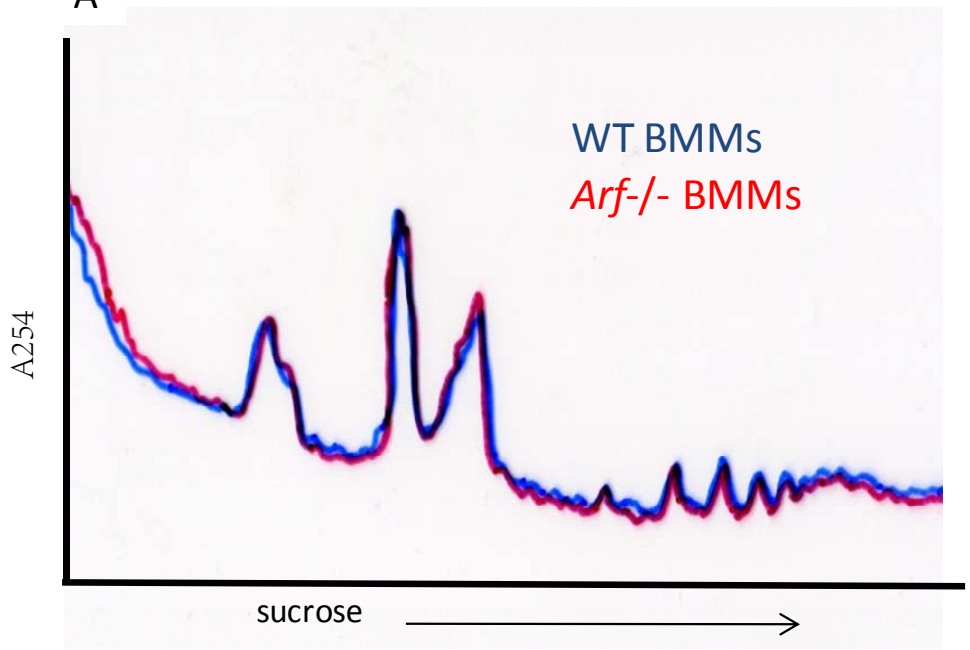
WT BMMs
Arf-/- BMMs
A254
sucrose

B

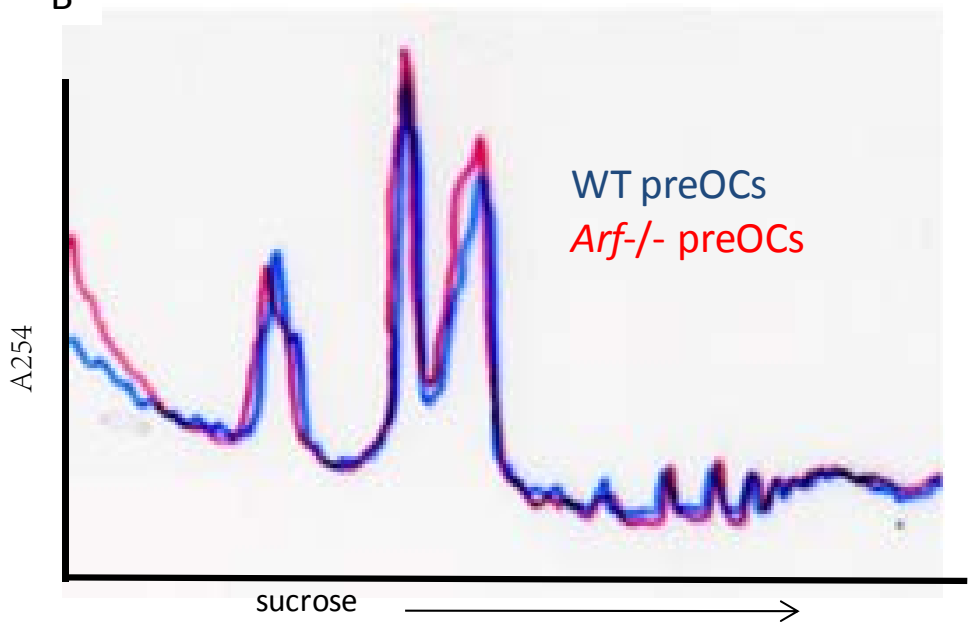
WT preOCs
Arf-/- preOCs
A254
sucrose

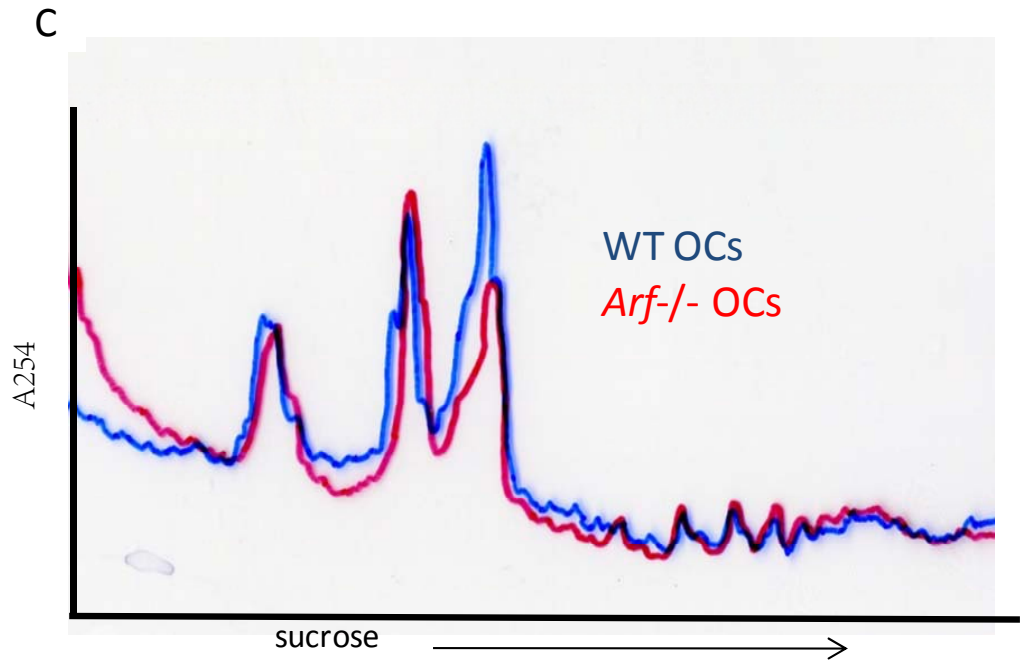

Figure 3.14.

Ribosome output is not different between wild-type and *Arf* $^{-/-}$ cells during osteoclastogenesis when mice are on different backgrounds, indicating the sensitivity of generating ribosome profiles to assess ribosome output. Bone marrow macrophages from either wild-type mice on a B6 background or *Arf*$^{-/-}$ mice on a B6/129 background were differentiated in 100mm dishes either in the presence of M-CSF alone (BMMs) or both M-CSF and 50ng/mL RANKL. Cells were then treated with 50ug/mL cycloheximide to freeze actively-translating ribosomes onto mRNAs at the appropriate days following the addition of RANKL (3 days post-RANKL for pre-osteoclasts and 5 days post-RANKL for osteoclasts, BMMs not given RANKL but harvested 24h after plating in the presence of M-CSF). 3 x 10^6 cells were lysed and cytosolic fractions were separated by centrifugation over a continuous sucrose gradient. RNA absorbance was

continuously monitored at 254nm to detect ribosomal subunits. WT = blue bars, *Arf*$^{-/-}$ = red bars. (A) Ribosome profiles of BMMs (B) Ribosome profiles of pre-osteoclasts (C) Ribosome profiles of osteoclasts

A

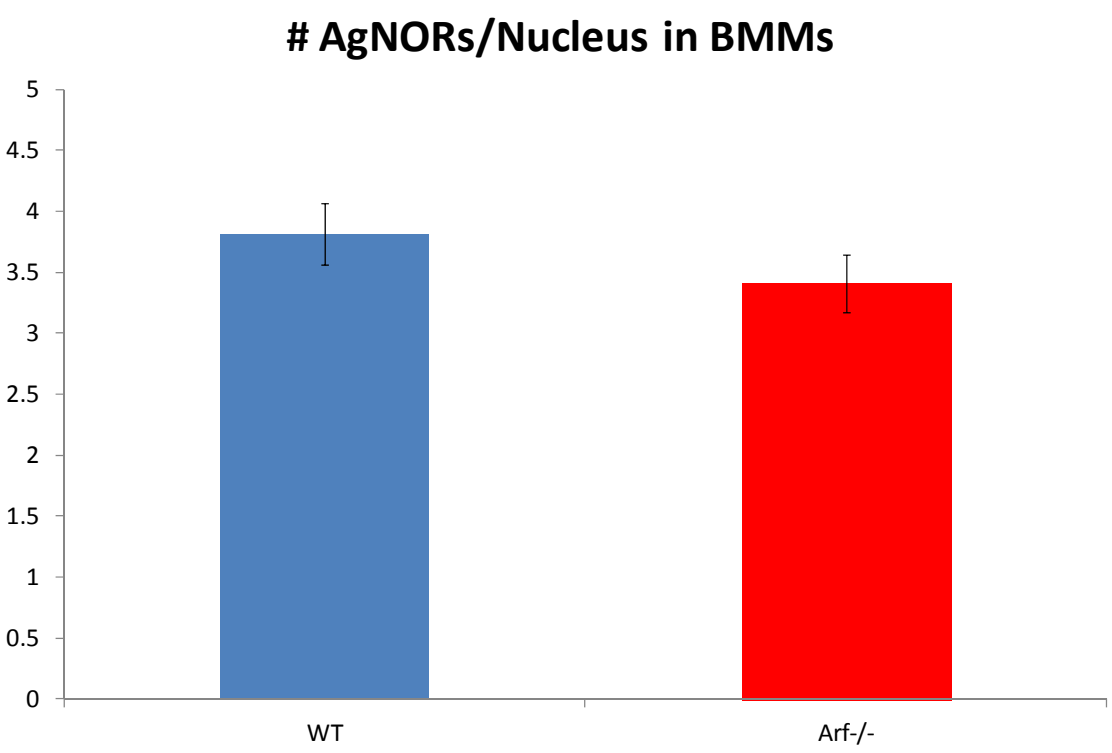
AgNORs/Nucleus in BMMs
5
4.5
4
3.5
3
2.5
2
1.5
1
0.5
0
WT
Arf-/-

B

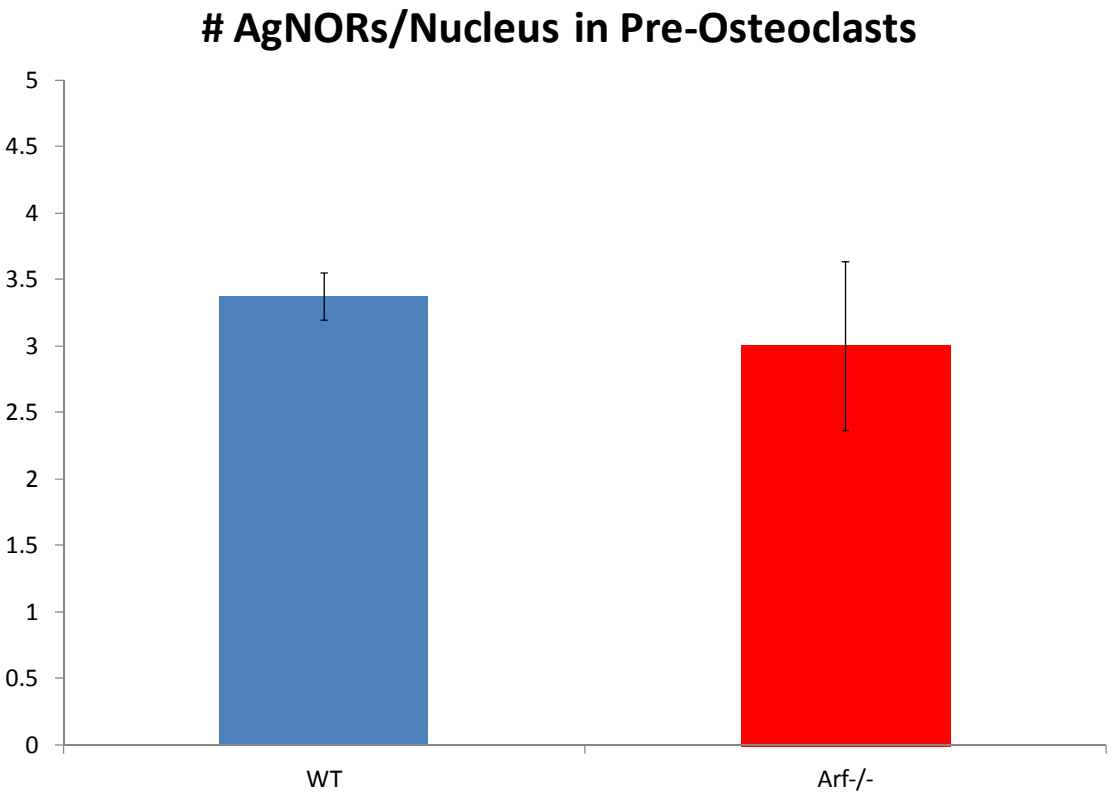
AgNORs/Nucleus in Pre-Osteoclasts
5
4.5
4
3.5
3
2.5
2
1.5
1
0.5
0
WT
Arf-/-

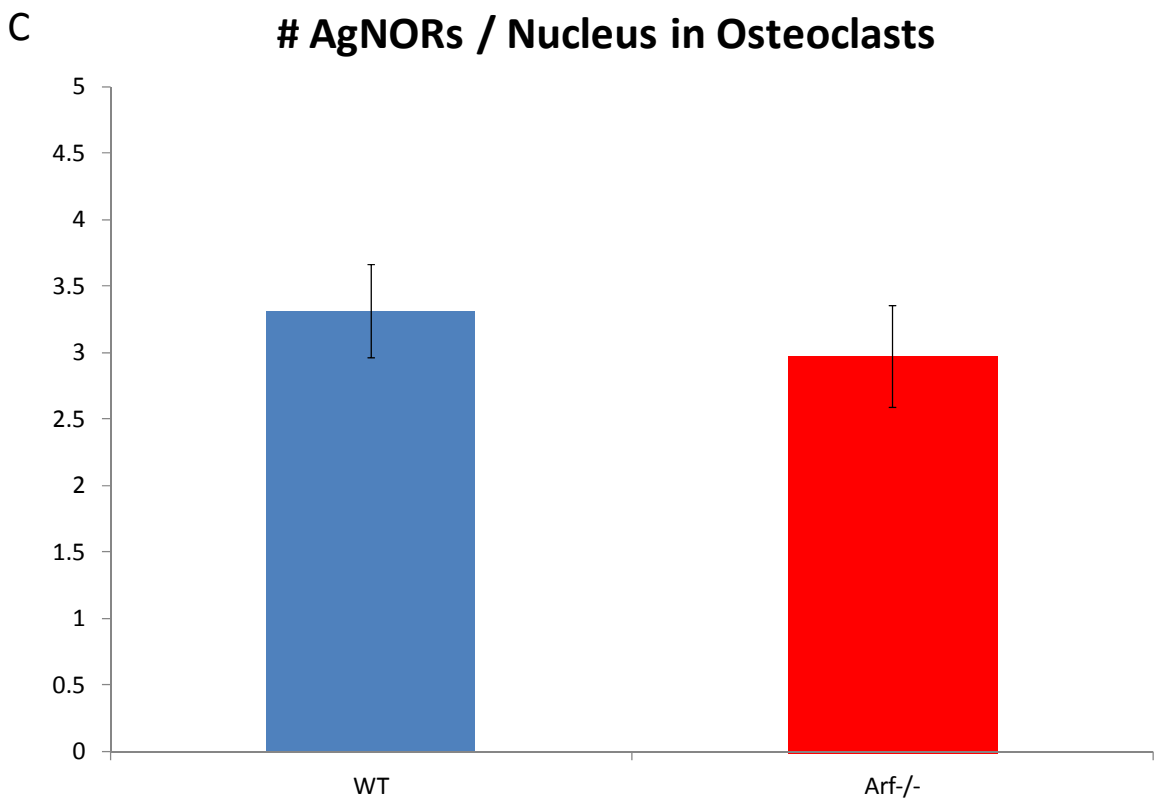

Figure 3.15.

***Arf* loss does not alter the number of AgNORs per nucleus during osteoclastogenesis.** Bone marrow macrophages from either wild-type or *Arf*$^{-/-}$ mice were differentiated in 100mm on coverslips in the presence of M-CSF alone (BMMs) or both M-CSF and 50ng/mL RANKL (pre-osteoclasts and osteoclasts). At the appropriate time during osteoclastogenesis (24h post-plating for BMMs, 3 days post-RANKL for pre-osteoclasts, and 5 days post-RANKL for osteoclasts) cells were fixed and processed to visualize AgNORs, and mounted on slides. AgNOR numbers in at least 50 nuclei on each coverslip for each genotype were blindly quantified. WT = blue bars, *Arf*$^{-/-}$ = red bars. (A) Average number of AgNORs per nucleus in BMMs (difference is not statistically

significant). (B) Average number of AgNORs per nucleus in pre-osteoclasts (difference is not statistically significant). (C) Average number of AgNORs per nucleus in osteoclasts (difference is not statistically significant).

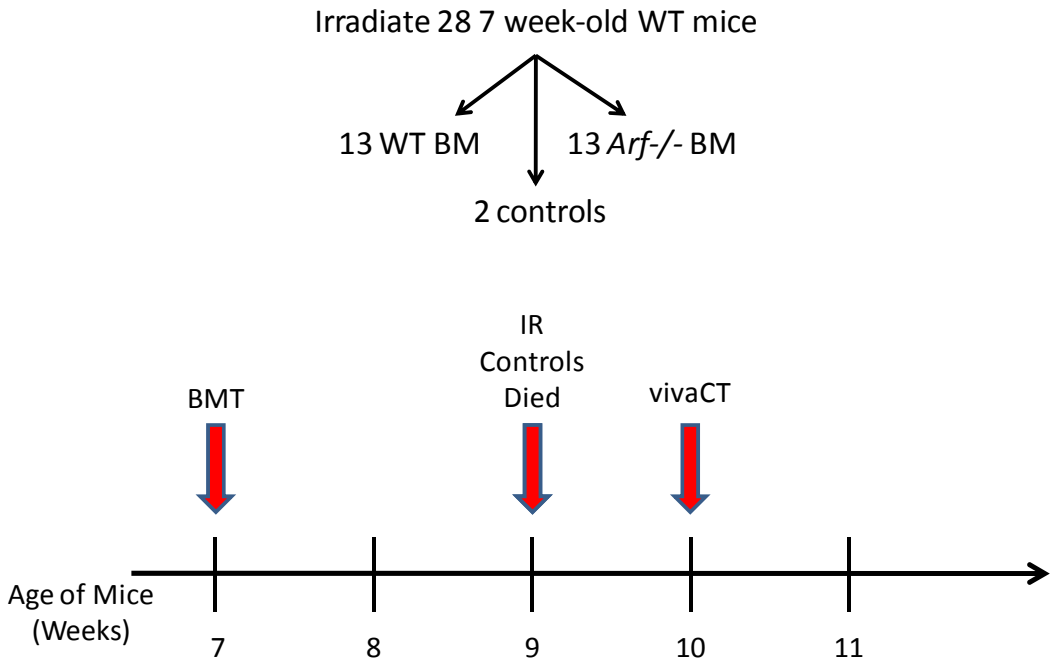

Figure 3.16.

Outline of initial experimental set-up to determine the role of ARF in osteoclasts *in vivo*. 24 hours after irradiating 28 7 week-old wild-type male mice, whole bone marrow was harvested from either wild-type or *Arf*$^{-/-}$ mice and 1 x 10^6 cells were injected intravenously into the irradiated mice. 13 mice received wild-type bone marrow, 13 received *Arf*$^{-/-}$ bone marrow, and 2 did not receive a transplant to control for the success of lethal irradiation. Mice that did not receive a transplant died 2 weeks following the irradiation. The remaining 26 mice were imaged by vivaCT 3 weeks following the irradiation and transplant.

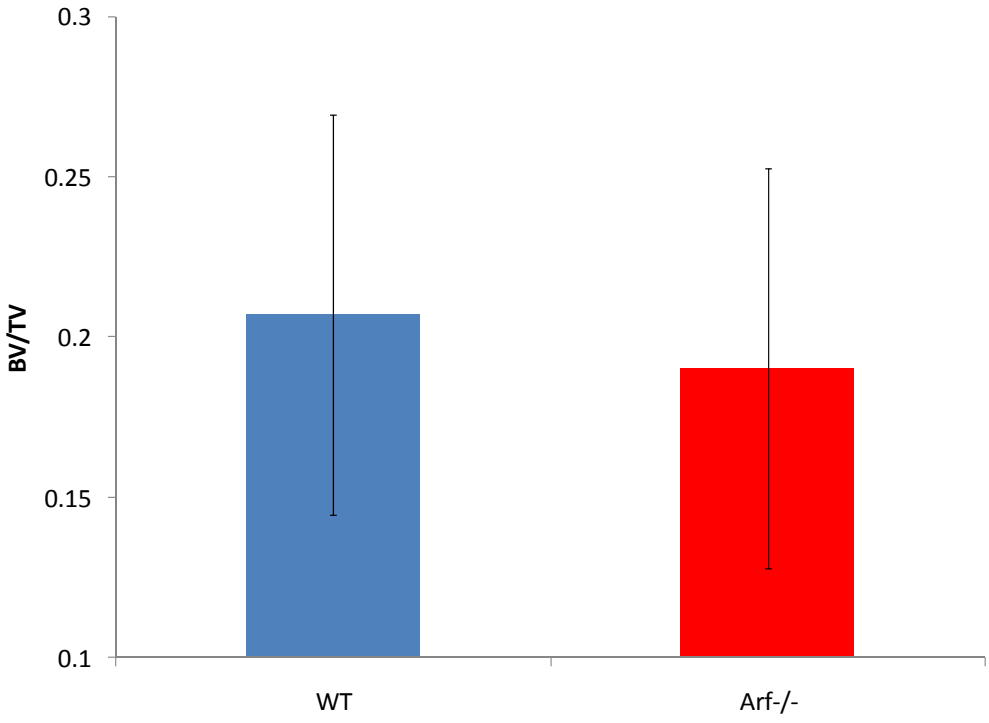

Figure 3.17.

Initial BV/TV results indicate that radiation chimeras must be challenged with RANKL. Radiation chimeras were subjected to vivaCT 3 weeks following the transplant to determine bone volume. There is no significant difference between wild-type mice that received bone marrow from wild-type donors and wild-type mice that received bone marrow from *Arf*$^{-/-}$ donors.

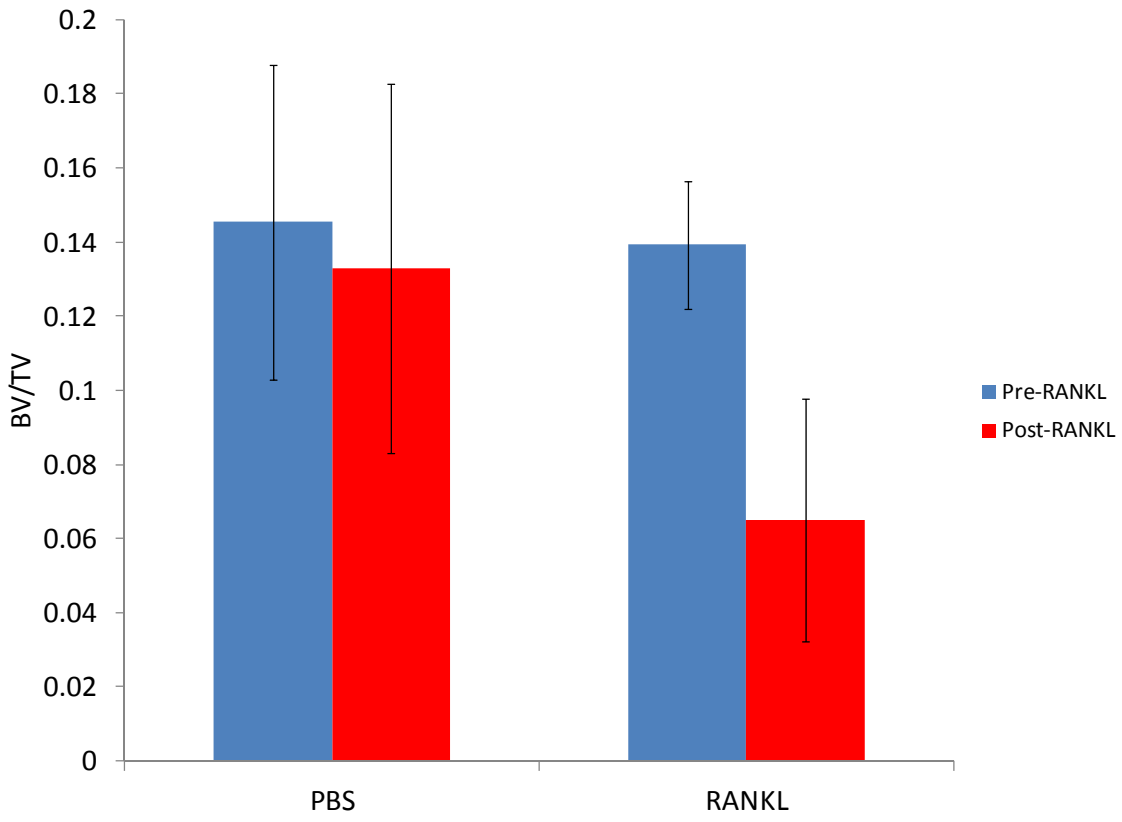

Figure 3.18.

Three consecutive daily doses of 2mg/kg RANKL given intraperitoneally causes a significant reduction in bone volume. Pre-RANKL bone volume was assessed by vivaCT anlysis for both groups less than 1 week prior to the initial injection of RANKL (blue bars). Three age-matched wild-type male mice were subsequently intraperitoneally injected daily with 2mg/kg RANKL for 3 consecutive days. Controls (n = 3) received daily intraperitoneally injections of equivalent volumes of PBS (based on individual weights) for 3 consecutive days. Post-RANKL bone volume was assessed by vivaCT analysis 1.5h following the final injection (red bars). The difference between pre-RANKL and post-RANKL BV/TV (bone volume/total volume) is not statistically

significant following PBS injections. The difference between pre-RANKL and post-RANKL BV/TV is statistically significant ($p \leq 0.05$)

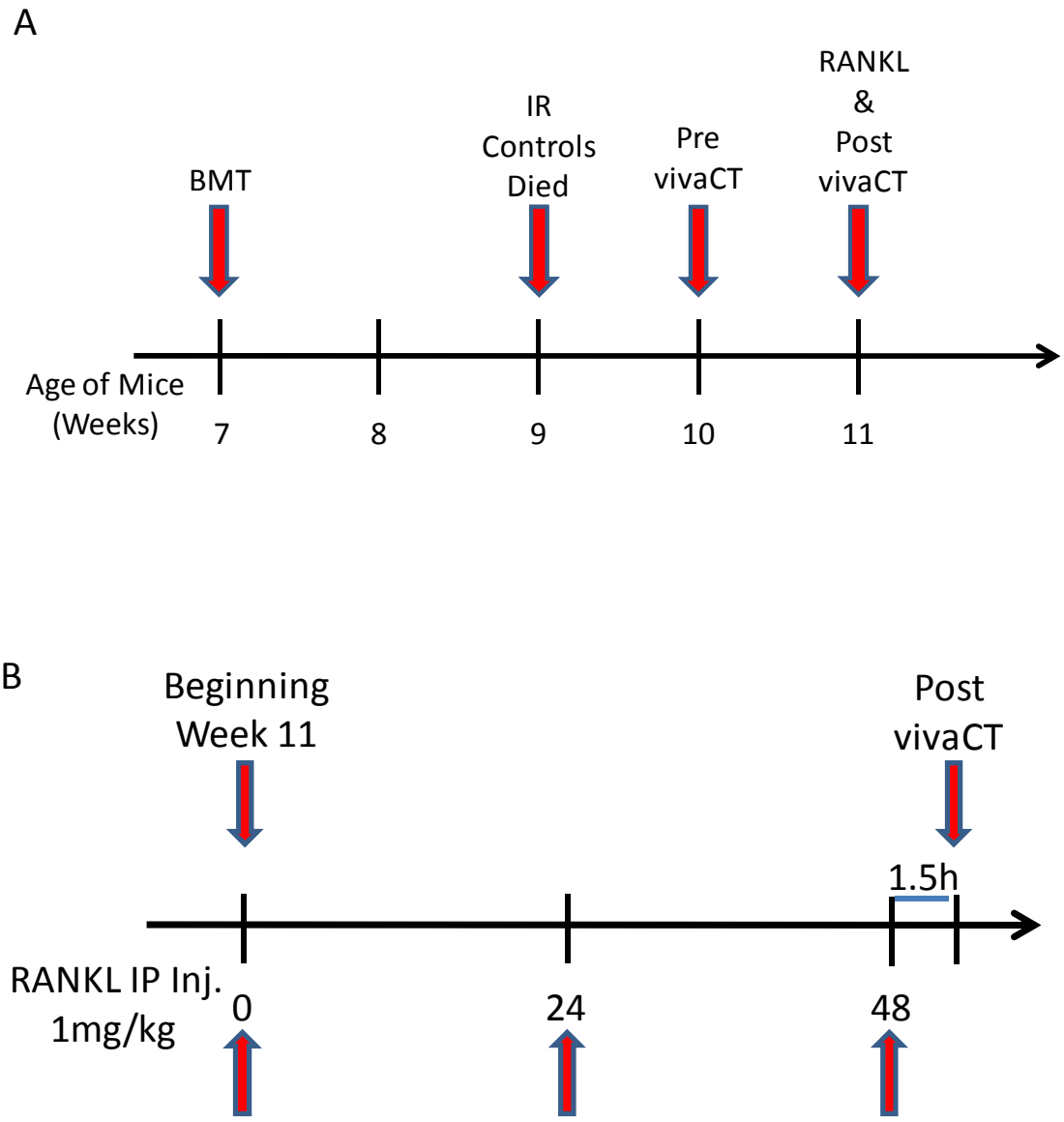

Figure 3.19.

Outline of final experimental set-up to determine the role of ARF in osteoclasts *in vivo*. (A) 24 hours after irradiating 28 7 week-old wild-type male mice, whole bone marrow was harvested from either wild-type or *Arf*$^{-/-}$ mice and 1 x 10^6 cells were injected intravenously into the irradiated mice. 13 mice received wild-type bone marrow, 13

received *Arf*$^{-/-}$ bone marrow, and 2 did not receive a transplant to control for the success of lethal irradiation. Mice that did not receive a transplant died 2 weeks following the irradiation. The remaining 26 mice were subjected to a pre-scan by vivaCT 3 weeks following the irradiation and transplant (pre vivaCT). One week following the pre-scan, mice were challenged with RANKL and subsequently imaged by vivaCT (post vivaCT). (B) Beginning at 11 weeks of age, mice were intraperitoneally injected with 3 consecutive daily doses of 1mg/kg RANKL (8 mice received WT bone marrow and RANKL, 8 mice received *Arf*$^{-/-}$ bone marrow and RANKL). Control mice were intraperitoneally injected with 3 consecutive daily doses of PBS (5 mice received WT bone marrow and PBS, 5 mice received *Arf*$^{-/-}$bone marrow and PBS). 1.5h following the last RANKL (or PBS) injection, mice were imaged by vivaCT (post vivaCT).

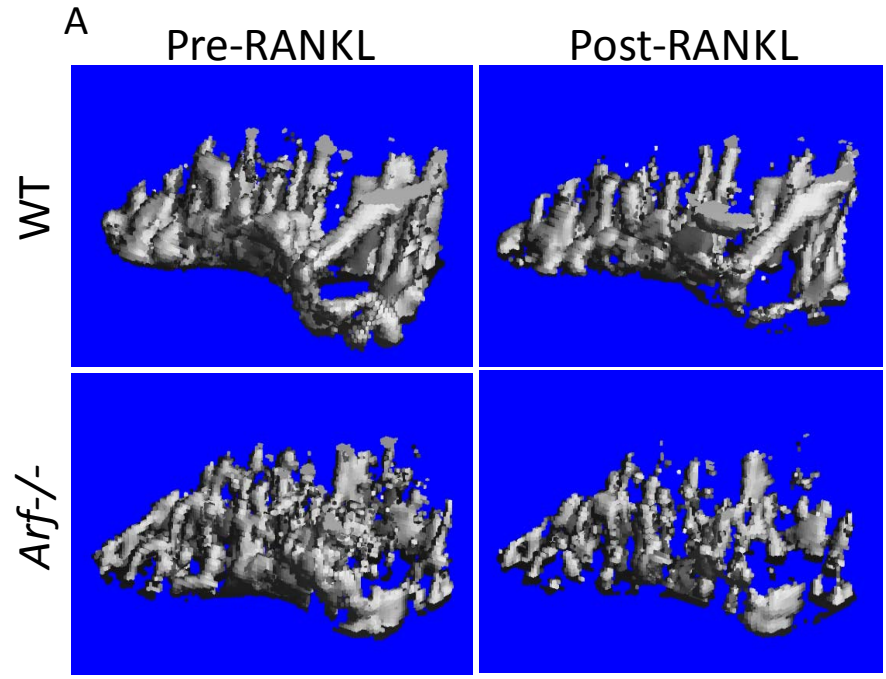
A
Pre-RANKL
Post-RANKL
WT
Arf-/-

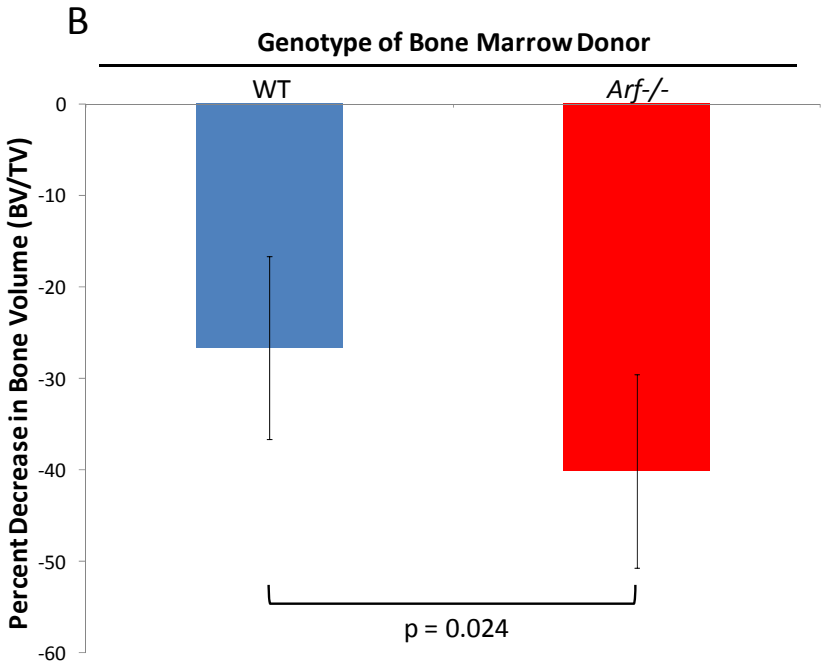
B
Genotype of Bone Marrow Donor
WT
Arf-/-
0
-10
-20
-30
-40
-50
-60
Percent Decrease in Bone Volume (BV/TV)
p = 0.024

C


Genotype of Bone Marrow Donor
WT
Arf-/-
0
-5
-10
-15
-20
-25
-30
-35
Percent Decrease in Trabecular Number
p = 0.017

D

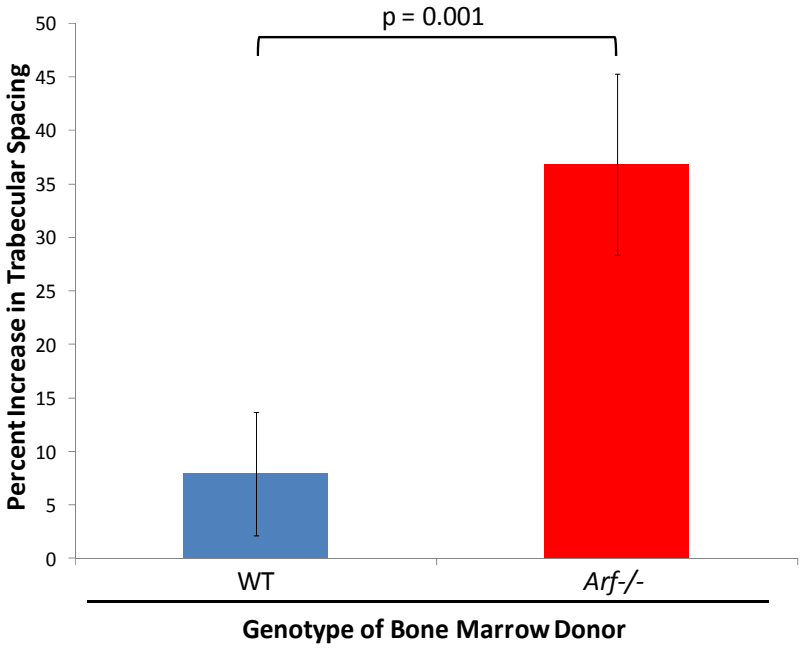
p = 0.001
50
45
40
35
30
25
20
15
10
5
0
Percent Increase in Trabecular Spacing
WT
Arf-/-
Genotype of Bone Marrow Donor

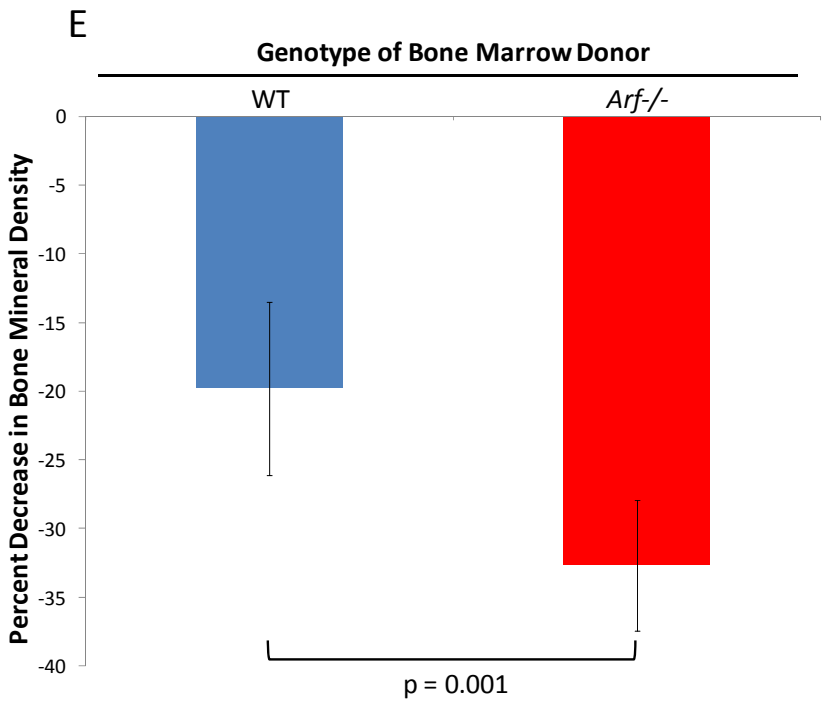

Figure 3.20.

Loss of *Arf* in osteoclasts results in increased bone resorption *in vivo* following RANKL stimulation. Pre-RANKL bone parameters were assessed by vivaCT analysis for both groups less than 1 week prior to the initial injection of RANKL. All mice were subsequently intraperitoneally injected daily with 1mg/kg RANKL for 3 consecutive days (n = 8 per group). Controls received daily intraperitoneally injections of equivalent volumes of PBS (based on individual weights) for 3 consecutive days. Post-RANKL bone parameteres were assessed by vivaCT analysis 1.5h following the final injection. For each animal, the difference between their pre-RANKL scan and post-RANKL scan was quantified and presented as present loss or gain. Animals receiving a WT bone marrow transplant are represented by blue bars and animals receiving an *Arf* $^{-/-}$ bone

marrow transplant are represented by blue bars. There were no statistically significant differences between WT and *Arf*$^{-/-}$ bone marrow recipients injected with PBS (data not shown). (A) Representative 3D images generated by vivaCT analysis show the trabecular bone in the tibia of a WT (top) and *Arf*$^{-/-}$ (bottom) bone marrow recipient before and after RANKL injection. (B) Animals receiving *Arf*$^{-/-}$ bone marrow lost significantly more bone volume following RANKL injections relative to animals receiving WT bone marrow ($p \leq 0.05$). (C) Animals receiving *Arf*$^{-/-}$ bone marrow had a significant decrease in trabecular number following RANKL injections relative to that in animals receiving WT bone marrow ($p \leq 0.05$). (D) Animals receiving *Arf*$^{-/-}$ bone marrow had a significant increase in trabecular spacing following RANKL injections relative to that in animals receiving WT bone marrow ($p \leq 0.05$).). (E) Animals receiving *Arf*$^{-/-}$ bone marrow had a significant decrease in bone mineral density following RANKL injections relative to that in animals receiving WT bone marrow ($p \leq 0.05$).

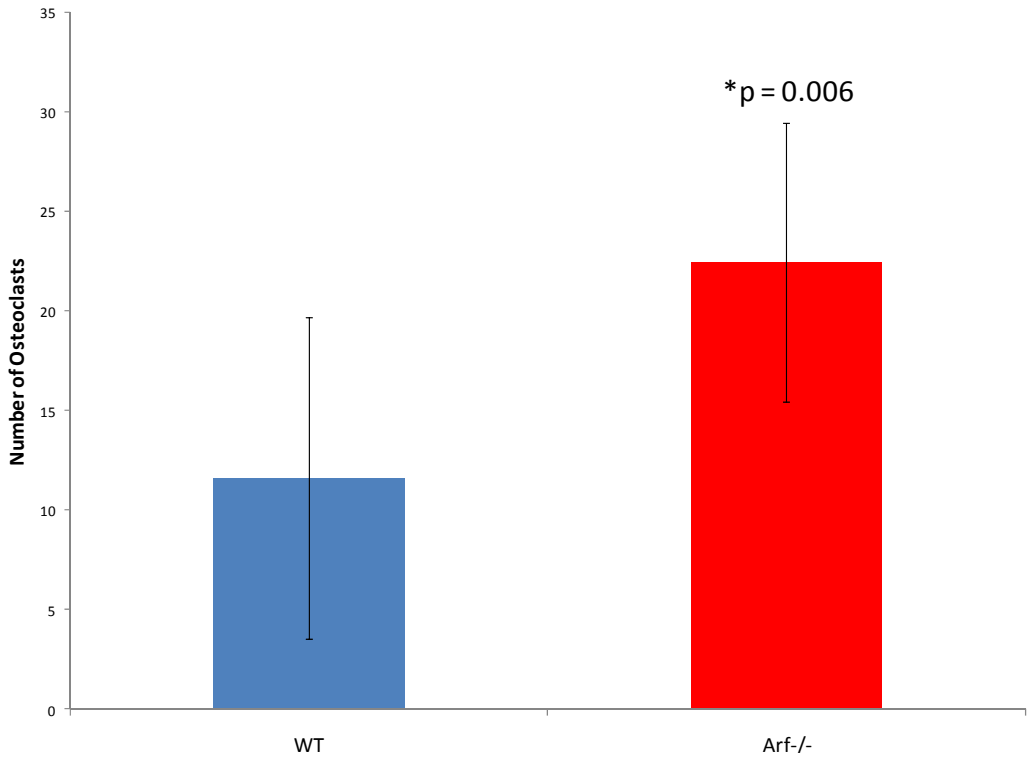

Figure 3.21.

Loss of *Arf* in osteoclasts results in an increase in osteoclast number *in vivo* following RANKL stimulation. Radiation chimeras were intraperitoneally injected daily with 1mg/kg RANKL for 3 consecutive days (n = 8 per group). Following the final injection of RANKL and vivaCT scan, tibias were harvested and formalin-fixed. Bones were then decalcified and incubated in increasing amounts of EtOH. Decalicified histological sections of proximal tibias were TRAP-stained and the number of OCs were blindly quantified in each section. Mice receiving WT bone marrow are represented by the blue bar and mice receiveing $Arf^{-/-}$ bone marrow are represented by the red bar. Difference is statistically significant ($p \leq 0.05$).

3.6 References

Aguilo, F., Zhou, M.M., and Walsh, M.J. Long Noncoding RNA, Polycomb, and the Ghosts Haunting INK4b-ARF-INK4a Expression. Cancer Res *71*, 5365-5369.

Apicelli, A.J., Maggi, L.B., Jr., Hirbe, A.C., Miceli, A.P., Olanich, M.E., Schulte-Winkeler, C.L., Saporita, A.J., Kuchenreuther, M., Sanchez, J., Weilbaecher, K.*, et al.* (2008). A non-tumor suppressor role for basal p19ARF in maintaining nucleolar structure and function. Mol Cell Biol *28*, 1068-1080.

Aubele, M., Biesterfeld, S., Derenzini, M., Hufnagl, P., Martin, H., Ofner, D., Ploton, D., and Ruschoff, J. (1994). Guidelines of AgNOR quantitation. Committee on AgNOR Quantitation within the European Society of Pathology. Zentralbl Pathol *140*, 107-108.

Ayrault, O., Andrique, L., Fauvin, D., Eymin, B., Gazzeri, S., and Seite, P. (2006). Human tumor suppressor p14ARF negatively regulates rRNA transcription and inhibits UBF1 transcription factor phosphorylation. Oncogene *25*, 7577-7586.

Ayrault, O., Andrique, L., Larsen, C.J., and Seite, P. (2004). Human Arf tumor suppressor specifically interacts with chromatin containing the promoter of rRNA genes. Oncogene *23*, 8097-8104.

Bernard, K., Litman, E., Fitzpatrick, J.L., Shellman, Y.G., Argast, G., Polvinen, K., Everett, A.D., Fukasawa, K., Norris, D.A., Ahn, N.G.*, et al.* (2003). Functional proteomic analysis of melanoma progression. Cancer Res *63*, 6716-6725.

Brady, S.N., Maggi, L.B., Jr., Winkeler, C.L., Toso, E.A., Gwinn, A.S., Pelletier, C.L., and Weber, J.D. (2009). Nucleophosmin protein expression level, but not threonine 198 phosphorylation, is essential in growth and proliferation. Oncogene *28*, 3209-3220.

Brady, S.N., Yu, Y., Maggi, L.B., Jr., and Weber, J.D. (2004). ARF impedes NPM/B23 shuttling in an Mdm2-sensitive tumor suppressor pathway. Mol Cell Biol *24*, 9327-9338.

Churchman, M.L., Roig, I., Jasin, M., Keeney, S., and Sherr, C.J. Expression of arf tumor suppressor in spermatogonia facilitates meiotic progression in male germ cells. PLoS Genet *7*, e1002157.

Cole, F., Keeney, S., and Jasin, M. Evolutionary conservation of meiotic DSB proteins: more than just Spo11. Genes Dev *24*, 1201-1207.

Furonaka, O., Takeshima, Y., Awaya, H., Ishida, H., Kohno, N., and Inai, K. (2004). Aberrant methylation of p14(ARF), p15(INK4b) and p16(INK4a) genes and location of the primary site in pulmonary squamous cell carcinoma. Pathol Int *54*, 549-555.

Grisendi, S., Bernardi, R., Rossi, M., Cheng, K., Khandker, L., Manova, K., and Pandolfi, P.P. (2005). Role of nucleophosmin in embryonic development and tumorigenesis. Nature *437*, 147-153.

Grisendi, S., Mecucci, C., Falini, B., and Pandolfi, P.P. (2006). Nucleophosmin and cancer. Nat Rev Cancer *6*, 493-505.

Gromley, A., Churchman, M.L., Zindy, F., and Sherr, C.J. (2009). Transient expression of the Arf tumor suppressor during male germ cell and eye development in Arf-Cre reporter mice. Proc Natl Acad Sci U S A *106*, 6285-6290.

Hainaut, P., Soussi, T., Shomer, B., Hollstein, M., Greenblatt, M., Hovig, E., Harris, C.C., and Montesano, R. (1997). Database of p53 gene somatic mutations in human tumors and cell lines: updated compilation and future prospects. Nucleic Acids Res *25*, 151-157.

Hall, M., and Peters, G. (1996). Genetic alterations of cyclins, cyclin-dependent kinases, and Cdk inhibitors in human cancer. Adv Cancer Res *68*, 67-108.

Haupt, Y., Maya, R., Kazaz, A., and Oren, M. (1997). Mdm2 promotes the rapid degradation of p53. Nature *387*, 296-299.

Hayman, A.R., Jones, S.J., Boyde, A., Foster, D., Colledge, W.H., Carlton, M.B., Evans, M.J., and Cox, T.M. (1996). Mice lacking tartrate-resistant acid phosphatase (Acp 5) have disrupted endochondral ossification and mild osteopetrosis. Development *122*, 3151-3162.

Honda, R., Tanaka, H., and Yasuda, H. (1997). Oncoprotein MDM2 is a ubiquitin ligase E3 for tumor suppressor p53. FEBS Lett *420*, 25-27.

Kamijo, T., Bodner, S., van de Kamp, E., Randle, D.H., and Sherr, C.J. (1999). Tumor spectrum in ARF-deficient mice. Cancer Res *59*, 2217-2222.

Kamijo, T., Zindy, F., Roussel, M.F., Quelle, D.E., Downing, J.R., Ashmun, R.A., Grosveld, G., and Sherr, C.J. (1997). Tumor suppression at the mouse INK4a locus mediated by the alternative reading frame product p19ARF. Cell *91*, 649-659.

Kang, Y.J., Olson, M.O., and Busch, H. (1974). Phosphorylation of acid-soluble proteins in isolated nucleoli of Novikoff hepatoma ascites cells. Effects of divalent cations. J Biol Chem *249*, 5580-5585.

Kang, Y.J., Olson, M.O., Jones, C., and Busch, H. (1975). Nucleolar phosphoproteins of normal rat liver and Novikoff hepatoma ascites cells. Cancer Res *35*, 1470-1475.

Kominami, K., Nagasaka, T., Cullings, H.M., Hoshizima, N., Sasamoto, H., Young, J., Leggett, B.A., Tanaka, N., and Matsubara, N. (2009). Methylation in p14(ARF) is frequently observed in colorectal cancer with low-level microsatellite instability. J Int Med Res *37*, 1038-1045.

Konishi, N., Nakamura, M., Kishi, M., Nishimine, M., Ishida, E., and Shimada, K. (2002). Heterogeneous methylation and deletion patterns of the INK4a/ARF locus within prostate carcinomas. Am J Pathol *160*, 1207-1214.

Kubbutat, M.H., Jones, S.N., and Vousden, K.H. (1997). Regulation of p53 stability by Mdm2. Nature *387*, 299-303.

Kuo, M.L., den Besten, W., Thomas, M.C., and Sherr, C.J. (2008). Arf-induced turnover of the nucleolar nucleophosmin-associated SUMO-2/3 protease Senp3. Cell Cycle *7*, 3378-3387.

Laud, K., Marian, C., Avril, M.F., Barrois, M., Chompret, A., Goldstein, A.M., Tucker, M.A., Clark, P.A., Peters, G., Chaudru, V.*, et al.* (2006). Comprehensive analysis of CDKN2A (p16INK4A/p14ARF) and CDKN2B genes in 53 melanoma index cases considered to be at heightened risk of melanoma. J Med Genet *43*, 39-47.

Maggi, L.B., Jr., Kuchenruether, M., Dadey, D.Y., Schwope, R.M., Grisendi, S., Townsend, R.R., Pandolfi, P.P., and Weber, J.D. (2008). Nucleophosmin serves as a rate-limiting nuclear export chaperone for the Mammalian ribosome. Mol Cell Biol *28*, 7050-7065.

McKeller, R.N., Fowler, J.L., Cunningham, J.J., Warner, N., Smeyne, R.J., Zindy, F., and Skapek, S.X. (2002). The Arf tumor suppressor gene promotes hyaloid vascular regression during mouse eye development. Proc Natl Acad Sci U S A *99*, 3848-3853.

Melendez, B., Malumbres, M., Perez de Castro, I., Santos, J., Pellicer, A., and Fernandez-Piqueras, J. (2000). Characterization of the murine p19(ARF) promoter CpG island and its methylation pattern in primary lymphomas. Carcinogenesis *21*, 817-821.

Nakamura, M., Watanabe, T., Klangby, U., Asker, C., Wiman, K., Yonekawa, Y., Kleihues, P., and Ohgaki, H. (2001). p14ARF deletion and methylation in genetic pathways to glioblastomas. Brain Pathol *11*, 159-168.

Nozawa, Y., Van Belzen, N., Van der Made, A.C., Dinjens, W.N., and Bosman, F.T. (1996). Expression of nucleophosmin/B23 in normal and neoplastic colorectal mucosa. J Pathol *178*, 48-52.

Qi, Y., Gregory, M.A., Li, Z., Brousal, J.P., West, K., and Hann, S.R. (2004). p19ARF directly and differentially controls the functions of c-Myc independently of p53. Nature *431*, 712-717.

Quelle, D.E., Zindy, F., Ashmun, R.A., and Sherr, C.J. (1995). Alternative reading frames of the INK4a tumor suppressor gene encode two unrelated proteins capable of inducing cell cycle arrest. Cell *83*, 993-1000.

Randerson-Moor, J.A., Harland, M., Williams, S., Cuthbert-Heavens, D., Sheridan, E., Aveyard, J., Sibley, K., Whitaker, L., Knowles, M., Bishop, J.N.*, et al.* (2001). A germline deletion of p14(ARF) but not CDKN2A in a melanoma-neural system tumour syndrome family. Hum Mol Genet *10*, 55-62.

Rauch, D.A., Hurchla, M.A., Harding, J.C., Deng, H., Shea, L.K., Eagleton, M.C., Niewiesk, S., Lairmore, M.D., Piwnica-Worms, D., Rosol, T.J.*, et al.* The ARF tumor suppressor regulates bone remodeling and osteosarcoma development in mice. PLoS One *5*, e15755.

Rizos, H., Puig, S., Badenas, C., Malvehy, J., Darmanian, A.P., Jimenez, L., Mila, M., and Kefford, R.F. (2001). A melanoma-associated germline mutation in exon 1beta inactivates p14ARF. Oncogene *20*, 5543-5547.

Roth, J., Dobbelstein, M., Freedman, D.A., Shenk, T., and Levine, A.J. (1998). Nucleo-cytoplasmic shuttling of the hdm2 oncoprotein regulates the levels of the p53 protein via a pathway used by the human immunodeficiency virus rev protein. EMBO J *17*, 554-564.

Saftig, P., Hunziker, E., Wehmeyer, O., Jones, S., Boyde, A., Rommerskirch, W., Moritz, J.D., Schu, P., and von Figura, K. (1998). Impaired osteoclastic bone resorption leads to osteopetrosis in cathepsin-K-deficient mice. Proc Natl Acad Sci U S A *95*, 13453-13458.

Serrano, M., Hannon, G.J., and Beach, D. (1993). A new regulatory motif in cell-cycle control causing specific inhibition of cyclin D/CDK4. Nature *366*, 704-707.

Sharpless, N.E. (2005). INK4a/ARF: a multifunctional tumor suppressor locus. Mutat Res *576*, 22-38.

Sherr, C.J. (1996). Cancer cell cycles. Science *274*, 1672-1677.

Sherr, C.J. (2000). The Pezcoller lecture: cancer cell cycles revisited. Cancer Res *60*, 3689-3695.

Sherr, C.J. (2001). The INK4a/ARF network in tumour suppression. Nat Rev Mol Cell Biol *2*, 731-737.

Sherr, C.J. (2006). Divorcing ARF and p53: an unsettled case. Nat Rev Cancer *6*, 663-673.

Shields, L.B., Gercel-Taylor, C., Yashar, C.M., Wan, T.C., Katsanis, W.A., Spinnato, J.A., and Taylor, D.D. (1997). Induction of immune responses to ovarian tumor antigens by multiparity. J Soc Gynecol Investig *4*, 298-304.

Silva, R.L., Thornton, J.D., Martin, A.C., Rehg, J.E., Bertwistle, D., Zindy, F., and Skapek, S.X. (2005). Arf-dependent regulation of Pdgf signaling in perivascular cells in the developing mouse eye. EMBO J *24*, 2803-2814.

Skaar, T.C., Prasad, S.C., Sharareh, S., Lippman, M.E., Brunner, N., and Clarke, R. (1998). Two-dimensional gel electrophoresis analyses identify nucleophosmin as an estrogen regulated protein associated with acquired estrogen-independence in human breast cancer cells. J Steroid Biochem Mol Biol *67*, 391-402.

Subong, E.N., Shue, M.J., Epstein, J.I., Briggman, J.V., Chan, P.K., and Partin, A.W. (1999). Monoclonal antibody to prostate cancer nuclear matrix protein (PRO:4-216) recognizes nucleophosmin/B23. Prostate *39*, 298-304.

Sugimoto, M., Kuo, M.L., Roussel, M.F., and Sherr, C.J. (2003). Nucleolar Arf tumor suppressor inhibits ribosomal RNA processing. Mol Cell *11*, 415-424.

Tago, K., Chiocca, S., and Sherr, C.J. (2005). Sumoylation induced by the Arf tumor suppressor: a p53-independent function. Proc Natl Acad Sci U S A *102*, 7689-7694.

Tanaka, M., Sasaki, H., Kino, I., Sugimura, T., and Terada, M. (1992). Genes preferentially expressed in embryo stomach are predominantly expressed in gastric cancer. Cancer Res *52*, 3372-3377.

Teitelbaum, S.L., and Ross, F.P. (2003). Genetic regulation of osteoclast development and function. Nat Rev Genet *4*, 638-649.

Tomimori, Y., Mori, K., Koide, M., Nakamichi, Y., Ninomiya, T., Udagawa, N., and Yasuda, H. (2009). Evaluation of pharmaceuticals with a novel 50-hour animal model of bone loss. J Bone Miner Res *24*, 1194-1205.

Wang, X., Kua, H.Y., Hu, Y., Guo, K., Zeng, Q., Wu, Q., Ng, H.H., Karsenty, G., de Crombrugghe, B., Yeh, J.*, et al.* (2006). p53 functions as a negative regulator of osteoblastogenesis, osteoblast-dependent osteoclastogenesis, and bone remodeling. J Cell Biol *172*, 115-125.

Weber, J.D., Jeffers, J.R., Rehg, J.E., Randle, D.H., Lozano, G., Roussel, M.F., Sherr, C.J., and Zambetti, G.P. (2000a). p53-independent functions of the p19(ARF) tumor suppressor. Genes Dev *14*, 2358-2365.

Weber, J.D., Kuo, M.L., Bothner, B., DiGiammarino, E.L., Kriwacki, R.W., Roussel, M.F., and Sherr, C.J. (2000b). Cooperative signals governing ARF-mdm2 interaction and nucleolar localization of the complex. Mol Cell Biol *20*, 2517-2528.

Weber, J.D., Taylor, L.J., Roussel, M.F., Sherr, C.J., and Bar-Sagi, D. (1999). Nucleolar Arf sequesters Mdm2 and activates p53. Nat Cell Biol *1*, 20-26.

Yu, Y., Maggi, L.B., Jr., Brady, S.N., Apicelli, A.J., Dai, M.S., Lu, H., and Weber, J.D. (2006). Nucleophosmin is essential for ribosomal protein L5 nuclear export. Mol Cell Biol *26*, 3798-3809.

Zemliakova, V.V., Strel'nikov, V.V., Zborovskaia, I.B., Balukova, O.V., Maiorova, O.A., Vasil'ev, E.V., Zaletaev, D.V., and Nemtsova, M.V. (2004). [Abnormal methylation of p16/CDKN2A AND p14/ARF genes GpG Islands in non-small cell lung cancer and in acute lymphoblastic leukemia]. Mol Biol (Mosk) *38*, 966-972.

Zhao, Q., Shao, J., Chen, W., and Li, Y.P. (2007). Osteoclast differentiation and gene regulation. Front Biosci *12*, 2519-2529.

Zheng, S., Chen, P., McMillan, A., Lafuente, A., Lafuente, M.J., Ballesta, A., Trias, M., and Wiencke, J.K. (2000). Correlations of partial and extensive methylation at the p14(ARF) locus with reduced mRNA expression in colorectal cancer cell lines and clinicopathological features in primary tumors. Carcinogenesis *21*, 2057-2064.

Chapter 4

Future Directions

4.1 Short-term future directions

Determine whether wild-type BMMs eventually "catch-up" with Arf$^{-/-}$ BMMs during osteoclastogenesis.

Our data from Chapter 3 suggest that *Arf* loss enhances osteoclastogenesis resulting in an increase in osteoclast number 5 days post-RANKL. In some cases, I have allowed both wild-type and *Arf*$^{-/-}$ macrophages to differentiate in osteoclastogenic media for 6 or more days. During these experiments, I have never observed a wild-type osteoclast phenotype that resembles that of *Arf*$^{-/-}$ osteoclasts. Specifically, I have not observed wild-type day 6 osteoclasts that phenocopy *Arf*$^{-/-}$ day 5 osteoclasts. However, this experiment remains to be formally completed and quantified. In thinking about how the results of this experiment might affect overall osteoclast number, we must also consider our results demonstrating that *Arf* loss extends the lifespan of osteoclasts *in vitro*. Therefore, even if wild-type BMMs eventually "catch-up" on day 6 to phenocopy their *Arf*$^{-/-}$ counterparts, they will still undergo apoptosis before the *Arf*$^{-/-}$ cells. Ultimately, this means that at any given time, there will always be more *Arf*$^{-/-}$ osteoclasts. Furthermore, the number of osteoclasts is one component in the overall output of osteoclast activity (the other being the function of osteoclasts on a per cell basis as will be discussed in the following section), which means that in the context of equal numbers of precursors and identical concentrations of osteoclastogenic cytokines, there should always be more osteoclast output in the absence of *Arf*.

Determine whether Arf loss results in increase osteoclast function *in vitro*

As mentioned above, there are two components to overall osteoclast output (i.e. bone resorption): osteoclast number and osteoclast function. It remains to be determined whether *Arf* loss increases the function of osteoclasts on a per cell basis. Our lab has previously published that $Arf^{-/-}$ cells 3 days post-RANKL have more TRAP activity than equal numbers of wild-type cells post-RANKL (Apicelli et al., 2008), suggesting that *Arf* loss results in enhanced osteoclast function on a per cell basis. To further support this finding, I propose to monitor osteoclast function *in vitro* by quantifying actin rings and bone resorption. Specifically, day 3 wild-type and $Arf^{-/-}$ pre-osteoclasts can be lifted and replated at equal densities on bovine bone slices. After 24h, the osteoclasts can be fixed on bone and stained for actin rings. Actin rings are areas of active bone resorption. There may be multiple actin rings per osteoclasts. One can quantify total area of active resorption per total cell area to get a percentage of active area resorption. While useful, this experiment does not necessarily take into account the amount of enzymes being secreted in each area of active resorption. Therefore, we must assess bone resorption in parallel. This could be quantified by either determining the area of bone resorption after removing the osteoclasts (pit assay), by quantifying the amount of collagen fragments released into the culture media, or both.

Further examine the effects of Arf loss on mononuclear precursor fusion

One of the most prominent *in vitro* phenotypes of $Arf^{-/-}$ osteoclasts is their size. There are two main possibilities for why *Arf* loss would result in an increase in osteoclast size: (i) enhanced fusion of mononuclear precursors and (ii) excessive protein synthesis.

It is also possible that both contribute to increased size. Our data show that *Arf*$^{-/-}$ osteoclasts do not have more nuclei than wild-type osteoclasts, suggesting that increased size is not due to enhanced fusion in the absence of *Arf*. As an alternative and more precise way of assessing fusion, we could label the nuclei of wild-type bone marrow macrophage with one color and the nuclei of *Arf*$^{-/-}$ bone marrow macrophages with another color. The nuclei from each genotype could then be plated together in different ratios for osteoclastogenesis. Nuclei from mature osteoclasts could then be assessed. For example, if we label wild-type nuclei red and *Arf*$^{-/-}$nuclei green and plate wild-type: *Arf*$^{-/-}$ nuclei at a ratio of 2:1, then each mature osteoclasts should have 2 red nuclei for every 1 green nucleus. This result would suggest that *Arf* loss does not affect mononuclear precursor fusion. However, if mature osteoclasts present with a ratio of 2 red: 2 green, then it would suggest that *Arf* loss enhances nuclear fusion. In parallel, one might also assess DC-STAMP levels, particularly in pre-osteoclasts, as this is a protein necessary for the fusion of precursors (Kukita et al., 2004; Yagi et al., 2005).

Determine whether the translation of TRAP and Cathepsin K mRNAs are altered in the absence of Arf

We have shown in Chapter 3 that TRAP and Cathepsin K protein levels appear 24h early during osteoclastogenesis in the absence of *Arf in vitro*. Additionally, we now know that *Arf* loss enhances protein synthesis during osteoclastogenesis (Apicelli et al., 2008). It is therefore possible that *Arf* loss is allowing for the premature translation of TRAP and Cathepsin K mRNAs. To test this possibility, we can isolate mRNAs from various peaks of our pre-osteoclast ribosome profiles. mRNAs undergoing higher rates of

translation will be shifted to the right on the polysome profiles in *Arf*$^{-/-}$ pre-osteoclasts relative to wild-type pre-osteoclasts. It may also be necessary to assess the levels of TRAP and Cathepsin K mRNAs on the polysome during day 2 of osteoclastogenesis since we first begin to see levels of both proteins appear on day 3 of osteoclastogenesis. It is possible that using day 2 ribosome profiles, we may detect TRAP and Cathepsin K mRNAs on the polysome only in the absence of *Arf*.

Genetically determine whether enhanced osteoclastogenesis upon Arf loss is dependent on NPM

Our lab has previously reported that ARF can inhibit the nucleocytoplasmic shuttling activity of nucleophosmin (NPM) (Brady et al., 2004). We also know that NPM is essential for ribosome export and protein synthesis (Maggi et al., 2008; Yu et al., 2006). Apicelli *et al.* demonstrated that when NPM is knocked down in *Arf*$^{-/-}$ macrophages, the *Arf*$^{-/-}$ *in vitro* osteoclast phenotype is reverted to that of wild-type osteoclasts (Apicelli et al., 2008). Initially, we hoped to examine the role of NPM during osteoclastogenesis in wild-type and *Arf*$^{-/-}$ cells by taking advantage of a recently published small molecule inhibitor (Qi et al., 2008). The authors reported that this inhibitor disrupts the oligomer formation of NPM, which is hypothesized to be critical for its function given that NPM is found as an oligomer under native conditions (Herrera et al., 1996; Namboodiri et al., 2004). Preliminary results suggested that NPM is important for wild-type osteoclastogenesis (Figure 4.1). However, our lab has been unable to verify by native gel electrophoresis that the small molecule inhibitor of NPM disrupt its oligomer formation. Still, it is promising to see such a dramatic phenotype upon the

suspected loss of NPM function. Therefore, I propose an alternative approach to determining the role of NPM during osteoclastogenesis in both wild-type and *Arf*$^{-/-}$ cells.

To genetically determine the role of NPM in enhanced osteoclastogenesis upon *Arf* loss, we have crossed *Npm*$^{+/-}$ mice with *Arf*$^{-/-}$ mice and generated the following genotypes: *Npm*$^{+/-}$*; Arf*$^{+/+}$, *Npm*$^{+/+}$*; Arf*$^{-/-}$, and *Npm*$^{+/-}$*; Arf*$^{-/-}$. I would first examine the osteoclastogenesis phenotype of all three of these genotypes *in vitro* to determine if loss of one *Npm* allele reverses the *Arf*$^{-/-}$ osteoclastogenesis phenotype. Future studies could also examine protein synthesis in each of these genotypes by ^{35}S-methionine incorporation. First of all, we need to know the osteoclastogenesis phenotype of *Npm*$^{+/-}$*; Arf*$^{+/+}$ bone marrow macrophages. It has been reported that *Npm*$^{+/-}$ mouse embryonic fibroblasts (MEFs) have lower rates of proliferation compared to wild-type MEFs at early passage and are haploinsufficient in their control of genetic stability (Grisendi et al., 2005). Furthermore, *Npm*$^{+/-}$ mice have accelerated oncogenesis and develop a hematological syndrome (Grisendi et al., 2005). However, there have been no reports demonstrating changes in osteoclastogenesis upon loss of *Npm*. Given that we have shown relatively low levels of ribosome output (compared to that observed in MEFs), it is possible that *Npm*$^{+/-}$*; Arf*$^{+/+}$ cells will have no defect in protein production or osteoclastogenesis. If this is true, then we can directly compare the other two genotypes. If unrestrained NPM activity is at least partially responsible for elevated levels of protein synthesis observed during osteoclastogenesis upon *Arf* loss, then we would expect to see a decrease in protein synthesis in *Npm*$^{+/-}$*; Arf*$^{-/-}$ mice relative to *Npm*$^{+/+}$*; Arf*$^{-/-}$ mice. One could additionally examine ribosome output as well as the nucleocytoplasmic shuttling of

ribosomes in all of these mice. Finally, it would be interesting to know if loss of one allele of *Npm* in *Arf*$^{-/-}$ mice reverses the *in vivo* osteoclast phenotypes.

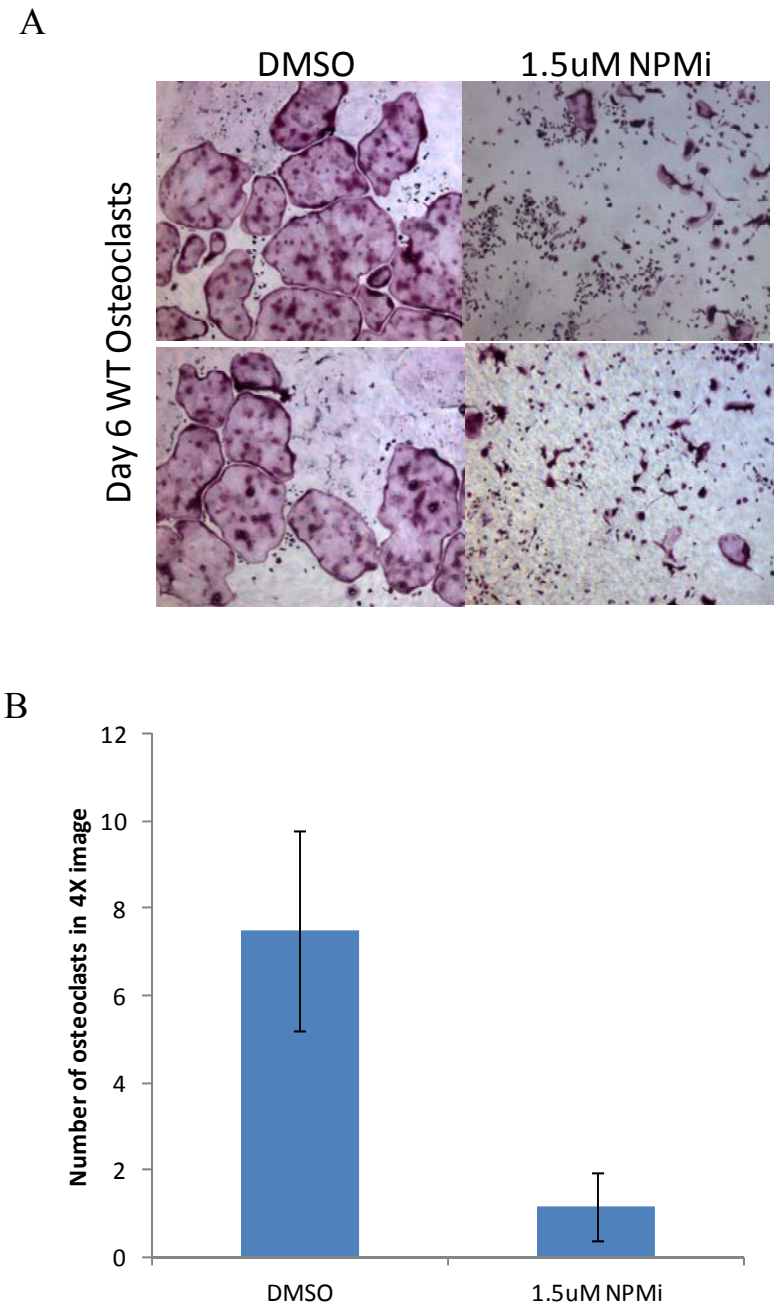

Figure 4.1

A small molecule inhibitor of nucleophosmin (NPM) retards osteoclastogenesis *in vitro*. (A) Wild-type bone marrow macrophages were plated in osteoclastogenic media in the presence of either DMSO or a small molecule inhibitor of NPM (NPMi) and allowed

to differentiate for 6 days. Osteoclasts are stained with TRAP. (B) Multinucleated TRAP-positive osteoclasts were quantified after 6 days. Three 4X fields were averaged from 4 individual wells. Difference is statistically significant ($p \leq 0.05$).

Genetically demonstrate that enhanced osteoclastogenesis in the absence of Arf is a result of increase protein synthesis

One of the major goals of this thesis has been to understand the role of ARF in regulating protein synthesis. While the previous experiment would strongly implicate ARF in impeding protein synthesis through the regulation of NPM, it does not rule out the possibility that ARF is prohibiting other functions that have been attributed to NPM and are not directly related to shuttling ribosomes and promoting protein synthesis (Grisendi et al., 2006; Okuwaki, 2008). Therefore, we have also crossed $Arf^{-/-}$ mice with mice containing a mutated allele of ribosomal protein L24. These mice are noted for their characteristic white belly spot and kinked tail and are thus referred to as the Belly Spot and Tail (Bst) mice (Oliver et al., 2004). $Rpl24^{Bst/+}$ cells have decreased rates of protein synthesis and proliferation relative to wild-type cells (Oliver et al., 2004). Aside from the aforementioned characteristics, the most notable phenotype of $Rpl24^{Bst/+}$ mice is a retinal defect (Rice et al., 1997; Rice et al., 1995; Smith et al., 2000; Tang et al., 1999). Interestingly, they also have some skeletal deformities including a triphalangeal first digit, an extra preaxial digit, a sixth lumbar vertebrae, and fused or wedge-shaped hemivertebrates, which result in the kinked tail phenotype (Oliver et al., 2004). Furthermore, homozygous loss of *Rpl24* is lethal (Oliver et al., 2004).

We now have the following genotypes: $Rpl24^{+/+}$; $Arf^{-/-}$, $Rpl24^{Bst/+}$; $Arf^{+/+}$, and $Rpl24^{Bst/+}$; $Arf^{-/-}$. The first experiment should be to isolate bone marrow macrophages from each of these mice and differentiate them into osteoclasts *in vitro* to determine if mutation of one *Rpl24* allele can reverse the $Arf^{-/-}$ osteoclast phenotype. I would expect that these osteoclasts would look more like wild-type osteoclasts and have decreased

protein synthesis and ribosome output relative to the *Arf*$^{-/-}$ cells. If this is true, it would be genetic evidence demonstrating a role for ARF in regulating protein synthesis during osteoclastogenesis. Moreover, bone marrow from *Rpl24*$^{Bst/+}$; *Arf*$^{-/-}$ could be used to generate radiation chimeras to compare wild-type mice receiving either wild-type or *Arf*$^{-/-}$ bone marrow transplants as we have done in Chapter 3.

Determine whether enhanced osteoclastogenesis upon Arf loss is dependent on p68

Our lab has recently isolated wild-type and *Arf*$^{-/-}$ nuclei in order to identify proteins whose nucleolar location is altered upon loss of *Arf*. This screen identified p68 (DDX5), which is an RNA helicase excluded from the nucleolus in the presence of ARF (Saporita et al., 2011). ARF prevents DDX5 from promoting ribosome biogenesis. Furthermore, the overall role of DDX5 in protein synthesis is demonstrated by the fact that its knockdown mimics ARF overexpression in TKO MEFs in terms of ribosome output (Saporita et al., 2011). *In vitro* and *in vivo* transformation experiments underscore the importance of the ARF-p68 interaction. In soft agar, *Arf*$^{-/-}$ MEFs are transformed in the presence of oncogenic Ras. However, knockdown of p68 in *Arf*$^{-/-}$ MEFs prohibited their transformation by Ras. Similarly, MEFs transduced with Ras and shp68 did not form tumors when inoculated into the flanks of nude mice whereas tumors did form in the presence of p68 (Saporita et al., 2011). Given that ARF limits protein synthesis in part by antagonizing the function of p68 in mitotic cells, it is possible that the ARF-p68 relationship is important during osteoclastogenesis. As a preliminary experiment, I have knocked down p68 in wild-type and *Arf*$^{-/-}$ cells during osteoclastogenesis. The data suggest that p68 is important for enhanced osteoclastogenesis upon *Arf* loss as there are

significantly less osteoclasts in the absence of *Arf* when p68 is knocked down relative to *Arf*$^{-/-}$ cells transduced with a control shRNA (Figure 4.2). Future studies could further examine the importance of p68 in enhanced osteoclastogenesis upon *Arf* loss by probing the steps of ribosome biogenesis, assessing ribosome output, and quantifying protein synthesis to determine if loss of p68 ultimately reverses the *Arf*$^{-/-}$ osteoclastogenesis phenotype.

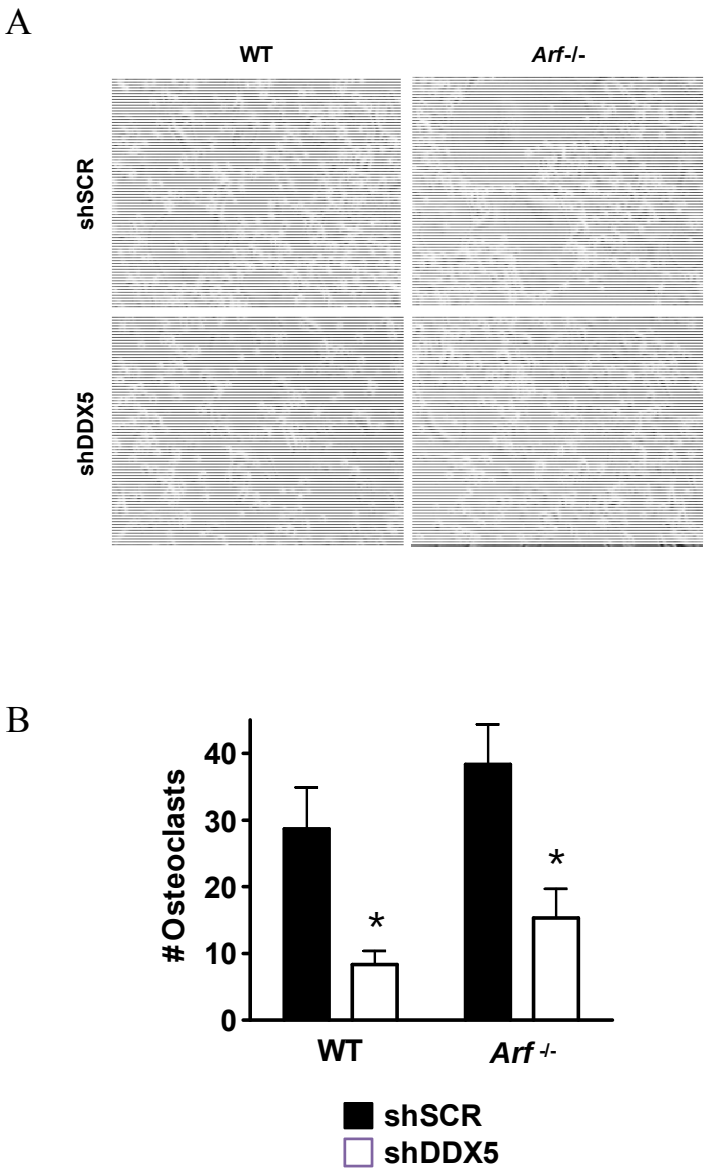

Figure 4.2.

Enhanced osteoclastogenesis upon in the absence of *Arf* is dependent on p68 (DDX5). (A) Representative 10X images of wild-type or *Arf*$^{-/-}$ day 5 osteoclasts that were lentivirally-transduced with either shSCRAMBLE or shDDX5. (B) Images were blindly quantified. Asterisks represent statistically significant differences between WT+shSCR and WT+shDDX5 or *Arf*$^{-/-}$+shSCR and *Arf*$^{-/-}$+shDDX5 ($p \leq 0.05$).

4.2 Long-term future directions

Examine the role of miRNAs during enhanced osteoclastogenesis upon Arf loss

Our lab has observed that *Arf* loss results in the selective translation of specific mRNAs in mouse embryonic fibroblasts (MEFs). In an effort to identify regulatory factors that may be controlling the translation of mRNAs upon *Arf* loss, we have initiated high throughput screens to assess the differences in miRNAs upon *Arf* loss in MEFs. Changes in the miRNA signature of a cell could significantly modulate the translation of various mRNAs as miRNAs are known to imperfectly base pair with target mRNAs and repress their translation (Calin and Croce, 2006). Upon observing differences in the miRNA prolife in MEFs, we first assessed day 5 wild-type and *Arf*$^{-/-}$ osteoclasts to see if any of the same miRNA changes exist between both mitotic and post-mitotic cells (Figure 4.3a). Of the tested miRNAs in day 5 osteoclasts, we were most interested in miRNA 223, as it has been reported to downregulated in both MEFs and osteoclasts, although it was only slightly downregulated in osteoclasts. However, it is also particularly interesting given that a recent study has shown that is downregulated in response to RANKL during osteoclastogenesis (Sugatani et al.). Furthermore, pre-miR-223 overexpression has been shown to block the formation of TRAP-positive multinucleated osteoclasts *in vitro* (Sugatani and Hruska, 2007). Together with published results, our data indicate that *Arf* loss may downregulate miR-223 to promote osteoclastogenesis. This hypothesis could be tested by overexpressing pre-miR-223 in *Arf* $^{-/-}$ macrophages upon plating in osteoclastogenic media. If the hypothesis is correct, I would expect to see a decrease in osteoclastogenesis with the overexpression relative to

what we have observed in *Arf*$^{-/-}$ cells. Additionally, we assessed the levels of two other miRNAs that have been reported in the osteoclast literature: miR-155 and miR-21 (Mann et al.; Sugatani et al.). We found that both of these miRNAs were slightly elevated in pre-osteoclasts upon *Arf* loss (Figure 4.3b). This would suggest that they may positively regulate osteoclastogenesis. In agreement with our results, Sugatani and colleagues have published that both of these miRNAs are upregulated in response to RANKL during osteoclastogenesis (Sugatani et al.). It would therefore be interesting to overexpress these in wild-type macrophages to see if they enhance osteoclastogenesis. Additionally, I would hypothesize that if they are knocked down in *Arf*$^{-/-}$ macrophages, then the enhanced osteoclast number and size may be, at least partially, reversed.

A

WT and Arf-/- OCs (Day 5)

miR	Fold Change	Taqman Array
132	1.86	2.86
127	N/A	1.86
129	2.27	2.43
142	1.10	---
223	1.22	17.02
34b	1.93	2.30
34c	2.24	2.34
182	5.25	2.39

B

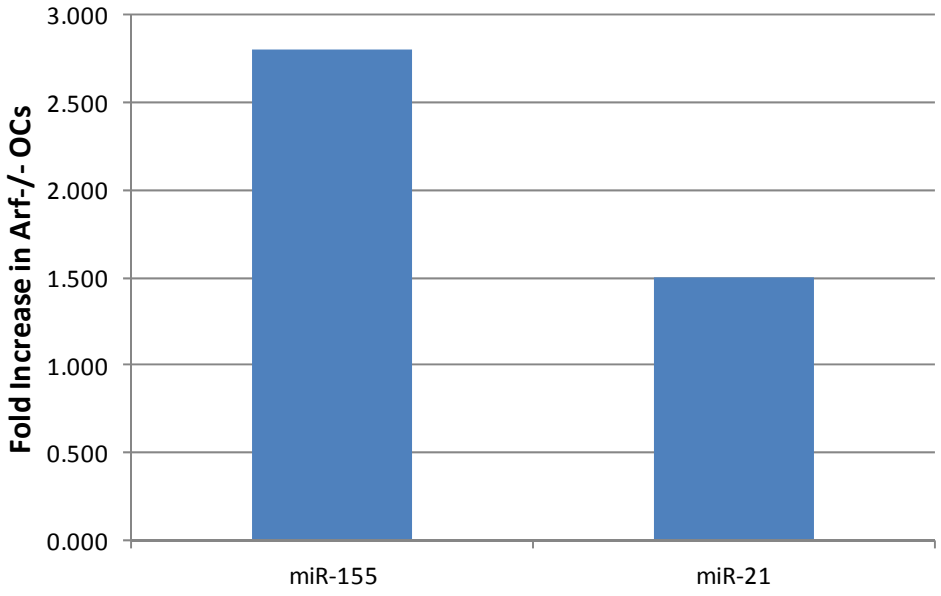

Figure 4.3

Changes in miRNAs during osteoclastogenesis. (A) Select miRNAs were assessed in wild-type and *Arf*$^{-/-}$ day 5 osteoclasts. Fold change is *Arf*$^{-/-}$ relative to wild-type. This is compared to results from a Taqman array done using wild-type and *Arf*$^{-/-}$ MEFs, in which the fold change represents *Arf*$^{-/-}$ MEFs relative to wild-type MEFs. (B) Taqman assays suggest that both miR-155 and miR-21 are elevated in *Arf*$^{-/-}$ pre-osteoclasts (day 3) relative to wild-type pre -osteoclasts.

Analyze the translatome of wild-type and Arf$^{-/-}$ osteoclasts

A central theme of this work is that *Arf* loss enhances protein synthesis to accelerate osteoclastogenesis, which begs the question: *which* mRNAs are being selectively translated (or not translated) when *Arf* is lost. Our lab and others have observed that some mRNAs are translated at rates that do not correspond with their levels of transcription (Pelletier et al., 2007; Rajasekhar et al., 2003). Furthermore, our lab has assessed the translatome (see Figure 4.4 for a description of the methods used in translatome analysis) of wild-type and *Arf*$^{-/-}$MEFs and found 109 mRNAs that are preferentially loaded (or unloaded) on the polysomes upon *Arf* loss. Additionally, we plan to perform the same assessment using *Arf*$^{-/-}$ prostate epithelial cells. It would be interesting to analyze the translatome of wild-type and *Arf*$^{-/-}$ pre-osteoclasts, as this is point at which we have observed significant changes in both ribosome output and protein synthesis during osteoclastogenesis. Not only would this data aid in the understanding of how *Arf* loss enhances osteoclastogenesis, but it would also be helpful to compare the translatomes of mitotic and post-mitotic cells. With such a comparison, we may be able to identify mRNAs whose translation is specifically important for cell growth independent of proliferation.

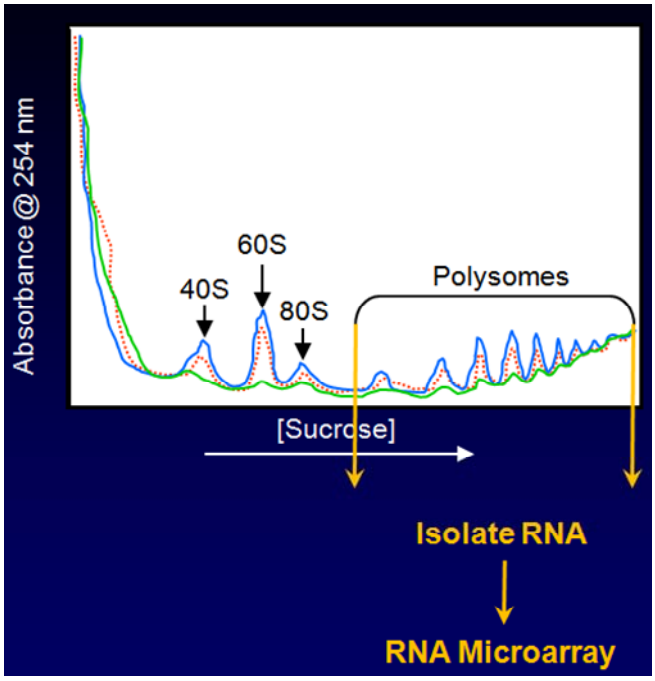

Figure 4.4

Schematic of methods used to determine mRNAs preferentially loaded or unloaded onto polysomes. mRNAs are "frozen" onto ribosomes by treating equal numbers of cells with cycoleximide. The cells are then lysed and the cytosolic fractions are separated using a sucrose density gradient. Polysome peaks will be collected and RNA from these peaks will be isolated. The RNA is then used in a microarray analysis (Illumina Mouse 8 array analysis done at Washington University). Each of the 8 arrays contains 24,000 known genes. The data is then statistically analyzed by the Microarray Core Facility at Washington University. All changes at the polysome are compared to changes at the total RNA level. Figure courtesy of Len Maggi.

4.3 References

Apicelli, A.J., Maggi, L.B., Jr., Hirbe, A.C., Miceli, A.P., Olanich, M.E., Schulte-Winkeler, C.L., Saporita, A.J., Kuchenreuther, M., Sanchez, J., Weilbaecher, K.*, et al.* (2008). A non-tumor suppressor role for basal p19ARF in maintaining nucleolar structure and function. Mol Cell Biol *28*, 1068-1080.

Brady, S.N., Yu, Y., Maggi, L.B., Jr., and Weber, J.D. (2004). ARF impedes NPM/B23 shuttling in an Mdm2-sensitive tumor suppressor pathway. Mol Cell Biol *24*, 9327-9338.

Calin, G.A., and Croce, C.M. (2006). MicroRNA signatures in human cancers. Nat Rev Cancer *6*, 857-866.

Grisendi, S., Bernardi, R., Rossi, M., Cheng, K., Khandker, L., Manova, K., and Pandolfi, P.P. (2005). Role of nucleophosmin in embryonic development and tumorigenesis. Nature *437*, 147-153.

Grisendi, S., Mecucci, C., Falini, B., and Pandolfi, P.P. (2006). Nucleophosmin and cancer. Nat Rev Cancer *6*, 493-505.

Herrera, J.E., Correia, J.J., Jones, A.E., and Olson, M.O. (1996). Sedimentation analyses of the salt- and divalent metal ion-induced oligomerization of nucleolar protein B23. Biochemistry *35*, 2668-2673.

Kukita, T., Wada, N., Kukita, A., Kakimoto, T., Sandra, F., Toh, K., Nagata, K., Iijima, T., Horiuchi, M., Matsusaki, H.*, et al.* (204). RANKL-induced DC-STAMP is essential for osteoclastogenesis. J Exp Med *200*, 941-946.

Maggi, L.B., Jr., Kuchenruether, M., Dadey, D.Y., Schwope, R.M., Grisendi, S., Townsend, R.R., Pandolfi, P.P., and Weber, J.D. (2008). Nucleophosmin serves as a rate-limiting nuclear export chaperone for the Mammalian ribosome. Mol Cell Biol *28*, 7050-7065.

Mann, M., Barad, O., Agami, R., Geiger, B., and Hornstein, E. miRNA-based mechanism for the commitment of multipotent progenitors to a single cellular fate. Proc Natl Acad Sci U S A *107*, 15804-15809.

Namboodiri, V.M., Akey, I.V., Schmidt-Zachmann, M.S., Head, J.F., and Akey, C.W. (2004). The structure and function of Xenopus NO38-core, a histone chaperone in the nucleolus. Structure *12*, 2149-2160.

Okuwaki, M. (2008). The structure and functions of NPM1/Nucleophsmin/B23, a multifunctional nucleolar acidic protein. J Biochem *143*, 441-448.

Oliver, E.R., Saunders, T.L., Tarle, S.A., and Glaser, T. (2004). Ribosomal protein L24 defect in belly spot and tail (Bst), a mouse Minute. Development *131*, 3907-3920.
Pelletier, C.L., Maggi, L.B., Jr., Brady, S.N., Scheidenhelm, D.K., Gutmann, D.H., and Weber, J.D. (2007). TSC1 sets the rate of ribosome export and protein synthesis through nucleophosmin translation. Cancer Res *67*, 1609-1617.

Qi, W., Shakalya, K., Stejskal, A., Goldman, A., Beeck, S., Cooke, L., and Mahadevan, D. (2008). NSC348884, a nucleophosmin inhibitor disrupts oligomer formation and induces apoptosis in human cancer cells. Oncogene *27*, 4210-4220.

Rajasekhar, V.K., Viale, A., Socci, N.D., Wiedmann, M., Hu, X., and Holland, E.C. (2003). Oncogenic Ras and Akt signaling contribute to glioblastoma formation by differential recruitment of existing mRNAs to polysomes. Mol Cell *12*, 889-901.

Rice, D.S., Tang, Q., Williams, R.W., Harris, B.S., Davisson, M.T., and Goldowitz, D. (1997). Decreased retinal ganglion cell number and misdirected axon growth associated with fissure defects in Bst/+ mutant mice. Invest Ophthalmol Vis Sci *38*, 2112-2124.

Rice, D.S., Williams, R.W., Ward-Bailey, P., Johnson, K.R., Harris, B.S., Davisson, M.T., and Goldowitz, D. (1995). Mapping the Bst mutation on mouse chromosome 16: a model for human optic atrophy. Mamm Genome *6*, 546-548.

Saporita, A.J., Chang, H-C., Winkeler, C.L., Apicelli, A.J., Kladney, R.D., Wang, J., Townsend, R.R., Michel, L.S., and Weber, J.D. (2011). RNA helicase DDX5 is a p53-independent target of ARF that participates in ribosome biogenesis. Cancer Res. In Press.

Smith, R.S., John, S.W., Zabeleta, A., Davisson, M.T., Hawes, N.L., and Chang, B. (2000). The bst locus on mouse chromosome 16 is associated with age-related subretinal neovascularization. Proc Natl Acad Sci U S A *97*, 2191-2195.

Sugatani, T., and Hruska, K.A. (2007). MicroRNA-223 is a key factor in osteoclast differentiation. J Cell Biochem *101*, 996-999.

Sugatani, T., Vacher, J., and Hruska, K.A. A microRNA expression signature of osteoclastogenesis. Blood *117*, 3648-3657.

Tang, Q., Rice, D.S., and Goldowitz, D. (1999). Disrupted retinal development in the embryonic belly spot and tail mutant mouse. Dev Biol *207*, 239-255.

Yagi, M., Miyamoto, T., Sawatani, Y., Iwamoto, K., Hosogane, N., Fujita, N., Morita, K., Ninomiya, K., Suzuki, T., Miyamoto, K*., et al.* (2005). DC-STAMP is essential for cell-cell fusion in osteoclasts and foreign body giant cells. J Exp Med *202*, 345-351.

Yu, Y., Maggi, L.B., Jr., Brady, S.N., Apicelli, A.J., Dai, M.S., Lu, H., and Weber, J.D. (2006). Nucleophosmin is essential for ribosomal protein L5 nuclear export. Mol Cell Biol *26*, 3798-3809.